1-1-2011

Mechanisms of translation arrest following focal brain ischemia

Monique K. Lewis
Wayne State University,

MECHANISMS OF TRANSLATION ARREST FOLLOWING FOCAL BRAIN ISCHEMIA

by

MONIQUE K. LEWIS

DISSERTATION

Submitted to the Graduate School

of Wayne State University,

Detroit, Michigan

in partial fulfillment of the requirements

for the degree of

DOCTOR OF PHILOSOPHY

2011

MAJOR: PHYSIOLOGY

Approved by:

_____

Advisor Date

_____

_____

_____

DEDICATION

This dissertation is dedicated to my mother, Constance Marshall. For as long as I can recall, she has made innumerable sacrifices to ensure that I would receive the best education possible, which includes her willingness to help by babysitting my children and sit through countless practice presentations while I pursued my PhD . My mother's unconditional love, support, encouragement and strength have motivated me throughout my life, especially during my time as a graduate student and I am eternally grateful to her.

In addition, I would like to dedicate this work to my amazing husband Lorrance Lewis. From our first meeting in 2007 up until now, he has been nothing but loving, supportive and patient as I worked to complete this program. My husband has encouraged, motivated and constantly prayed for me during my lowest moments while pursuing my degree, especially when I wanted to give up or questioned the relevance of my work. Words can't express how grateful I am to him.

Last, but not least, I would like to dedicate this work to my family, many of whom have been afflicted with diabetes and stroke. They are the reason why I work to provide a better understanding of these diseases and hopefully contribute to the development of more effective treatment in the future.

ACKNOWLEDGMENTS

I would like to thank the members of my dissertation committee, Drs. Joseph Dunbar, Jose Rafols and Jan Schwartz, as well as the entire Physiology department for their time and support of my education and research.

I want to especially thank Dr. Natalie Rizk, who took time out of her busy schedule as a medical student to patiently teach me how to perform the middle cerebral artery occlusion surgery. I'd also like to thank Jie Wang for teaching me how to do perfusion-fixation and many of the staining techniques utilized in our lab. I am forever grateful for their support, friendship and time, without which I wouldn't have been able to perform my experiments.

I want to thank Foaz Kayali and Jill Jamison for their important work developing the pA FISH and IF staining techniques and work on ribonomics following brain ischemia and reperfusion.

Also, I want to thank Dr. George Roberts, Jeff Szymanski whom have offered invaluable technical support.

I would like to extend special thanks to Dr. Donald J. DeGracia, my advisor and mentor, for his patience, encouragement, and his unyielding dedication to my education.

This work was supported by grants from the National Institutes of Health (NIGMS 2 R25 GM58905-10 IMSD and NINDS NS057167 DJD).

TABLE OF CONTENTS

LIST OF TABLES

LIST OF FIGURES

LIST OF ABBREVIATIONS

4EBPs, 4E binding proteins

ACA, anterior cerebral artery

CA, Cornu Ammonis

CA/R, cardiac arrest and resuscitation

CCA, common carotid artery

COX IV, cytochrome c oxidase subunit IV

DG, dentate gyrus

DND, delayed neuronal death

ECA, external carotid artery

eIF2, eukaryotic initiation factor-2

eIF2(αP), eIF2 when alpha subunit is phosphorylated in holoenzyme

eIF2B, eukaryotic initiation factor-2 B

eIF2α, alpha subunit of eIF2

eIF2α(P), phosphorylated alpha subunit of eIF2

eIF2α, eukaryotic initiation factor-2 (α-subunit)

eIFs, eukaryotic initiation factors

eIF4, eukaryotic initiation factor-4

ER, endoplasmic reticulum

eNOS, endothelial nitric oxide synthase

FFA, free fatty acids

FISH, fluorescent in situ hybridization

GM130, cis-golgi matrix marker 130 kDa

HSP70, heat shock protein 70 kDa

ICA, internal carotid artery

ICAM-1, Inter-Cellular Adhesion Molecule 1

IF, immunofluorescence histochemistry

IP, intraperitoneal

IPC, ischemic preconditioning

I/R, ischemia and reperfusion

IRES, internal ribosome entry sites

K/X, ketamine and xylazine

LDF, laser Doppler flowmetry

LWA, linear weighted averaging

LONI, Laboratory of Neuroimaging (at UCLA)

MCA, middle cerebral artery

MCAO, middle cerebral artery occlusion

MIP, maximum intensity projection

MMP, matrix metalloproteinase

NeuN, neuronal nuclei

NF H/M, neurofilament heavy and medium weight chains

PA, protein aggregates

pA, poly-adenylated mRNAs

PABP, poly-adenylated mRNA-binding protein

PDI, protein disulfide isomerase

pMCAO, permanent MCAO

RPA, ribosomal P antigen

SG, Stress granules

S6, constituent protein of the 40S small ribosomal subunit

STZ, Streptozocin

Ternary complex, complex of eIF2/GTP/$tRNA_i^{met*}$

TA, Translation arrest

TGN38, trans-golgi network 38 kDa antigen

TIA-1, T-cell internal antigen

tPA, tissue plasminogen activator

TTC, 2,3,5 Triphenyltetrazolium chloride

TTP, tristetraprolin

TUNEL, terminal deoxynucleotidyl transferase-mediated dUTP nick end labeling

UPR, unfolded protein response

UTR, untranslated regions

2VO/HT, two vessel occlusion and hypovolemic hypotension

CHAPTER ONE: Background

I. Introduction

The loss of blood flow to the brain is termed ischemia and the subsequent resumption of blood flow is termed reperfusion. Brain ischemia and reperfusion (I/R) occurs primarily following resuscitation from cardiac arrest and/or stroke and presents one of the most significant clinical challenges. At present, there are no clinically effective pharmacologic interventions to halt brain damage following I/R. The major Aim of this dissertation will be to investigate possible mechanisms involved in neuron death following brain I/R, which may potentially lead to the development of effective therapies.

A second major facet of this dissertation will be to address the issue of stroke and diabetes. It is very well established clinically that stroke outcome in diabetic patients is significantly worse than in non-diabetic patients. Diabetes has negative effects throughout the whole body and multiple different causes have been attributed to worsened stroke outcome. As both diabetes and ischemia are stress to cells, I hypothesize that the worsened damage following ischemic stroke in diabetes is due to a cumulative or additive effect of each condition on neuronal stress responses.

Neuronal death following brain I/R injury is a result of a variety of damage pathways[5]. The focus of the work here is on a specific aspect of I/R injury: the persistent inhibition of protein synthesis, or translation arrest (TA), which occurs in neurons in response to I/R injury. TA is of significance because, as I discuss in detail below, it correlates with neuronal death[1,2]. The purpose of this Dissertation is to investigate mechanisms of TA in the brain following focal ischemia, with and without diabetes. There has been extensive research on persistent TA in global models of brain I/R, whereas research in focal ischemia, as occurs in stroke, has not been as extensive. Therefore, there is a need to further study mechanisms of TA in the focal model.

After a thorough literature review, I have found no studies of the possible role of TA in worsened stroke outcome in diabetics, making this line of investigation completely novel.

Below, I will review our current understanding of I/R brain injury and how diabetes worsens outcome. I will discuss clinical outcomes, the major mechanisms, and especially focus on TA following brain I/R. The most current ideas on TA link it to intracellular stress responses and the formation of subcellular particles involved in mRNA metabolism such as stress granules and mRNA granules. My Background discussion will introduce my hypotheses about mechanisms of prolonged TA following focal brain I/R and the possible effect of diabetes on these mechanisms. In subsequent chapters I will present my study designs and results. The Dissertation will close with a chapter discussing the significance of my finding in light of the existent literature and in terms of new ideas about cell injury dynamics that are being developed in our laboratory.

II. Brain Ischemia and Reperfusion Defined

Ischemia is a significant decrease or cessation of blood flow to the brain, and reperfusion is resumption of normal or near normal blood flow. The brain is the most sensitive organ to I/R injury. I/R brain injury takes two major forms: global and focal. Global ischemia is a cessation of blood flow to the entire brain and occurs in humans during drowning or during cardiac arrest. Focal ischemia is ischemia of a localized region of the brain and is due to many possible causes such as artery occlusion, ruptured hematomas, gliomas, etc. Stroke is the focal ischemia that most often occurs in humans. Both focal and global ischemias are lethal to neurons and there is great clinical interest in determining the mechanisms of injury so as to be able to treat these conditions.

III. Focal Ischemia and Reperfusion Brain Injury

Stroke is the most common form of focal ischemic insult to the brain and is the third most

common cause of death and disability in the United States.[3] Ischemic stroke accounts for approximately 80% of all strokes and results from an embolic or thrombotic occlusion of a major cerebral artery or its branches. This is most often the middle cerebral artery (MCA). Occlusion of a specific blood vessel results in injury to the corresponding volume of brain tissue fed by the occluded vessel. Loss of the brain functions associated with the ischemic brain volume occurs rapidly. Damage to the brain results from either a transient ischemic attack, where neuronal function will be restored ~24 hrs after the development of symptoms[4], or from a stroke, where neuronal function is lost forever due to irreversible death of the brain tissue.

Unlike global ischemia, which leads to neuronal cell death in very specific neuron populations, there is a morphological complexity to stroke injury.[5] Focal ischemia produces a mass of damaged brain tissue termed the infarct. Damage is expressed as the volume of the infarct. A necrotic core forms at the site of the occlusion, consisting of dead brain tissue including neurons, glia and vascular tissue. Surrounding the core is a penumbra characterized by hypoperfusion and other metabolic and functional disturbances. If the vessel remains occluded, an increasing number of cells, further away from the core, will eventually be affected. These cells define the penumbral region, and their death occurs many hours, days or in some cases, months, after the initial ischemia. Penumbral neurons that die after the ischemia are distinguished from the immediate necrosis of the core by the term "delayed neuronal death" (DND).[6]

In permanent ischemia, the initial infarct is seen after 3-12 hrs.[7] The infarct begins in the core but reaches close to its maximal size, which includes core and penumbra, 8-24 hrs after the onset of ischemia. The infarct continues to grow after 1 day, so that between 24 and 72 hrs it can grow by approximately 30%.[8] Thus damage continues to increase in penumbral regions. Different durations of temporary ischemia lead to graded involvement of different regions in the

infarct as measured after 1-2 days reperfusion.[9] Studies have demonstrated that 1 hr of ischemia leads to infarct in the core, with infarct in the penumbra developing fully within 2-3 hr of temporary occlusion.[10] As little as 30 minutes of transient ischemia leads to an infarct in the core region, but this only first appears after 3 days and takes 2-3 weeks to mature to its full size.[11]

Individual cell death within the infarct develops slowly, but more rapidly than delayed cell death in global ischemia. Cell death first becomes significant at approximately 6-12 hrs in the core of the lesion, with a major increase between these two time points. At 12 and 24 hrs, approximately 80% of the neurons died.[12] The final stage of infarct development in focal ischemia is pan-necrosis, in which neuronal death is accompanied by glial and vascular cell death and loss of cellular elements.[5]

To conclude, development of the necrotic infarct occurs within a few hours of focal ischemia, but matures over up to several days, drawing in penumbral regions and resulting in a larger mass of dead brain tissue.

IV. Diabetes and Worsened Stroke Outcome

A. Diabetes Defined

Diabetes mellitus is a metabolic disorder characterized with chronic degenerative changes in various tissues, with the two major forms being type 1, insulin-dependent, and type 2, noninsulin-dependent diabetes. In the United States, 25.8 million people, or 8.3 % of the population, have diabetes, with 1.9 million new cases of diabetes diagnosed in people aged 20 years or older in 2010.[13] Type 2 diabetes accounts for ~90% of the population diagnosed with diabetes in the United States. Diabetes is not just an epidemic of the US but is considered a global health problem, affecting over 340 million people worldwide.[14]

Type 1 diabetes is an autoimmune disorder characterized by the destruction of pancreatic islet cells, including the insulin-producing beta cells. However, many factors contribute to the

onset of type-2 diabetes, including genetic, lifestyle and dietary. Type 2 diabetes is characterized by insulin resistance, relative insulin deficiency at later stages, and excessive hepatic glucose production, all leading to hyperglycemia. The primary events are believed to be an initial deficit in insulin secretion and, in many patients, relative insulin deficiency in association with peripheral insulin resistance[15]. Dysfunction of pancreatic beta cells, which produce insulin, is necessary for the development of the disease, but the nature of the primary beta cell defect is still unknown.

Initiation of the insulin response depends upon the transmembranous transport of glucose and coupling of glucose to the glucose sensor on the beta cell. The glucose/glucose sensor complex then induces an increase in glucokinase by stabilizing the protein and impairing its degradation. The induction of glucokinase serves as the first step in linking intermediary metabolism with the insulin secretory apparatus. Glucose transport in beta cells of type 2 diabetes patients appears to be greatly reduced, thus shifting the control point for insulin secretion from glucokinase to the glucose transport system[16]. Other defects in beta cell function in type 2 diabetes include defective glucose potentiation in response to substances that cause non-glucose-dependent insulin secretion, asynchronous insulin release, and a decreased conversion of proinsulin to insulin.

A hallmark of type 2 diabetes is increased secretion of insulin, hyperinsulinemia, early on. In later stages, because of the chronic insulin resistance in muscle and adipose cells and impaired beta cell function, there is a loss of the early insulin release in response to hyperglycemic stimuli[17]. Thus, when insulin binds to its receptors, it is not able to bring about a response of increased glucose utilization in these cells. With the impaired insulin production and secretion, glucose synthesis and output from the liver increases. Thus, the liver in type 2 diabetes is programmed to both overproduce and under use glucose.

Furthermore, in addition to the ineffectiveness of insulin in inhibiting glucose production in the liver, free fatty acids are deposited into tissues and inefficiently stored in adipose tissue, resulting in elevated circulating levels. The elevated FFA levels also lend to the increased glucose production by the liver[18]. The ensuing glucose toxicity leads to a multitude of disturbances in various tissues, disrupting homeostasis throughout the body. Chronic hyperglycemia and hyperlipidemia can exert deleterious effects on beta cell function. Over time, both of these phenomena contribute to the progressive deterioration of glucose homeostasis characteristic of this disease and various long-term complications. The long-term complications markedly increase the susceptibility to cardiovascular disease, including ischemic stroke.

B. Impact of Diabetes on Stroke Occurrence and Recovery

People with diabetes are two to four times more likely to have an atherotherombotic stroke than people who do not have the disease[13]. Diabetes particularly affects the risk of stroke among younger individuals, with a more than 10-fold increase risk of stroke in the stroke population younger than 55 years[13]. It has been demonstrated that diabetes is associated with vascular alterations, including cerebrovascular atherosclerosis and other abnormalities[19]. There is compromised collateral flow throughout arterial networks, leading to a decrease in blood flow to the brain that further complicates stroke. In addition, people with diabetes often have high blood pressure, which can also cause abnormalities in the small blood vessels of the brain and contribute to the increased susceptibility to stroke. Because diabetes has the tendency to exert such deleterious effects on the vascular system, these factors render diabetics, at least in part, to be more susceptible to ischemic brain damage and worsened outcome following stroke.

In order to investigate the impact of diabetes on stroke, neuronal cell death was assessed following permanent focal ischemia using the middle cerebral artery occlusion (MCAO) technique. The infarct core includes the striatum and overlying cortex, areas directly fed by the

MCA. Areas peripheral to the core encompass the piriformis and parietal cortex.[20] However, the hippocampus did not display an infarct and is therefore not considered to be in the core. As explained above, the current understanding is that neuronal cell death is due to necrosis occurring in the core and to DND in the penumbra.[21] The core of the focal lesion undergoes massive ion and metabolite changes that, by some indicators such as ATP levels and ion gradients, appears to recover after transient ischemia. However, during the reperfusion period, it is near impossible to prevent formation of an infarct in the core by any interventions, despite the initial appearance of recovery.[22]

In contrast, in the MCAO model, the penumbra can be rescued by many interventions[5,122], indicating different mechanisms of damage in the two regions. This is why defining the penumbra and the mechanisms by which neurons die in that region is of particular interest. Terminal deoxynucleotidyl transferase-mediated dUTP nick end labeling (TUNEL) was used to assess nucleosomal DNA fragmentation in situ in normal and diabetic animals with or without MCAO[22]. No TUNEL positive cells were found in the cortex of normal animals, whereas the diabetic animals did show positive TUNEL staining in the cortical cells. After permanent MCAO, TUNEL positive cells were present in the piriform and parietal cortices in the normal animals and were further increased in the diabetic group. Furthermore, caspase-3 was also found to be increased following MCAO in normal animals and was increased above that in the diabetic group.[22] Caspase 3 activation is most often associated with apoptosis, but in neurons, its activation has also been associated with neuronal remodeling that is not associated with cell death.[23]

These studies demonstrated that focal ischemia produces cell death in the core of the infarct and ensuing cell death in the penumbral region, with the amount of cell death being augmented by the presence of diabetes. To consider mechanisms by which diabetes worsens

stroke outcome, we first turn to a discussion of the established mechanisms of brain I/R injury.

V. Established Mechanisms of Brain I/R

Following focal ischemia, the core is not salvageable. However, the DND associated with the penumbra provides a time window for therapeutic interventions. Therefore, it is the goal of stroke research to understand DND in the penumbra to be able to limit stroke damage to only the core infarct. The DND of penumbra is very similar in both time course and mechanisms to the DND found in selectively vulnerable neurons after global ischemia, and therefore, findings in the global ischemia models are brought to bare on the focal case.

It needs to be emphasized that, in spite of a very large amount of information (a PubMed search of the term "brain ischemia" gives 78,805 papers!), the cell death pathways causing DND following I/R injury are not known with certainty. The "acid test" of current knowledge is the fact that all pharmacologic clinical trials following either stroke[122] or cardiac arrest and resuscitation[24] have fully failed. Therefore, it is safe to conclude our current knowledge, in spite of its volume, is incomplete. It is anticipated that a full and correct understanding of DND will lead to the development of clinically effective therapies. In the following paragraphs, we review (1) the established damage mechanisms associated with I/R injury and (2) the stress response expressed by neurons following I/R injury.

A. Ischemia

Ischemia, independent of reperfusion, brings about various forms of cell damage, all surrounding the rapid loss of ATP, which is secondary to the loss of glucose and oxygen influx following cessation of cerebral blood flow. In the brain, ATP loss most directly affects the Na^+/K^+-ATPase electrogenic pump, accounting for approximately 50% of ATP utilization in the neuron.[25] Consequently, ATP loss in the brain leads to a series of events known as excitotoxicity.

1. Excitotoxicity

Under normal conditions in a neuron, the binding of glutamate to NMDA and AMPA receptors causes depolarization of postsynaptic neurons via rapid influx of Na^+ and Ca^{2+}. Depolarization also induces Ca^{2+} influx through the voltage gated L- and T- calcium channels. This calcium influx is reversed when extra- and intracellular ion concentrations are reset, ultimately via the Na^+ gradient created by several ATP-dependent Ca^{2+} pumps. Also, continued glutamate excitability is halted as a result of glutamate reuptake by astroglia, in an ATP dependent manner.

Following ischemia, ATP levels drop in cells because of a lack of delivery of oxygen and glucose and a high rate of ATP expenditure in these cells. ATP levels are 50% of baseline in the first min of ischemia, and essentially zero at 4 min ischemia[26]. Loss of ATP halts the function of the Na^+-K^+-ATPase allowing uncontrolled ion influx, mainly through "leak channels" initially, and allowing ions to approach their Nernst equilibria. The net result of the attempt of ions to equilibrate is a net depolarized state in the neuron. The depolarization results in the release of excessive amounts of excitotoxic amino acids, namely glutamate, from presynaptic neurons into the extracellular space.[27] Glutamate then acts by activation of NMDA and AMPA receptors. This leads to an uncontrolled positive feedback loop: net depolarization results in neurotransmitter release, the majority of which are excitatory, inducing ligand-gated depolarization, which causes further excitatory transmitter release, inducing further depolarization. This feedback continues until releasable transmitter is depleted. This sequence of events is called excitotoxicity.

Long durations of ischemia will cause such extreme ion equilibration that cells will die by bursting due to a net ion influx carrying water by osmotic forces. However, with moderate and clinically relevant ischemia durations, ion influx is not sufficient to burst cells, but leads to a

pathologically high cytoplasmic Ca^{2+} concentration. Silver and Erecinska in 1990 demonstrated that, during ischemia, intracellular Ca^{2+} concentration in neurons goes from about 10 nM to about 800 nM after 7 min of complete ischemia[28].

During focal ischemia, the impact of intra-ischemic depolarization is not completely known. Previous studies have found that there is a wave-like spread of increased extracellular K^+ and glutamate from the core of the lesion in a phenomenon known as "spreading depression"[29]. The frequencies of the depolarizations are halved by either AMPA or NMDA antagonists, indicating that glutamate-mediated depolarization contribute at least 50%.[30]. The evidence linking the development of damage in the penumbra to these depolarizations is extensive, but mainly correlative[31]. The most convincing direct evidence that these depolarizations are damaging came about by using either KCl or electrical stimulation, which increased the number of depolarizations by twofold. This resulted in an increase in the size of the infarct and peri-infarct damage by 30-100%[31-32]. Based on these findings, the damage caused by the induced depolarizations suggests that the endogenous depolarizations are also damaging during ischemic conditions. However, pharmacological targeting, in an effort to more directly establish the importance of the depolarizations, has proven to be difficult[31].

The contribution of excitotoxicity to DND has not been resolved. One study has shown significant ultrastructural alterations in post-synaptic densities following I/R that persisted to at least 24 hr reperfusion in CA1 compared to dentate gyrus (DG)[33]. However, this study failed to evaluate these parameters in CA3, which is also well known to have very high excitatory transmission, which underlies the development of temporal lobe epilepsy[34]. Perhaps most important, the extracellular levels of excitatory transmitters found in ischemic brain is much less than those generated by exogenous application of the transmitters required to generate cell death solely by an excitotoxic mechanism[35]. Thus, any notion that excitotoxicity is the sole factor in

DND has been proven false. Other lines of evidence suggest that the main contribution of an excitotoxic mechanism to DND is to allow a massive dys-regulation of cytoplasmic Ca^{2+}.

B. Reperfusion Damage Mechanisms

Reperfusion results in additional damage mechanisms that compound the damage evoked during ischemia. These include: free radical production, lipid peroxidation, nitrosylation, further alterations in cellular signaling pathways, and persistent TA.

1. Free Radicals

There is substantial evidence that free radical damage (today commonly known as reactive oxygen species or ROS) contributes to DND following brain I/R. One consequence of the abnormal calcium influx in neurons during ischemia is a rapid increase in intracellular arachidonic acid concentration by Ca^{2+}-activated phospholipases[36-37]. Once reperfusion begins, the accumulated arachidonic acid can be converted to hydroperoxides by lipoxygenase. The hydroperoxides can participate in lipid peroxidation by Fenton-like reactions[38]. Thus, oxidative damage occurs in reperfused neurons on the membrane as a result of lipid peroxidation[39].

Oxygen supply to ischemic cells is restored with reperfusion. Oxygen is an essential substrate of the enzyme cyclooxygenase which catalyzes the addition of two oxygen molecules to arachidonic acid producing prostaglandin G. Prostaglandin G is subsequently peroxidized, forming an oxygen radical, superoxide (O2-) and prostaglandin H[26]. While the prostaglandins are known inflammatory mediators, they can also increase in lipid peroxidation in cell membranes that will result in changes in lipid permeability and fluidity. This, in turn, will disrupt the functions of receptors, ion channels, and other proteins located on the cell membrane. Perturbations within the cell membrane occur as a result of the glutathione depletion during ischemia[40], resulting in the cell's inability to recover from damage caused by lipid peroxidation.

In addition to reactive oxygen species, the oxygen radicals can react with nitric oxide

(NO) through a reaction catalyzed by NOS, forming peroxynitrite[19], a reactive nitrogen species (RNS). Peroxynitrite, in turn, oxidizes Fe^{2+} ions resulting in greater lipid peroxidation[41]. In addition, under ischemic conditions there is a resultant burst of free oxygen radicals and the release of pro-apoptotic molecules due to the formation of mitochondrial permeability transition pores[42]. Following ischemia, free radicals are generated during the inflammatory response[43].

In focal ischemia, there is very little free radical change in the core as compared to the penumbra; this is in contrast to the ion and metabolite changes that occur.[44] Free radical production, as measured by hydroxylation of salicylic acid, remained elevated 3 hours after the onset of ischemia in the penumbra, and further elevated with the onset of reperfusion. In contrast, there was no increase in the core during 3 hours of ischemia, but there was an increase at about 4 hours reperfusion[45]. Therefore, core exposure to free radicals during the main periods of injury development during ischemia is considered minimal with free radical production largely restricted to the penumbra[5].

In addition, studies have definitively shown that free radical and NO production are elevated for at least 6-12 h following focal ischemia[46]. It has been demonstrated that elevated levels of superoxide, in concert with NO production, result in increased peroxynitrite production. It has been well established that free radicals are generated during and after both focal and global ischemia and conditions that reduce their accumulation should ameliorate damage, if the free radicals are in fact damaging. However, cell death, induced by arachidonate activation, in NB-104 cells is not inhibited after cells were treated with radical scavengers[47]. But in the same study, cell death induced by lipid hydroperoxides was prevented when treated with radical scavengers[47]. Despite the apparent connection between oxygen radical formation and lipid peroxidation in causing cell death, studies have proven otherwise. Although the contribution of free radical damage to reperfusion injury is significant, it is only part of the picture.

C. Inflammation

Inflammation has been implicated as a secondary injury mechanism following stroke. A growing number of recent investigations have established a critical role for leukocytes in bringing about tissue damage after ischemia and reperfusion in stroke. The vascular endothelium promotes inflammation through the upregulation of adhesion molecules like intercellular adhesion molecule (ICAM)-1, E-selectin, and P-selectin, that bind to circulating leukocytes and facilitate their migration into the CNS[48]. Once in the CNS, the production of cytotoxic molecules may facilitate cell death. The macrophage and microglial response to injury may either be beneficial by scavenging necrotic debris or detrimental by facilitating cell death in neurons that would otherwise recover.

Using MCAO, several studies have demonstrated that inflammatory events occurring at the blood-endothelium interface of cerebral capillaries underlie the resultant ischemic tissue damage. Inflammatory cell adhesion molecules, chemokines, and cytokines have all been implicated in the pathogenesis of damage. Following transient and permanent MCAO, pro-inflammatory cytokines such as interleukin (IL)-1β and IL-6 act upon the vascular endothelium to increase the expression of ICAM-1, P-selectin, and E-selectin, which promote leukocyte adherence and accumulation.[5] It has been shown that application or overexpression of the IL-1β receptor antagonist, IL-1rα, reduces infarct size[49] and blockage of IL-1β converting enzyme reduces brain injury through decreased formation of IL-1β[50].

In addition, cell surface receptors called integrins are activated and mediate intracellular inflammatory signals. These inflammatory signals promote leukocyte migration across the endothelium and mediate inflammatory cascades resulting in further cerebral damage. There is also an accumulation of neutrophils, which are phagocytotic white blood cells, in infarcted tissue

24 h after permanent or temporary focal ischemia[51]. Neutrophils have been observed within the vessels and the parenchyma of ischemic brain after reperfusion[52]. Depletion of neutrophils from the circulation using anti-neutrophil antibodies reduces the brain injury associated with ischemia and reperfusion[53], suggesting a causative, but minor, role for neutrophils in brain injury. Further investigation of the underlying mechanisms of inflammation may play an important role in the development of therapeutic treatment of stroke.

D. Post-Ischemic Translation Arrest

In 1971, Kleihaus and Hossmann discovered that during reperfusion, protein synthesis was inhibited, in spite of return of normal ATP levels[54]. This post-ischemic translation arrest (TA) has proven to be an important observation. Subsequently research established that: (1) TA occurs in all post-ischemic brain regions for at least several hours[1], (2) translation recovers in surviving brain regions, but not in regions that will die by DND, and (3) the TA appeared to involve a defect at the initiation stage of translation[1].

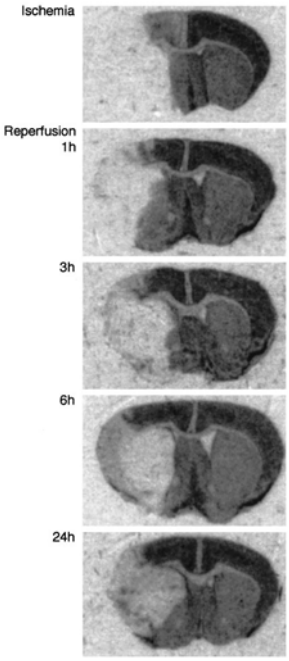

Figure 1 : TA after focal ischemia and reperfu-sion. Image from[2].

Figure 1 illustrates TA following focal ischemia induced by MCAO in a study conducted by Dr. Wulf Paschen[2]. In this study, following 2 hr MCAO and durations of reperfusion indicated in the figure, animals were administered radioactive amino acid, and autoradiograms prepared. Following ischemia, the ipsilateral hemisphere showed no protein synthesis in the MCA territory. In the penumbral area of cerebral cortex, a slight recovery occurred at 6 hr reperfusion, but by 24 hr reperfusion, the recovery was not sustained and incorporation was lower than the 6 hr time point. The core lesion in the basal ganglia never recovered translation because the cells were necrotic. But significantly,

translation never recovered in the cortical penumbra and these neurons subsequently died.

VI. Translation Arrest and Brain I/R

For many years, TA was considered a damage mechanism induced by I/R injury. However, continued work in this area has caused a shift in this viewpoint. Instead of being seen as a damage mechanism, TA is now recognized as a marker of protective intracellular stress responses, and the persistent TA that correlates with cell death is considered a symptom of a dysfunctional stress response on the part of post-ischemic neurons. What I will do in this section is first, discuss what has been discovered about the causes of TA during I/R, and then discuss how these discoveries have linked post-ischemic TA with neuronal stress responses. I will discuss the role of TA in the general response of cells to exogenous stressors. These ideas will provide the basis for the dissertation work I proposed.

Most studies conducted on TA following I/R have used global ischemia models. Therefore most of the evidence I will discuss will be based on global models. TA has been less studied in focal models, and the experiments I will propose will be aimed precisely at clarifying mechanisms of TA after focal ischemia, with and without diabetes.

A. Translation Initiation

Kleihaus and Hossmann[54] in 1971 showed in their seminal study that polysomes dissociated immediately with the onset of reperfusion and that protein synthesis was inhibited. Because it was known even then that polysome dissociation was a marker of inhibition of translation initiation, these authors inferred that translation initiation was inhibited in the reperfused neurons. Much subsequent research investigated translation initiation following I/R so I will now explain translation initiation.

Protein translation consists of three steps; initiation, elongation, and termination. More than a dozen globular protein initiation factors are involved in the initiation step, working in

concert to promote the binding of mRNA, the small 40S ribosomal subunit, the large 60S ribosomal subunit, and the methionine-conjugated initiator tRNA. After the formation of the initiation complex, initiation factors dissociate and elongation factors are recruited to allow the ribosome to move on the mRNA in the 5' → 3' direction, by which the mRNA sequence is translated into a primary protein sequence. A critical aspect of the elongation phase is the binding of chaperone proteins to the nascent peptide, which help it to fold into its mature three-dimensional tertiary conformation. The termination step takes place when a special tRNA binds to a stop codon on the mRNA, signaling elongation termination and dissociation of the nascent peptide.

There are two rate-limiting steps in translation initiation that serve as almost universal regulatory targets, from bacteria, through yeast, to complex metazoans including humans. These steps involve eIF2, which delivers the charged initiator tRNA and eIF4, which delivers the mRNA to the 40S subunit. eIF4F is a heterotetramer, consisting of eIF4E, eIF4A, eIF4B, and eIF4G subunits[55]. eIF4E binds the 5' m7-G cap of the mRNA. eIF4A is a helicase that, in association with its cofactor eIF4B, unwinds the secondary structure of the mRNA, allowing the ribosome to scan the mRNA. Finally, eIF4G is a scaffold protein, providing a surface on which many of these binding interactions occurs[56]. eIF4 is controlled by several concurrent mechanisms[55] and the main result of eIF4 regulation is to control which mRNAs get translated.

eIF2 determines the global rate of protein synthesis and contributes to the initiation of protein translation by forming a ternary complex with GTP and Met-tRNA. Binding of the ternary complex to the small 40S ribosomal subunit forms the 43S preinitiation complex. Addition of the mRNA-eIF4 complex forms the 48S preinitiation complex. Once initiation is completed, the 60S large ribosomal subunit joins, and hydrolysis of eIF2-GTP to GDP occurs, followed by the dissociation of eIF2 from the completed ribosomal 80S complex. The exchange

of GDP bound to eIF2 for GTP is mediated by eIF2B, a guanine nucleotide exchange factor, and is a crucial step for the recycling of eIF2. This is important because eIF2-GDP cannot bind the methionyl charged initiator tRNA to form the ternary complex and prepare eIF2 for another round of initiation. Thus, the quantity of available eIF2B is the rate-limiting factor for normal rates of translation initiation.

Phosphorylation of the alpha subunit of eIF2 causes a decrease in total protein synthesis rate. Mechanistically, when the alpha subunit of eIF2 is phosphorylated [eIF2(αP)], it binds eIF2B with a much higher affinity than dephosphorylated eIF2.[57] The sequestration of eIF2B by eIF2(αP) effectively removes it from the reaction cycle. This in turn results in an accumulation of eIF2-GDP that is not able to form the ternary complex and leads to the subsequent stalling of ribosomes during initiation, while awaiting delivery of the initiator methionine.

There are two established mechanisms of eIF4F regulation: (1) by phosphorylation of eIF4E, which increases its affinity for eIF4G, thereby increasing the formation of the eIF4 complex[58] and (2) by 4E binding proteins (4EBPs), when dephosphorylated, compete with eIF4G for binding to eIF4E, preventing the formation of eIF4[56]. eIF4G regulation is not well understood, but what is known is that following infection with a picornavirus, eIF4G is degraded[59]. The main effect of decreasing available eIF4 is a quantitative shift in which types of mRNA are translated and a net decrease in protein translation[59].

Fragmentation of eIF4G disables 5'-capped mRNAs to be delivered to the ribosome; however uncapped viral mRNAs contain special nucleotide sequences in their 5' untranslated regions known as an internal ribosome entry site (IRES). The IRES allows cap-independent translation of viral mRNAs[60]. In addition, degradation of eIF4G via caspase-3 proteolysis occurs during apoptosis, where important apoptotic mRNAs such as the FAS receptor and DAP5 (an eIF4G homolog) contain IRES sequences[61].

B. Changes in eIF2 and eIF4 during reperfusion

Studies of translation initiation following brain ischemia and reperfusion have revealed that eIF2α is phosphorylated and eIF4G is degraded[62,63,64,65,66]. In 2004, Garcia *et al* demonstrated that eIF2α phosphorylation occurred with or without ischemic preconditioning (IPC). IPC is an exposure to a brief, nonlethal duration of ischemia followed by a lethal dose two days later.[67] Cell death does not occur when IPC is performed[68] and therefore, eIF2α(P) itself is not directly involved in DND since it occurs with or without IPC. However, degradation of eIF4G occurred only with long ischemia durations, while eIF2α(P) occurred even with the shortest ischemia durations.

Studies of eIF2α(P) showed that it is a transient and acute response. While eIF2α(P) occurs rapidly, it also dephosphorylated rapidly. Therefore, the consensus has emerged that eIF2α(P) cannot be responsible for the prolonged TA associated with DND[2,69,75,86].

Studies of eIF4 following brain I/R showed that there was no change in eIF4E, but there was degradation of eIF4G, which was greatest in the CA1 region of the hippocampus[64,70]. The main finding of studies of eIF4 subunits is the calpain-mediated degradation of eIF4G following brain I/R. It is not known at present in which cell types changes in eIF4G occur or the significance of the changes in eIF4G. As cell death can be induced in global models without degradation of eIF4G[72,102], its degradation cannot be considered essential to DND in global models.

C. Mechanisms of Prolonged Translation Arrest

To try to discover the cause of the persistent TA, recent work has studied mechanisms of TA other than the regulation of translation initiation. There are two main models and both share the common idea that translational machinery is sequestered into molecular complexes that cannot perform protein synthesis. These models are called cotranslational aggregation and the

ribonomic dysfunction models.

1. Cotranslational Aggregations

The first model is called cotranslational aggregation proposed by Dr. Hu's laboratory[71-72]. Extensive studies on neurodegenerative diseases, such as Alzheimer's disease, Parkinson's disease, and prion-like diseases demonstrated an increase in unfolded proteins in pathological neurons[73]. An improperly folded protein, like amyloid-beta peptide precursor in Alzheimer's disease, is ubiquinated and accumulated as protein aggregates throughout the cytoplasm[73]. Ubiquination of improperly folded and non-functional proteins is a signal for transport to the proteosome and subsequent degradation. However, since the quantity of the unfolded proteins exceeds the rate at which they are degraded by the proteosomes, these abnormal proteins clump together irreversibly throughout the cytoplasm.

The basis for Dr. Hu's model of cotranslational aggregation is similar to changes seen in chronic neurodegenerative disorders. Studies from the Hu lab showed that two types of ubiquinated particles accumulate in post-ischemic neurons[74,71]. The first particle was termed "ubi particles" because it was cytoplasmic, relatively large (diameter ~ 1 micron) and contained ubiquitin. Ubi-particles are visible under the light microscope, forming in all post-ischemic neurons immediately with reperfusion. However, the ubi-particles disappear from resistant areas by 24 hr reperfusion, but persist in the ischemic vulnerable CA1 in an altered form. The second particle, termed protein aggregates (PAs), is visible only under the electron microscope and was roughly 200 nm in diameter. PAs persisted in the soma and dendrites of CA1 neurons after 24 hr reperfusion, but were absent in resistant neurons, such as the dentate gyrus. Later studies from Dr. Hu's lab investigated the composition of PAs[75]. Proteins that were shown to accumulate in the PAs were: (1) initiation factors, such as subunits of eIF2 and eIF4, (2) protein folding chaperones such as HSC70, and (3) proteins that make up the 40S ands 60S ribosomal subunits

such as ribosomal protein S6. Therefore, the composition of the PAs suggested they were involved in prolonged TA by sequestering components needed for translation. Further, that PAs occurred only in ischemic vulnerable neurons such as CA1 was an unambiguous correlation with the time course of persistent TA and DND, something that has not been demonstrated to this point when only changes in initiation factors have been studied.

Based on this evidence, Dr. Hu has proposed the following model of cotranslational aggregation for prolonged TA in post-ischemic CA1 neurons. He proposes that I/R cause misfolding of nascent peptides during the process of translation elongation. These then: (1) become targets for ubiquination, and (2) clump together. When the misfolded nascent peptides clump together, they also draw the ribosomes into the aggregates of misfolded proteins, thereby sequestering ribosomes. This process is what is meant by the term "cotranslational aggregation". Cotranslation aggregation provides an alternative pathway, other than eIF2α phosphorylation, that could potentially explain why there is irreversible prolonged TA in reperfused neurons destined to DND.

Although there is good evidence to support this model, it has two main weaknesses. The first is quantitative. The total amount of translational components that get sequestered in the PAs is ~ 10-15% of ribosomal components, and ~ 35% of co-translational chaperones. PAs have not been shown to quantitatively sequester any single translational component[69]. A second weakness of this model is that it does not take into account the regulatory changes in initiation factors that were described above, namely the phosphorylation of eIF2α and the degradation of eIF4G. We now develop our main ideas of an alternative model for prolonged TA.

2. Ribonomics

This model is the working model we use in our laboratory and is the outcome of work in Dr. DeGracia's lab over the past ~7 years. Unlike Dr. Hu's model, the ribonomic dysfunction

model takes into account the changes in translation initiation that have been identified by Dr. DeGracia, Dr. Burda, Dr. Paschen and other investigators over the past years[2,63,65,]. Before explaining the ribonomic dysfunction model, I will first define the term ribonomic.

The term "ribonomic" is similar to the idea of genomic or proteomic, in that it refers to a total complement of mRNAs in the cell at any given instant. There is more to this idea however. The idea is meant to capture the fact that there are many layers of regulation of the cellular mRNAs that begin from the point of mRNA transcription and continue to the point an mRNA is ultimately degraded in the cytoplasm. In between, an mRNA molecule undergoes complex patterns of localization and regulation via a large number of binding partners. Therefore, the idea of ribonomic refers to the regulatory interactions of mRNA molecules with either proteins or microRNAs[76].

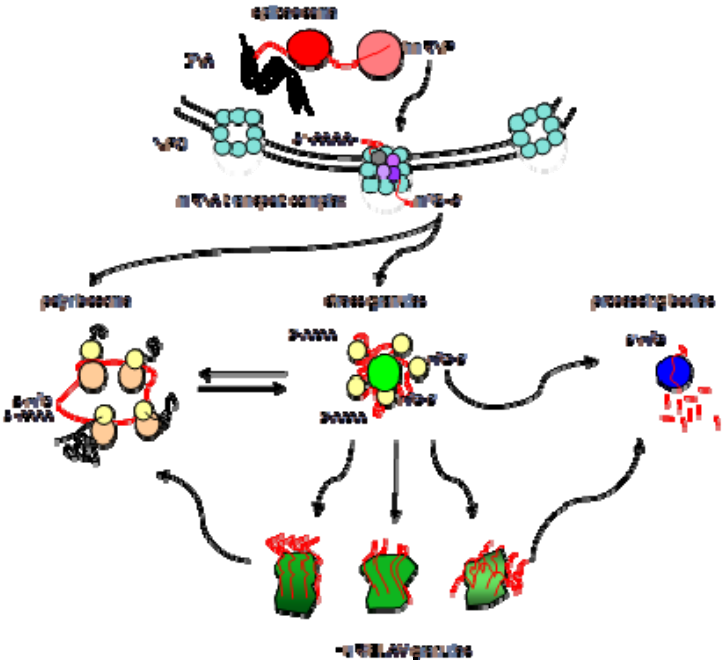

Figure 2. The ribonomic network.

An important aspect of the cellular ribonome is that mRNAs undergo very specific subcellular localization via a number of structures that have been identified to be involved in mRNA function (Figure 2). The known structures in the nucleus are the splicesome and the mRNA nuclear transport complex. In the cytoplasm, the structures that localize mRNAs are stress granules (SGs), processing bodies, HuR granules, and polysomes. Each of these structures plays a role in mRNA function. Stress granules are like a train station and route mRNAs

amongst the other ribonomic structures[77]. Processing bodies are the particles that degrade mRNAs, and in this regard are similar to what the proteosome is to proteins[78]. Polysomes are now viewed as one of these mRNA control particles[69], and these are where the genetic information coded in an mRNA gets converted to protein. HuR granules are structures that are thought to bring functionally related mRNAs together to carry out complex genetic programs[79,80]. Dr. Jack Keene, one of the leaders in studying HuR granules, invented the idea of "mRNA operons"[81]. Similar to bacterial operons, in which several genes with a coordinated function are translated at the same time, the mRNA operon is the HuR granule that brings together functionally related mRNAs so that they may be acted upon at the same time in eukaryotic cells. This action may involve coordinated translation, coordinated silencing (e.g. the mRNAs are present but not translated), or coordinated degradation (by routing the groups of mRNAs to processing bodies for degradation).

VII. The Ribonomic Model and Brain I/R

The ideas surrounding the concept of ribonomic regulation of mRNA offers new insights into possible mechanisms of persistent TA following brain I/R. Since the seminal work of Kleihaus and Hossmann[54] the field has been focused on changes in ribosomes as the cause of TA. However, mRNA is just as important to protein synthesis as ribosomes are, and there has been a relative neglect in the field at understanding changes in mRNA and its regulation, and its possible role in TA.

There are many, many studies in the field looking at the changes in specific mRNAs following I/R, either by in situ hybridization or PCR. But there are only two papers that looked at global changes in mRNAs following I/R. Maruno & Yanagihara[82] showed a decrease in total mRNA in reperfused CA1 compared to other brain regions. A decrease in mRNA would contribute to TA. Matsumoto *et al*[83], showed, using gradient centrifugation, that there was a

change in the subcellular fractionation of mRNAs in vulnerable neurons following ischemia[83]. The interesting point here is that, if there are indeed major changes in mRNA following brain I/R, such as could be envisioned looking at the ribonomic network, then this brings into question the interpretations of all of the many studies that have evaluated individual mRNAs. To date, there has only four studies that looked at the ribonomic network, and these have all been carried out in Dr. DeGracia's lab[101-102]. I will now review these studies.

A. SGs in Reperfused Neurons

In 2005, Kayali *et al*. evaluated SGs in rat hippocampal formation using the cardiac arrest and resuscitation model of global brain ischemia[101]. SGs are known to form following phosphorylation of eIF2α when cells undergo stress[77]. SGs have been shown to function to move mRNAs around the cell into other ribonomic structures where the most focus to date has been the movement of mRNAs from polysomes to processing bodies[84]. Since eIF2α phosphorylation was a well established change in reperfused neurons[65], Kayali *et al* hypothesized that there might be a difference in SGs between resistant (e.g. CA3) and vulnerable (CA1) post-ischemic neurons. This hypothesis linked to what was already a well-established fact of reperfused neurons, unlike Dr. Hu's model of cotranslational aggregation.

A 10-minute global brain ischemia was induced by cardiac arrest followed by reperfusion durations of 10 min, 90 min, or 4 hours. Double-labeling immunofluorescence (IF) for two SG components, S6 and TIA-1, was used for evaluation. SGs in resistant regions, such as CA3, hilus, and dentate gyrus (DG) increased at 10 min reperfusion and returned to control levels by 4 hr reperfusion (4hR), however, this was not the case in vulnerable CA1. At 4hR, S6 was solely localized within SGs only in CA1 pyramidal neurons. This study led to the conclusion that prolonged TA in reperfused CA1 pyramidal neurons was due to loss of the 40S ribosomal subunits and the complete sequestration of the remaining 40S ribosomal subunits in SGs at a

time when eIF2α(P) has dephosphorylated substantially[85]. This conclusion related SGs and the persistent TA in CA1 to the acute phase of TA mediated by eIF2α phosphorylation[86]. It also provided a mechanism of the continued inhibition of protein synthesis in reperfused CA1 pyramidal neurons after eIF2α had been dephosphorylated.

B. Problems with the SG Mechanism

The main limitation of the Kayali *et al* study was that it looked only to 4 hr reperfusion, which is well before the time of DND at ~ 72 hr reperfusion[101]. This was a technical limitation due to the difficulty of keeping rats alive for longer durations following cardiac arrest and resuscitation. Following cardiac arrest, rats experience severe peripheral organ damage, which was studied by Dr. Montie[87-88]. Because of these limitations the cardiac arrest model was unsuitable for studying longer reperfusion durations to assess the role of SGs in neuronal death.

The experiment was repeated with a different model of global ischemia, the bilateral carotid artery occlusion plus hypovolemic hypotension model (2VO/HT) of Smith *et al*[89]. This model does not cause peripheral organ damage, so animals can be reperfused for any duration. When 10 min of ischemia was applied with the 2VO/HT model, although CA1 death occurred at 72 hr reperfusion, there was no loss of S6 or sequestration of S6 in SGs at 4 hr reperfusion[69]. That S6 sequestration in SGs did not occur at 4 hr following 2VO/HT indicated that the SG mechanism of prolonged TA was not general. In the 2VO/HT model, the number of SGs increases similarly in both CA1 and CA3: there was a transient increase at 10 min reperfusion which returned to control levels for the remainder of reperfusion[69].

In the 2VO/HT model, DeGracia *et al*[90] showed that SGs eventually fuse with protein aggregates, showing that Dr. Hu's model and Dr. DeGracia's model were not only compatible, but that the mechanisms converged. However, even in this case, there was not a wholesale sequestration of any tested ribosome component in the SG/PA hybrid particles.

Dr. Hu performed a study of protein aggregates following stroke[75], and in this study stained brain slices for ribosomal protein S6. He showed a loss of S6 staining similar to that observed in the cardiac arrest model in the Kayali *et al* study[101]. However, SGs were not evaluated in this study. It is of interest to note the loss of S6 staining in the Liu *et al* study because below, in our results with Long Evans rats, we show that of the 14 antigens stained for following focal ischemia, all 14 showed loss of staining in the core region.

C. mRNA Granules

In a second ribonomic-oriented study using the cardiac arrest model, DeGracia *et al* [91], immuno-mapped eIF4G following global brain I/R. Here it was observed that in the cytoplasm of reperfused neurons, the eIF4G staining took the form of granular "clumps". This paper suggested that the eIF4G "clumps" might represent degradation products of eIF4G, or possibly that eIF4G had been sequestered in the form of the ubi-protein complexes identified by Dr. Hu's laboratory.

In recent work from our lab, in which I participated, we used fluorescent *in situ* hybridization (FISH) to visualize poly-adenylated mRNAs (pA) in reperfused neurons using a poly(T) probe[102]. We also performed colocalization studies of pA with a number of antigens by double staining with pA FISH and immunofluorescent histochemistry (IF).

Figure 3 Figure 3shows the main result of this study. We observed the pA staining in non-ischemic controls (NIC) as diffuse in the cytoplasm. However, with reperfusion, the pA also took the form of granular "clumps" in the cytoplasm, very similar to what was observed with eIF4G in the DeGracia *et al* (2006)[91] study. The granulated form of mRNA in the cell cytoplasm we termed "mRNA granules".

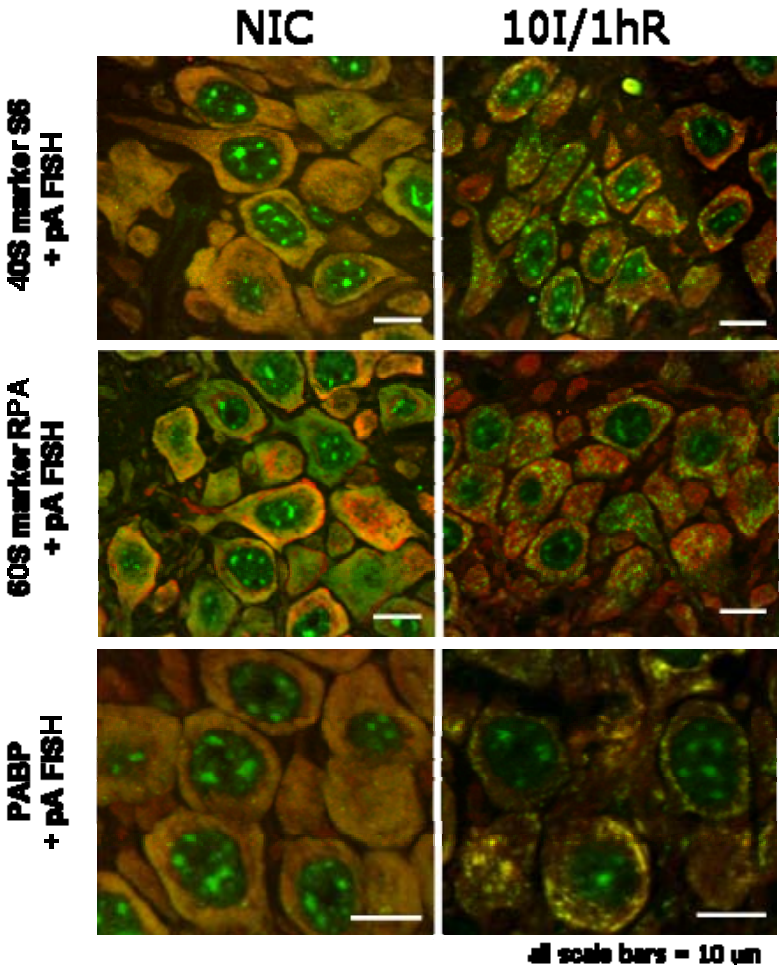

Figure 3 : Detection of mRNA granules by pA FISH and co-IF for 40S, 60S and PABP. Left, non-ischemic controls (NIC) where the pA and proteins had a "smooth" and relatively homogeneous staining pattern in the cell cytoplasm. Right: following 10 min global brain ischemia and 1 hr reperfusion, the pA staining patterned formed granular structures, the mRNA granules. The mRNA granules did not colocalize with markers of the 40S and 60S ribosomal subunits, but did colocalize with pA-binding protein (PABP). Images adapted from [102].

In the Jamison *et al* (2008)[102] study, the mRNA granules colocalized with eIF4G indicating that the eIF4G granulation reported in the DeGracia *et al*., (2006)[91] study were not degradation products, but were eIF4G localized in the mRNA granules. The mRNA granules did not colocalize with TIA-1, proving they were not SGs. They did not colocalize with TTP, a marker of processing bodies[92], proving they were not processing bodies. The mRNA granules did colocalize with HuR, and we therefore believe that the mRNA granules are the HuR granules discussed above, which have been described and studied by the Keene Laboratory.

Most significantly, as shown in Figure 3, when double labeling for pA and S6, a marker of the 40S ribosomal subunit, or pA and ribosome P antigen, a marker of the 60S subunit[93], was performed, the mRNA granules did not colocalize with either antigen. That is, the mRNA

granules did not colocalize with either the 40S or 60S ribosomal subunits. On the other hand, as shown in Figure 3, in non-ischemic controls, pA/S6 and pA/RPA strongly colocalized in the form of a diffuse cytoplasmic staining. The Jamison *et al*[102] study also evaluated in vivo translation after administration of radioactive amino acids. The result was obtained that every reperfusion time point in which neurons showed the presence of the mRNA granules also showed inhibition of in vivo protein synthesis. Therefore, we now believe that the mRNA granules sequester mRNAs away from ribosomes, and that this provides a second mechanism, in addition to the cotranslational aggregation model of Dr. Hu, of prolonged TA in reperfused CA1 neurons.

In fact, on the basis of the pA staining patterns presented in the Jamison *et al* study, it appears that the pA signal is quantitatively present in the mRNA granules. This then is the first observation of any change in a translational component that: (1) correlates precisely with the full time course of TA, and (2) represents a quantitative transformation that would mechanistically explain the prolonged TA during reperfusion.

VIII. Summary and Hypothesis

To summarize the main points of the background, above it was discussed how a prolonged TA correlates exactly with the DND of neurons following both focal and global brain ischemia. Many different mechanisms of prolonged TA have been tested. Changes in ribosome regulation occur mostly at the early reperfusion time points and do not explain the prolongation of TA. Some percent of ribosome components get sequestered in PAs, which can contribute to prolonged TA, but cannot fully explain it. To date, the only observation of changes in the translational system that is both apparently quantitative and correlates precisely with the time course of TA is the observation of mRNA granules following global brain I/R. It is currently unknown if a similar sequestration of mRNA away from ribosomes occurs following focal brain

I/R, leading therefore to the main hypothesis of my Dissertation:

Hypothesis 1 : Focal brain ischemia causes sequestration of mRNA away from ribosomal subunits.

Above it was also discussed how diabetes worsens outcome following brain I/R. To the best of my knowledge, and after a thorough literature review, the translation system in the reperfused brain of diabetics has not been studied. Since TA correlates precisely with cell death, and cell death is increased in diabetics, I therefore offer the second main hypothesis of my dissertation:

Hypothesis 2 : Diabetes worsens the TA associated with focal ischemia to increase the amount of cell death.

IX. Factors Affecting Experimental Designs

The above hypotheses will be tested by the following experimental strategies.

1) Determine the formation of mRNA granules in the focal ischemic brain, with and without diabetes.
2) Correlate the extent of mRNA granule formation with the extent of brain cell death in the focal ischemic brain.

The methods utilized to carry out these experimental strategies included (1) an animal model of focal brain ischemia based on MCAO, (2) an animal model of diabetes using streptozocin (STZ)-induced destruction of pancreatic beta cells, (3) the use of standard staining methods to determine the extent of necrotic infarcts by the lack of brain slice staining with the compound 2,3,5 triphenyltetrazolium chloride (TTC), and (4) detection of pA mRNAs via fluorescent in situ hybridization, and a determination of their colocalization with a variety of protein antigens via immunofluorescent histochemistry. Before proceeding to Methods and Results, some further rationalization of the Experimental Designs is in order.

A. Transient or Permanent Focal Brain Ischemia.

Below we describe the use of the MCAO model of focal brain ischemia. Unlike the global ischemia models used routinely in the lab, MCAO results in an incomplete ischemia, meaning that cerebral blood flow is never reduced to zero. Even during the ischemic period in which the filament blocks the MCA, the remainder of the brain blood flow is normal and intrinsic brain and vascular reflexes are activated to enhance blood flow to the MCA territory via collateral anastomoses, creating a complex and only partially understood blood flow gradient[124]. Thus, blood flow in the occluded territory during the ischemic period of MCAO can range from between 20-50% normal[117], which itself is animal strain dependent (see below).

In contrast, with models of global brain ischemia, there is a discreet and well-defined period of zero blood flow (the ischemic period) followed by discreet periods of reperfusion. Also, the onset of ischemia and subsequent onset of reperfusion are often rapid. Thus, the ischemic insult with global models can be thought of as a square wave. But a similar logic does not hold for the MCAO focal model.

These considerations are important with respect to the translational system as follows. In global models, where blood flow is zero during ischemia, intracerebral ATP levels also go to zero, and ATP dependent processes come to a halt. The phosphorylation of the alpha subunit of eIF2 requires ATP as a substrate. Thus, in global models of brain ischemia there is no phosphorylation of eIF2α during the ischemia period[64]; this phosphorylation event occurs within the first minutes of reperfusion after ATP levels have increased enough to allow it to proceed. On the other hand, in a study by Wulf Paschen's lab, the levels of eIF2α(P) were observed to be at their *maximum* at the end of a 2 hr period of MCAO[2]. During the subsequent reperfusion period the levels of eIF2α(P) decreased from this maximum and returned to pre-ischemic

(control) levels by 6 hr reperfusion. Thus, the focal case is much different from the global case with respect to the phosphorylation of eIF2α, which is a key event in the regulation of translation in neurons following I/R.

Therefore, the logic of our study design is different from a typical study using a global ischemia model that would use a fixed time of ischemia (usually 10 min) followed by a time course of reperfusion. Because the "ischemic" period in an MCAO model is actually a complex mix of ischemia and reperfusion occurring in the same brain, the main focus of the studies we shall describe involve what is (perhaps not so accurately) called "permanent" focal ischemia, in which we will evaluate increasing durations of MCAO. We feel this is a necessary set of studies to perform before any attempt to perform a fixed value of ischemia followed by increasing durations of reperfusion, or what is commonly referred to as "transient" MCAO. The use of transient MCAO for the major studies reported here (e.g. those involving the Long Evans rat strain described in Chapter 3) was used primarily to validate the model by demonstrating production of a necrotic infarct.

B. Rat Strain Effects following MCAO

There is a substantial literature showing differences in outcome amongst different strains of rodents, specifically with the MCAO model[94]. For example, a study by Prieto *et al* (2005)[117] showed statistically significant differences in cerebral blood flow during the MCA occlusion period in different rat strains. In this study, Wistar showed the highest blood flows (average ~ 50%), Sprague Dawley was intermediate (average ~ 38%), and Long Evans showed the lowest blood flows (average ~ 28%). Why different strains demonstrate different blood flows is not a topic we study here. But it is a factor we attempt to account for by performing our studies on two different rat strains: Wistar and Long Evans. By using the Wistar strain, we can compare our results to previous studies of the effect of diabetes after MCAO[95,96,104]. By using the Long

Evans strain, we can compare our results to the reported studies of the translation system and the mRNA granulation process in post-ischemic brain[64-65,90,101-102].

C. Effect of Anesthetic on Outcome from MCAO

The effect of anesthetic on outcome following brain I/R is a highly researched area. Hundreds of published studies have reported that anesthetics can affect outcome either to the positive or negative. It is interesting to note, however, that, as with every other agent that has shown laboratory neuroprotection, the ostensible neuroprotective properties of anesthetics has no bearing at all on clinical anesthesia in a practical clinical setting[97]. The common inhalation anesthetic halothane was used for the majority of studies reported here. However, in my initial work with the Wistar strain, some experimental groups were performed using the also common combination of the dissociative anesthetic ketamine and the muscular relaxant xylazine. I report these results below even though no significant differences were observed.

X. Overview of Experimental Plan

Given the above considerations, the overall experimental plan is illustrated in Figure 4. The general plan was that experimental groups were performed, from which tissue slices were made and then stained to detect either the infarct (TTC) or molecular markers. Specific designs and analytic methods are reported in subsequent chapters. The different experimental groups are illustrated schematically in Figure 4 and broken out into three categories: (1) animals strain (Wistar vs. Long Evans), (2) type of focal ischemia (transient vs. permanent), and anesthetic used (ketamine/xylazine (K/X) vs. halothane). The main experimental groups, all of which used halothane anesthetic are listed in Table 1. The following chapters describe the Methods and Results as follows: Chapter 2 describes the Wistar strain studies; Chapter 3 describes studies with untreated Long Evans rats, and Chapter 4 describes the studies with diabetic Long Evans rats. Chapter 5 will then discuss the integrated results.

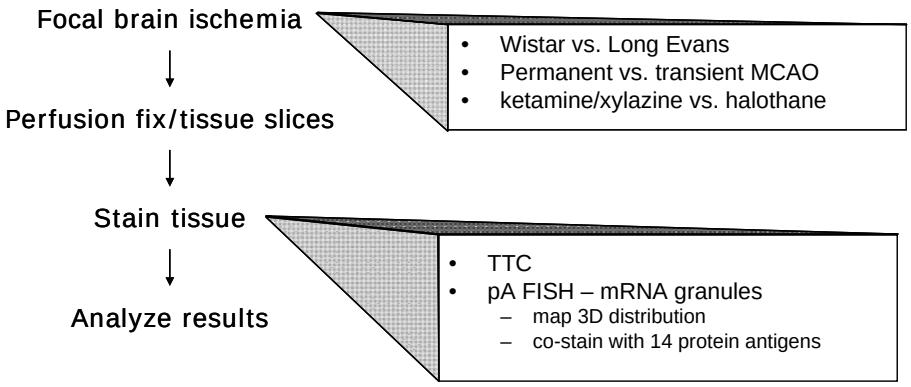

Figure 4: Overview of Experimental Designs

Table 1: Experimental Groups Overview, including number of animals per group (n).

Strain	Ischemia	Reperfusion	Group name
Wistar	2 hr	-	2I
(n = 3/grp)	2 hr	4 hr	2I/4R
	2 hr	24 hr	2I/24R
	2 hr	7 days	2I/7dR
Long Evans	2hr	-	2I
(n = 5/grp)	2hr	24 hr	2I/24R
	4 hr	-	4I
	6hr	-	6I
	8hr	-	8I
Long Evans	0.5 hr	-	0.5I
Diabetic	1hr	-	1I
(n = 4/grp)	4 hr	-	4I
	6hr	-	6I

CHAPTER TWO: Studies on Wistar Strain - Methods and Results

I. Rationale

Since my 2nd major hypothesis sought to evaluate the effect of diabetes on the translation components, I began my work by evaluating the Wistar rat strain so I could compare to previous studies of diabetes and focal brain ischemia[95,96,104]. Specifically, the 2005 study of Rizk, Rafols and Dunbar[104] provided the starting point for my investigations. This study showed that 2 hr transient MCAO plus 24 hr reperfusion did not generate an infarct in non-diabetics but that diabetic animals showed a large infarct at this same end point, and that neurons of the diabetic brains showed substantial activation of apoptotic pathways *before* the application of MCAO. I therefore sought to evaluate the same time course of MCAO with and without diabetes. The intent of the studies described in this Chapter was to first establish a baseline of mRNA granule formation along a time course of transient MCAO in non-diabetic Wistar rats, and then repeat the studies using diabetic animals.

To briefly summarize the results of the studies in Wistar rats, I was unable to detect mRNA granules at any time point of reperfusion, out to 7 days. Instead, I observed only a very minor formation of mRNA granules at the 2 hr ischemia-only time point. We considered that the negative result may have been due to two factors. First, it may be been an anesthetic effect. Second, we considered that at 2 hr MCAO, the small number of mRNA granules detected reflected either the beginning or end of a time course, and that more mRNA granules might be identifiable at either earlier or later ischemia durations. I therefore conducted a series of studies, shifting from halothane to K/X, and also evaluating various durations of ischemia. The results of these studies were also essentially negative. Although mRNA granules were sporadically detected in the 2 hr MCAO + K/X group, their frequency was not apparently different from the halothane group. In general, the frequency of mRNA granules was much lower than would have

been expected from our experience with the global brain ischemia model[102].

Being unable to establish a baseline of mRNA granule formation, studies of diabetes in the Wistar strain were not conducted. It is for these reasons I turned to the Long Evans strain and those studies are described in Chapters 3 and 4. Here I report my observations of low frequency mRNA granule formation in the Wistar strain neurons. Because the frequency of mRNA granule formation was so low in the Wistar strain, there is not a comprehensive analysis such as described for the Long Evans strain in Chapter 3. Additionally, because of the link between TA and stress responses, I stained to determine if the Wistar rats translated HSP70 protein during the reperfusion time course.

II. Materials

HuR primary antiserum was purchased from Santa Cruz Biotechnology, Inc (Santa Cruz, CA). Rabbit polyclonal anti-PABP was purchased from Abcam (Cambridge, MA). Mouse monoclonal ribosomal protein S6 was purchased from Cell Signaling (Danvers, MA). HSP70 antiserum was from Stressgen (Ann Arbor, MI). Alexa FluorR 488 donkey anti-goat IgG, Alexa FluorR 555 donkey anti-rabit IgG and Alexa FluorR 555 anti-mouse IgG, used for IF histochemistry were purchased from Molecular Probes (Eugen, OR). A 5' biotinylated 50-mer oligo-dT probe used for FISH was made by Integrated DNA Technologies, Inc. (Coralville, IA). Prehybridization and hybridization buffers were obtained from the mRNA locator In Situ Hybridization Kit (Ambion, Austin, TX). TTC was purchased from Sigma-Aldrich (St. Louis, MO).

III. Methods

A. Animal Model

All animal experiments were approved by the Wayne State University Animal Investigation Committee and were conducted following the *Guide for the Care and Use of*

Laboratory Animals (National Research Council, revised 1996). Every effort was made to minimize animal suffering and the total number of animals used. Unilateral focal brain ischemia was induced in male Wistar rats (weight 275-300g; Harlan, Indianapolis, IN) using the MCAO intraluminal suture model of Hatashita *et al*[98]. The experimental groups, anesthetic, and number of animals per group is shown in Table 2:

Table 2: Experimental groups and anesthetic for studies of Wistar rat strain.

Experimental group	anesthetic	n	Ischemia duration	Reperfusion duration
2I	halothane	3	2 hr	0
2I/4R	halothane	3	2 hr	4 hr
2I/24R	halothane	3	2 hr	24 hr
2I/7dR	halothane	3	2 hr	7 days
0.5I	K/X	3	½ hr	0
1I	K/X	3	1 hr	0
1.5I	K/X	3	1 ½ hr	0
2I	K/X	3	2 hr	0
4I	K/X	3	4 hr	0

Anesthesia was initiated with either a single intraperitoneal (IP) injection of 0.25 ml/kg and 0.8 ml/kg K/X or 5 % halothane and maintained with 1.5 % halothane via facemask for the duration of the surgery. Animals were supine and core body temperature was maintained at 37 ± 0.5˚ C by a homeostatic blanket system (Harvard Apparatus) using a rectal thermometer. Rats were maintained normothermic during the entire surgery period. After shaving the cervical region and cleansing the area with betadine, a midline cervical incision was made in order to expose the omohyoid and sternomastoid muscles, which were separated using a retractor to expose the right common (CCA) and its bifurcation. The right CCA was dissected free of surrounding tissue and nerves. All branches of the external carotid artery (ECA) were isolated and coagulated. The CCA was clamped using a vascular clip and the internal carotid artery (ICA) was isolated and also clamped. Under an operating scope, a small cut was made in the ECA and a nylon filament ~ 18.5 mm in length was inserted into the CCA and secured. The

vascular clip was then removed from the ICA and the stump of the ECA was transected in order to facilitate maneuvering of the nylon filament into the ICA. The filament was carefully passed up into the lumen of the ICA, blocking the MCA at its origin. Laser Doppler flowmetry (LDF) from the ipsilateral cortex, at a coronal level approximately 1 mm anterior to Bregma was used to confirm a reduction in blood flow. Once the LDF readings stabilized, the vascular clip was removed from the CCA and all incisions were closed. Rats were then returned to their cages and allowed to recover. Upon regaining consciousness, rats displayed paresis of the left forelimb and unilateral circling.

B. 2,3,5 Triphenyltetrazolium Chloride Staining

Immersion staining of TTC was used to measure tissue viability and evaluate infarct size. The principle of TTC staining relies on the oxidation of the tetrazolium salt by intact mitochondrial dehydrogenase into a red, lipid-soluble formazan, which yields the carmin red product, formazan[99]. Viable tissue therefore stains deep red, whereas infarcted (necrotic) tissues lack dehydrogenase activity and therefore do not stain. Thus, the infarcted area (white) can be easily distinguished from the surrounding intact tissues[99-100]. At the appropriate times, the rats were decapitated, the brains rapidly removed, and placed in ice cold 0.9% NaCl for 5 minutes. The brains were then sectioned into 2 mm thick coronal sections using a brain matrix and then placed in a 2% solution of TTC in 0.9% NaCl, covered and allowed to incubate for 30 minutes at 37 ˚C on a shaker. At the end of the incubation period, the sections were removed and placed in 4% paraformaldehyde (PFA) at 4˚C for post-fixing. Digital images of the brain sections were taken 48 hours later.

C. Double-labeling Immunofluorescence and Fluorescent In Situ Hybridization

At the end of the permanent ischemia or reperfusion periods, the animals were re-anesthetized and transcardially perfused with 50 ml of 0.9% sodium chloride followed by 250 ml

of 4% PFA in 0.1M PBS at a flow rate of 20 ml/min. The brains were removed and post-fixed overnight in the PFA solution at 4˚C. Using a vibratome, 50 micron slices through the anterior forebrain were obtained and stored at -20˚C in cryostat solution until used.

IF histochemistry for HSP70 was performed as follows. Brain slices were washed in 0.1M PBS for 10 minutes x4 then blocked in 10% normal donkey serum (NDS) in 0.1M PBS containing 0.3% Triton X-100 (PBS-TX) solution for 25 minutes, following by washing x3 for 10 min in 0.1M PBS. Slices were then immersed in primary antibodies in 1% NDS in PBS-TX at room temperature on a shaker overnight. The following day, slices were washed x3 for 10 min in 0.1M PBS and then incubated in secondary antibody solution, in the dark, for 2 hours and washed again x3 for 10 min in 0.1M PBS.[101] HSP70 antiserum was used at a 1:200 dilution.

Double IF/FISH was performed exactly as described previously[102] with poly-T probe at 50 ng/ml and the following primary antisera dilutions: 1:25, anti-HuR; 1:250, anti-PABP; 1:25, anti-S6. Secondary antisera dilutions in 1% NDS in PBS-TX were: 1:300, Alexa 488; 1:300, Alexa 555.

Briefly, Double IF/FISH was performed in a two stage procedure in which the FISH procedure was a modification of that described in Bessert and Skoff (1999)[103]. The first stage IF procedure was as described above. The second FISH stage was performed under low light illumination or in the dark. At the end of the IF procedure slices were mounted on lysine-coated slides. IF-stained sections were fixed in 3.6 % formaldehyde in PBS for 10 min at room temperature and then drained and blotted. Prehybridization was carried out in a box humidified with 50% formamide/4X SSC inside an incubator at 32oC for 3 hr in prehybridization buffer (mRNAlocator In Situ Hybridization Kit, Ambion, Austin, TX). Slides were then incubated overnight in the same apparatus in a solution of 50 ng/ml of a 5'-biotinylated 50-mer oligo-dT probe (Integrated DNA Technologies, Inc., Coralville, IA), dissolved in hybridization buffer

(mRNA Locator In Situ Hybridization Kit). The next day, all subsequent processing was performed at room temperature. Slides were washed x2 in 2X SSC for 10 min and then incubated in 1:500 Alexa 488-labeled streptavidin (S32354, Invitrogen, Carlsbad, California) in 4X SSC/0.1% Triton X-100 for 60 min. Slides were then washed once in 4X SSC for 10 min followed by incubation in 2X SSC/0.1% Triton X-100 containing 1: 667 of biotinylated goat anti- streptavidin (BA-0500, Vector Laboratories, Burlingame, CA) for 60 min. Slides were again washed once in 4X SSC for 10 min and then incubated in 1:667 Alexa 488-labeled streptavidin in 2X SSC/0.1% Triton X-100 for 60 min. Slides were then washed sequentially in 4X SSC for 10 min and 2X SSC for 10 min, and then coverslipped for viewing.

Slides were examined on an Axioplan 2 Imaging System (Carl Zeiss, Oberkochen, Germany) equipped with an ApoTome. Excitation at 488 nm and 568 nm, and emission at 518 nm and 600 nm were used for Alexa 488 (green) and Alexa 555 (red), respectively. Optical sectioning was performed using the X63 oil immersion objective to generate z-stacks as previously described[101]. Fluorescent micrographs shown in the figures are orthographic projections of 2.45 micron z-stacks (7 x 0.35 micron optical sections), unless otherwise stated. Validation of antisera staining was previously described[101-102].

IV Results

A. TTC staining

As a means to validate the MCAO model and evaluate infarct volume, TTC staining was performed on male Wistar rats that underwent 2 hours of MCAO followed by 4 hours, 24 hours and 7 days of reperfusion. 2 hours of MCAO did not lead to an appreciable necrotic core, at any reperfusion duration, even to 7 days reperfusion (Figure 5). This finding was consistent with previous studies conducted in this strain where no visible infarct was seen with TTC staining, following 2 hours of ischemia and 24 hours of reperfusion[104].

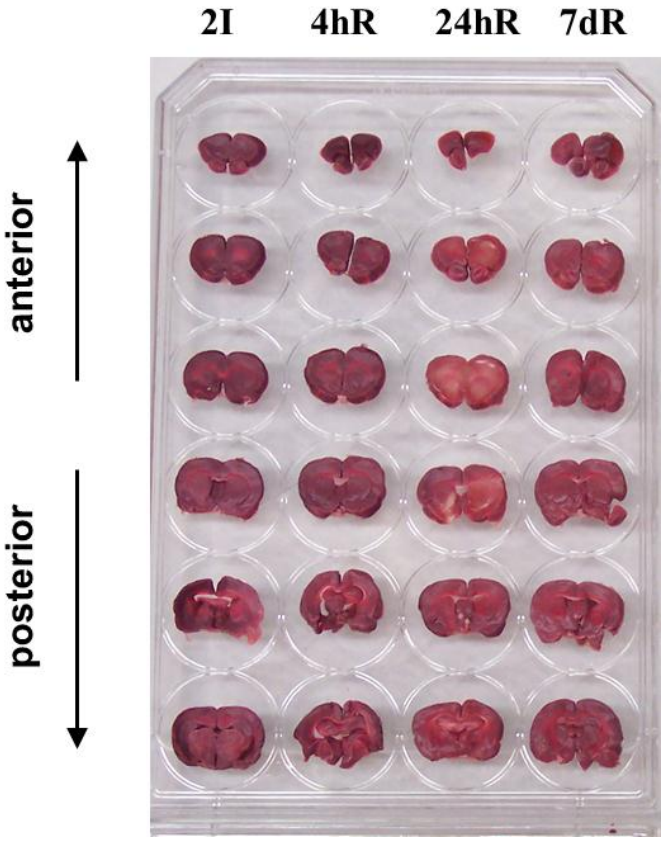

Figure 5: TTC staining of Wistar rat strain following transient focal ischemia.
Male Wistar rats were subjected to normothermic, unilateral MCAO for 2 hours of ischemia only (2I), 2 hours of MCA ischemia plus: 4 hours of reperfusion (4hR), 24 hours of reperfusion (24hR) and 7 days of reperfusion (7dR). Representative 2 mm slices arranged anterior (top) to posterior (bottom), encompassing the MCAO territory which includes the striatum.

B. Frequency of mRNA granule formation

Microscopic studies conducted to investigate whether or not mRNA granule formation took place following MCAO in the Wistar rat revealed that mRNA granules formed only at a low frequency. Granulation of mRNA was detected in only 2 of the 15 animals tested with K/X and 2 of the 12 animals tested using halothane (Table 3). Significantly, for both anesthetics, the only experimental group showing mRNA granules was the 2 hr MCAO ischemia group. mRNA granules were not detected in any reperfused samples. The use of the injectable anesthetics ketamine and xylazine or the inhalational anesthetic halothane had no effect the outcome remained the same. With respect to the experimental groups, therefore, the frequency of mRNA granule formation was 67% for both the K/X and halothane 2 hr MCAO groups, and zero for all other groups. Wistar rats, in general, have been shown to be more resistant to ischemic insults

when compared to other strains with comparable physical and physiologic parameters[105,106]. The lack of mRNA granule formation in this instance, consistent with the TTC staining result, indicates the Wistar strain did not experience a severe enough ischemic insult to induce mRNA granulation.

Table 3: Frequency of mRNA granule formation in the Wistar rat following MCAO.

Anesthetic	total n	n with mRNA granules
K/X	15	2 (13.3 %)
halothane	12	2 (16.7 %)

Animals were tested using either ketamine/xylazine (K/X) or halothane anesthesia.

C. Histological assessment of mRNA granules in Wistar rats

In spite of their low frequency of occurrence, I assessed the mRNA granules in the 2I Wistar rat group to determine if their colocalization properties were similar to that observed following global brain ischemia. In the four samples displaying neurons containing mRNA granules, these neurons were sparsely scattered in clustered areas on the ipsilateral hemisphere as shown in Figure 6. A crude estimate would put their area to be less than 5% of the total hemispheric area, and they tended to be more medially located in the ipsilateral hemisphere.

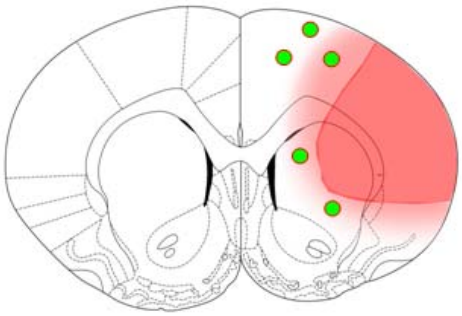

Figure 6: A rough indication of the distribution of mRNA-granule containing neurons in Wistar rats at 2hr MCAO. Green circles indicate scattered areas where the neurons showed mRNA granulation. The dark red area is where a necrotic core would be expected based on the MCA territory, and the surrounding light red area represents where penumbra is expected.

Figure 7, panels A, B and C, show photomicrographs of mRNA-granule containing neurons co-stained with pA FISH and IF for S6, PABP and HuR, respectively. For each co-staining pair, sham operated non-ischemic control (NIC) animals are shown along with the 2I samples. The first column is the merged image, the second column the pA channel (green) and the third

column is the respective red channel for the protein antigen.

Figure 7A shows pA/S6 staining in layer II cerebral cortical neurons. The NIC samples showed a smooth and homogeneous pattern of pA/S6 colocalization in the cell cytoplasm. This colocalization likely represents normal mRNA-ribosomal association during the protein translational process. Neurons in the ipsilateral region of the 2I sample formed mRNA granules that did not colocalize with S6, which is better visualized by observing the separate channels. In the pA channel there is concentration of the pA signal that is not present in the S6 channel. Compared to the results of layer II cortical staining I will show in Chapter 3, the amount of mRNA granulation in Figure 7A can be considered only partial.

A more obvious mRNA granulation was apparent in the layer V pyramidal neurons seen co-stained with PABP in Figure 7B and HuR in Figure 7C. For pA/PABP, it is again seen how the NIC showed a diffuse cytoplasmic colocalization. For the 2I sample, both the pA and PABP signal show granulation, which colocalize to form yellow mRNA granules in the merged image. For pA/HuR (Figure 7C), the mRNA granules were quite obvious compared to NIC samples. Although the merged image of pA/HuR does not produce yellow mRNA granules, it can be seen that HuR is indeed granulated in the HuR channel of the ischemic but not NIC sample.

In the Jamison *et al* (2008) study of mRNA granules in global ischemia, identical patterns were seen in which S6 did not, but PABP and HuR did colocalize with the mRNA granules. Therefore, in spite of the relatively infrequent occurrence of mRNA granules in the Wistar rat strain following focal I/R, the mRNA granules are similar to those discovered following global ischemia with regard to colocalization with these three antigens.

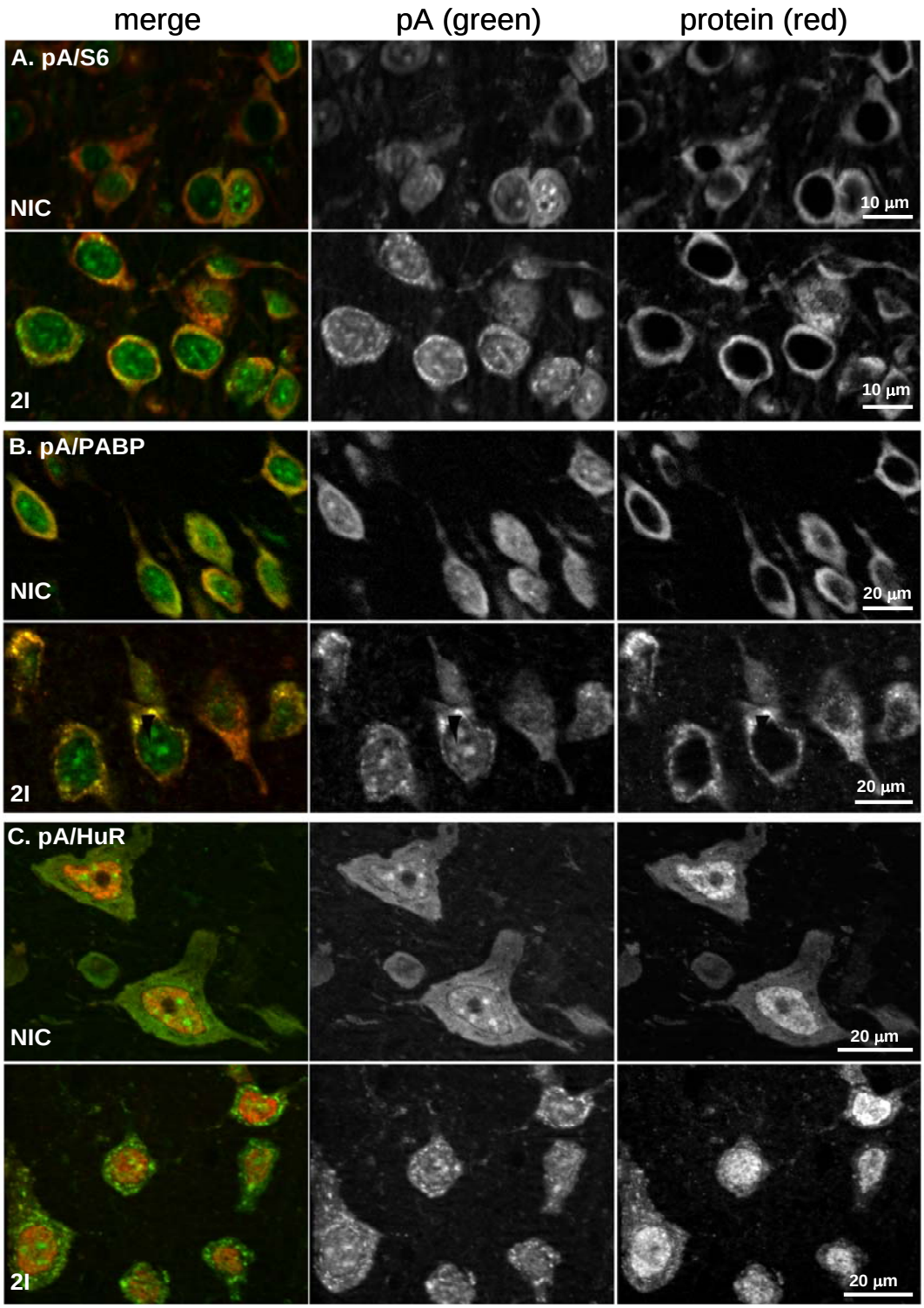

Figure 7: Colocalization studies of mRNA granules with S6, PABP & HuR in 2hr MCAO Wistar rats.
(A) pA/S6 in layer II of cerebral cortex, (B) pA/PABP in layer V or cererbral cortex, (C) pA/HuR in layer V of cerebral cortex. Merged images, pA green channel and protein antigen red channels as indicated. Scale bars apply to each respective row.

D. "Intermediate" pA phenotypes of some layer V neurons

As seen in Figure 7C, the layer V neurons showed distinctly identifiable mRNA granules in the 2I samples. However we occasionally observed a phenotype that appeared "intermediate" between fully granulated mRNA as seen in Figure 7C and the relatively smoother pA signal in the cytoplasm of NICs. The rarity of these "intermediate" neurons made systematic study of them implausible and I simply note and record their occurrence here.

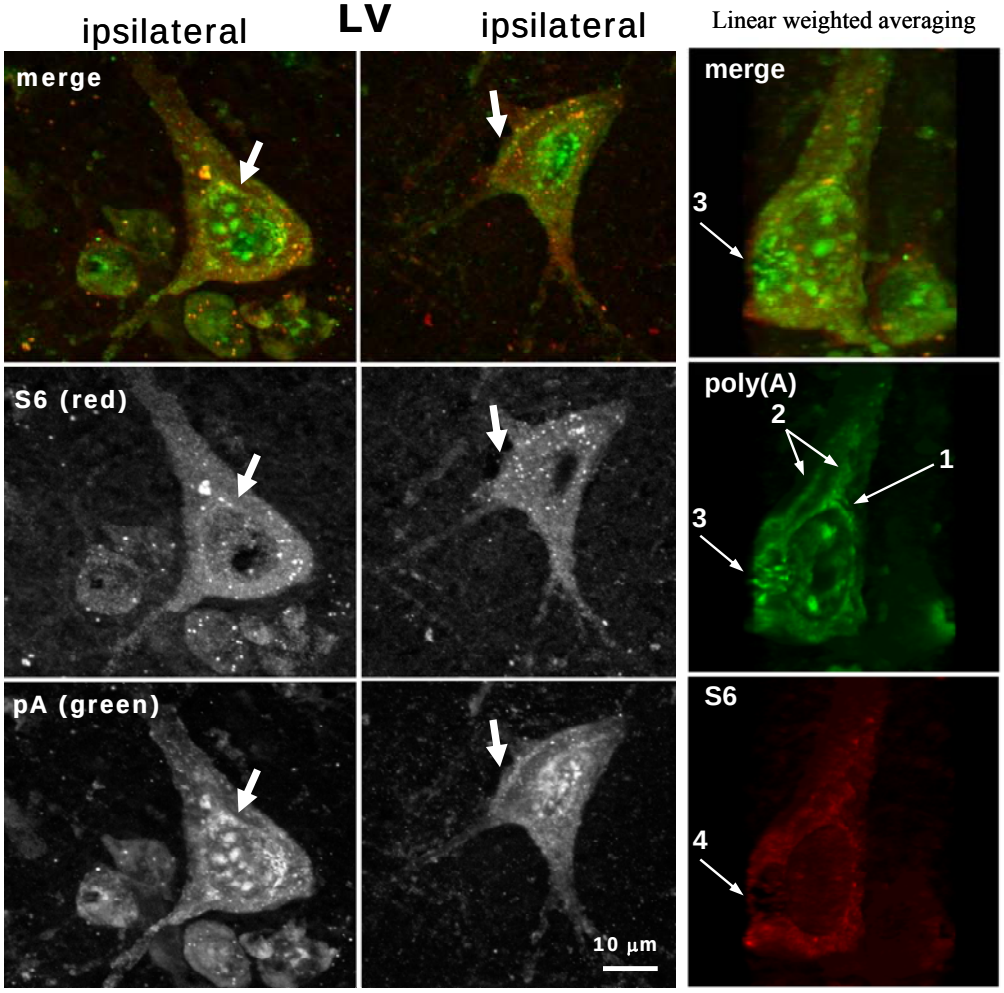

Figure 8 illustrates two of these layer V pyramidal neurons each of which displayed a prominent ridge-like pA staining pattern, which was not present in the S6 channel. The "ridges" appeared as either perinuclear or as tracks that appeared to run along the plasma membrane and apical dendrite.

For the neuron in the first column of Figure 8, a "deep stack" of 37 optical sections with a z-depth of 13 microns was acquired. This z-stack was volumetrically rendered using a method called linear weighted averaging (LWA) to better visualize the pA staining pattern of the cell. LWA is a non-transparent method of superimposing the optical sections that allows 3D structures such as the ridge-like structures along the nucleus (arrow labeled 1) and plasmalemma of the apical dendrite (arrows labeled 2) to be more readily seen. Additionally, a reticulated structure (arrow labeled 3) was prominently visible; at this same location in the cell there was no staining at all for ribosomal protein S6 (arrow labeled 4). Again, the relative rarity of these prevented any type of systematic study. In Chapter 3, where systematic colocalization studies are performed with the mRNA granules, I found these did not colocalize with markers of the endoplasmic reticulum, Golgi apparatus, microtubules or intermediate filaments, and it is possible the ridge-like structures identified here would also not colocalize with these structures.

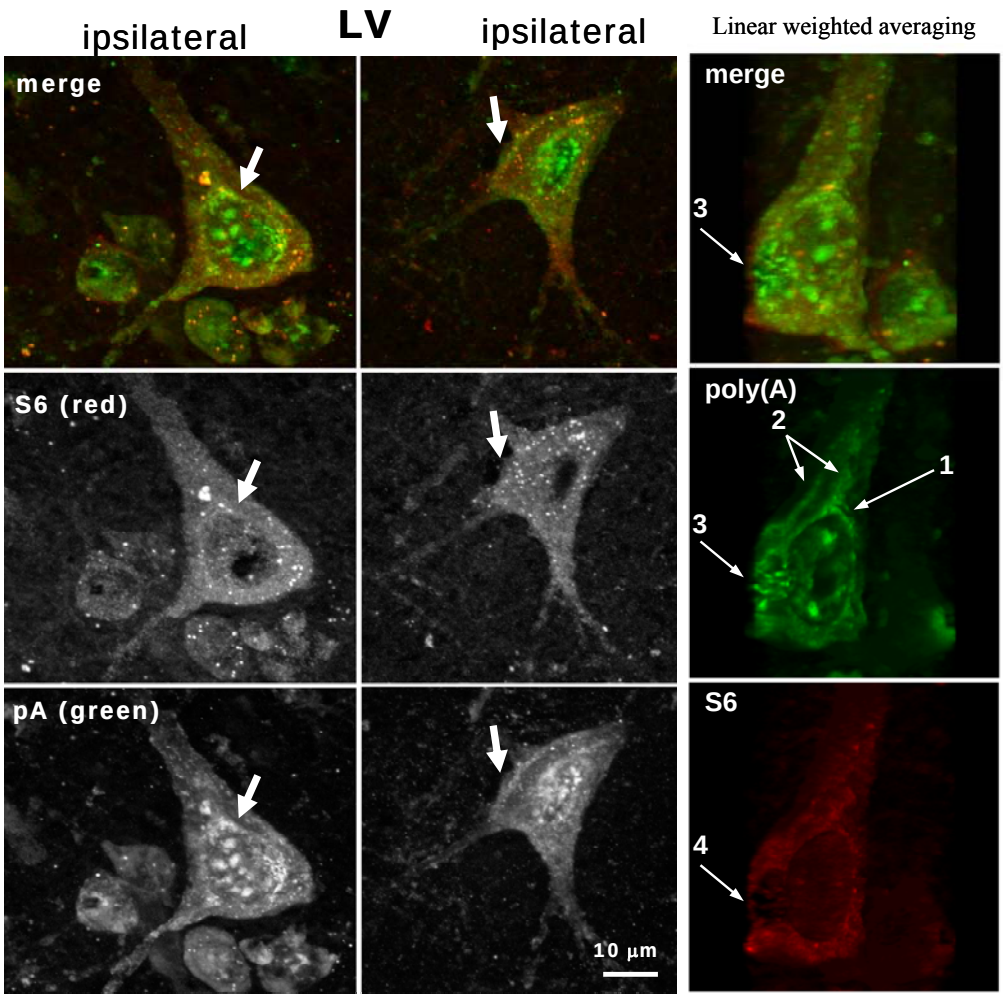

Figure 8: Layer V neurons with an "intermediate" pA phenotype in Wistar rats.
First and second columns show single layer V neurons containing "ridge-like" pA structures that are not present in the S6 channel. Third column shows a 3D reconstruction of the neuron in the first column using linear weighted averaging volume rendering that enhanced the visibility of the pA structures.

E. HSP70 immunostaining

The heat shock response is a well-documented stress response that occurs in cells following perturbations in its environment. HSP70 protein belongs to the family of heat shock proteins that are upregulated when a cell is stressed. Previous studies have shown that hsp70 mRNA and HSP70 protein are upregulated primarily in endothelial cells of large blood vessels following MCAO ischemia[107] and that the upregulation of its translation correlates with the

colocalization of HuR with mRNA granules[102]. Additionally, translation of HSP70 has been shown to be a protective response following brain I/R[108]. Given that Wistar rats did not form an infarct at any time point tested (Figure 5), I assessed the expression of HSP70 protein in order to see if there was a correlation with the TTC staining results.

Following 2 hours of ischemia, HSP70 was expressed in different structures as a function of reperfusion duration (Figure 9). At 4hR, only contractile cells wrapped around the surface of endothelial cells known as pericytes stained for HSP70 in the penumbral cortex and striatum. The morphology of the pericytes was visualized by 3D reconstruction of z-stacks of HSP70 staining (Figure 9D). At 24hR, striatal neurons prominently stained for HSP70. At 7dR only endothelial cells of blood vessels throughout the ipsilateral hemisphere stained for HSP70. These results show that a complex pattern of HSP70 expression occurred in the brains of the Wistar rats following transient MCAO. The successful translation of HSP70 protein is consistent with the lack of an infarct in the Wistar strain following MCAO.

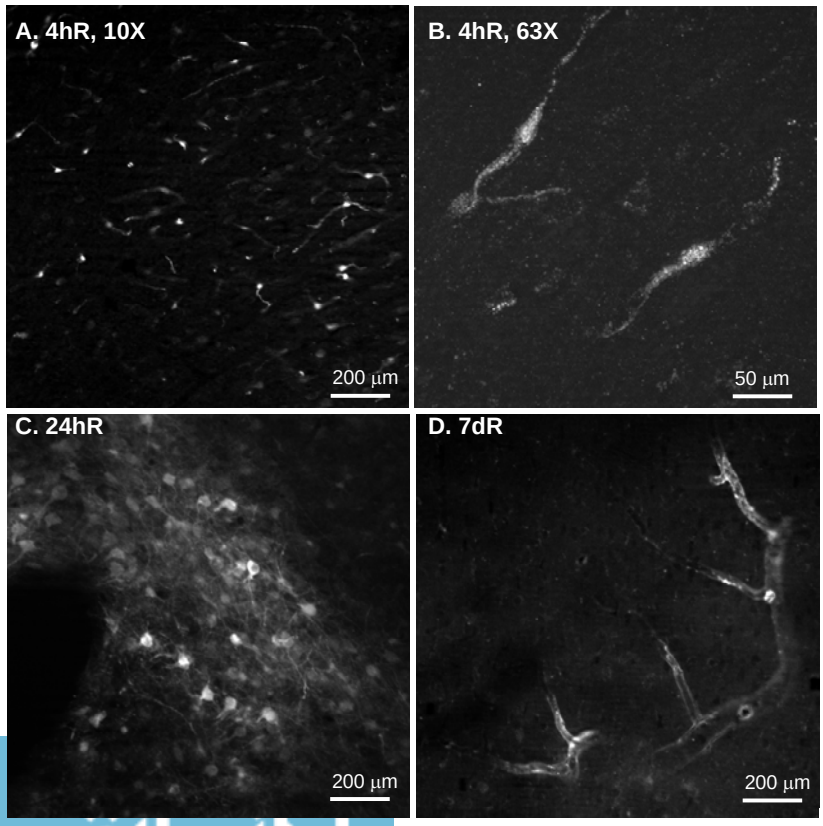

Figure 9 : HSP70 protein expression in different cell types as a function of reperfusion duration.
2 hours of MCAO ischemia followed by: (A) 4 hours reperfusion (4hR) only showed HSP70 expression in pericytes. (B) High magnification, 3D reconstruction of HSP70 reveals the characteristic morphology of pericytes. (C) At 24hR, penumbral neurons stained for HSP70 and (D) at 7dR endothelial staining of HSP70 occurred in blood vessels.

CHAPTER THREE: Studies on Long Evans - Methods and Results

I. Rationale

Although the Wistar rat strain evidenced neurons containing mRNA granules following 2 hr MCAO, and these had characteristics in common with those identified in neurons following global brain ischemia[102], their frequency of occurrence in both the experimental groups and in terms of the area of brain tissue affected was far too small to use as a baseline for studies of the effect of diabetes on the translational system following focal brain ischemia. Since mRNA granules had been initially discovered in the Long Evans rat strain[102], I undertook MCAO studies in the Long Evans rat strain.

This turned out to be a fortuitous decision because the Long Evans rat strain displayed abundant mRNA granulation of neurons in response to focal brain ischemia as I will describe in this chapter. Because the Long Evans gave a positive result with respect to mRNA granule formation, I undertook a systematic analysis of their distribution along a time course of ischemia duration. A reperfusion time course was not studied here because it was first necessary to study the degree to which mRNA granules formed at different durations of ischemia. To characterize the mRNA granules along a time course of ischemia, three main types of analysis were performed: (1) a study of different histological regions in the MCAO brain, (2) a three dimensional (3D) study along the rostral-caudal extent of the brain, and (3) a comprehensive colocalization analysis of the mRNA granules with two categories of markers: (a) mRNA interacting proteins, and (b) markers of subcellular organelles.

II. Materials

Table 4 lists the antisera, what they are markers of, vendors and dilutions used in the present study. All other antibodies were purchased from companies previously described in Chapter 2. I will briefly describe each marker in the Results section ahead.

Table 4: Antisera used for colocalization studies.

Antisera	Marker for	Vendor	Catalog #	Dilution
α-tubulin	microtubules	Sigma	T6199	1:100
APRIL	HuR ligand	Abcam	ab4224	1:100
COX IV	mitochondria	Abcam	ab16056	1:50
GM130	cis-Golgi apparatus	BD Biosciences	610822	1:100
HuR	mRNA BP	Santa Cruz	sc-5261	1:25
NeuN	nucleus	Millipore	MAB377	1:500
NF H/M	intermediate filaments	Sigma-Aldrich	N2912	1:300
PDI	Endoplasmic reticulum	Thermo Scientific	MA3-019	1:200
pp32	HuR ligand	Enzo Life Sciences	ADI-905-234-100	1:250
RPA	60S subunit	ImmunoVision	HPO-0100	1:5000
S6	40S subunit	Cell Signaling	2317	1:25
TGN38	trans-Golgi apparatus	Thermo Scientific	MA3-063	1:200

Abbreviations and a brief description of the antigens is provided in the text.

A. Animal Model

Unilateral focal brain ischemia was induced in male Long Evans rats (weight 275-300g; Charles River Laboratories International, Inc., Wilmington, MA) using the same model of MCAO described in Chapter 2. The experimental groups and number of animals used are listed in Table 5.

Table 5: Experimental groups used in Long Evans studies.

Experimental Group	Ischemia	Reperfusion	n
Sham controls	-	-	3
2I	2hr	-	5
2I/24R	2hr	24 hr	5
4I	4 hr	-	5
6I	6hr	-	5
8I	8hr	-	5

III. Methods

A. TTC Staining

TTC staining was performed as previously described in Chapter 2.

B. Immunofluorescence and FISH

Double IF/FISH was performed exactly as described in Chapter 2. Primary antisera

dilutions are listed in Table 4. Secondary antisera dilutions in 1% NDS in PBS-TX were the same as that previously described in Chapter 2.

C. Systematic histological analysis of MCAO brain

As described in Chapter 1, focal ischemia results in heterogeneous damage in the brain producing, at minimum, a core, penumbra, and the remaining nonischemic brain tissue. Therefore, for all samples, each of these regions was analyzed. In addition, since the MCA feeds both the cerebral cortex and striatum, I evaluated both regions histologically. The rat cerebral cortex, while functionally six layered, shows 3 anatomical demarcations at the coronal levels I investigated (around 1 mm anterior to Bregma). Layers II and III form one large layer most proximal to the brain surface, under which are layers V and then VI. Thus, I routinely analyzed 4 histological regions: striatum, and layers II/III, V, and VI. In total, to systematically study the brain after focal ischemia, for every experimental animal I routinely photographed from the 12 different areas in a given coronal section. The different MCAO-induced areas and histological regions are illustrated in Figure 10.

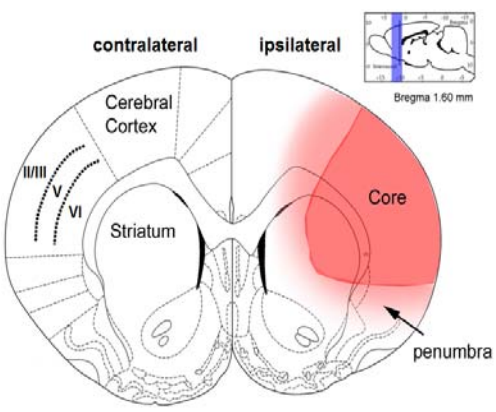

For a given animal, 12 separate z-stacks were taken:

Contralateral
1. striatum
2. layer II/III
3. layer V
4. Layer VI

Penumbra
5. striatum
6. layer II/III
7. layer V
8. Layer VI

Core
9. striatum
10. layer II/III
11. layer V
12. Layer VI

Figure 10: Regions systematically analyzed in Long Evans MCAO brains.
Histological regions are listed on the left of the coronal section, and MCAO-induced areas are displayed on the right hemisphere. The coronal section used for analysis of histological regions was at approximately 1 mm anterior to Bregma. Purple area in sagittal inset shows the rostral-caudal extent used for 3D reconstructions described in section IV.D below. Images adapted and modified from[109].

D. Volumetric reconstruction of pA staining

For computer reconstructions of the 3D rostral to caudal spatial distribution of neurons containing mRNA granules, sixteen coronal slices, 100 microns apart, were evaluated between approximately 1.32 mm to – 0.60 mm anterior to Bregma, containing the MCA territory.

Slices were stained by double labeling with pA FISH and PABP IF. Areas with mRNA granules-containing neurons and areas with shrunken/distorted neurons (described in Results below) were determined for each slice under 20X magnification and marked on photocopies of corresponding coronal sections taken from the Paxinos and Watson Rat Brain Atlas[109]. Since PABP strongly colocalizes with mRNA granules[102], all mRNA granule-containing regions were confirmed by inspection under the 40X objective for both pA and PABP stains. Determination of areas containing neurons with either mRNA granules or with shrunken/distorted neurons was conducted by two independent observers blinded to the identity of the experimental groups; the independent mappings generally agreed to > 90%.

Hand-drawn images were then digitized as BMP files on a flat bed scanner and imported into Amira 5.2.0 (Visage Imaging, San Diego, CA, USA) to perform 3D reconstructions. The mRNA granule-containing and shrunken/distorted neuron-containing areas were traced onto cross sections at approximately the same Bregma coordinates of the corresponding images of the digital rat brain dataset from the Laboratory of Neuro Imaging (LONI) from the University of California at Los Angeles[110]. The LONI dataset used was the series of coronal images through the entire rat brain sampled at 30 micron intervals and digitized at 1024 x 1024 pixels, 8 bit resolution. (This data is available for download at: www.loni.ucla.edu/Atlases/Atlas_ Detail.jsp?atlas_id=1)

For both illustration purposes and for quantitation (described below) the 3D reconstructed volumes were embedded within the LONI dataset. The LONI dataset was masked to include

only the brain, and volumetrically rendered in Amira from slice (using the exact file names of the LONI dataset) cor_0979.gif (at Bregma -0.66 mm) through slice cor_1043.gif (at Bregma +1.34 mm) using the Voltex method with 'mip' (mean intensity projection) and 'color table' options selected, and a constant color of RGB = (0.894, 0.894, 0.894).

From the 16 sequential brain sections of FISH/IF staining, 3D volumes were generated in Amira 5.2.0 as per user manual instructions. Two volumes were constructed per each experimental animal: the volume containing shrunken/distorted neurons (colored red in the figures and labeled "core") and the volume of mRNA granule-containing neurons (colored green in the figures and labeled "granular"). Magnitudes of each volume were taken as the number of voxels contained in each volume as calculated by built-in Amira routines. The "total volume" was taken as the number of voxels in one hemisphere of the masked LONI dataset between coordinates +1.34 to -0.66 mm anterior to Bregma. "Total affected volume" was the sum of the core and granular voxels in an animal. Two different percents were calculated to express the volumetric data. Relative percent volume calculated the relative proportions of the core and granular volumes occupying the total affected volume. Absolute percent volume calculated the percent of the total LONI dataset volume occupied by the granular and/or core volumes. Calculated percents for experimental groups were compared using ANOVA, and Tukey post hoc where appropriate, with significance was set at $p < 0.05$. Using the pre-core volume as an example, the percentage formulas were.

$$relative\ percent\ = \frac{\#\ \text{voxels pre-core}}{\#\ \text{voxels pre-core} + \#\ \text{voxels granular}} x100$$

$$absolute\ percent = \frac{\#\ \text{voxels pre-core}}{\#\ \text{voxels in LONI dataset between Bregma +1.34 mm to -0.66 mm}} x100$$

IV. Results

A. TTC staining

When permanent MCAO (pMCAO) was evaluated out to 8 hr ischemia in the Long Evans rats, none of the pMCAO samples showed an infarct by TTC staining (Figure 11). However, TTC staining of Long Evans rats showed an infarct in the 2 hr ischemia plus 24 hr reperfusion group (Figure 11). This result contrasts to the Wistar groups, where no infarct was seen as far out as 7 days of reperfusion (Figure 5).

The 2I/24R TTC result provided a rough guide to our use of the terms "penumbra" and "core" in the 3D reconstructions described below. In the pMCAO ischemia-only samples, neurons located in the areas devoid of TTC staining in the 2I/24R samples generally had a shrunken and distorted appearance, and often had weak staining for protein antigens. Therefore, in spite of TTC staining the pMCAO brains from 2 to 8 hr ischemia-only, the neurons displayed characteristics that are not revealed by TTC, but can be detected by other stains[111], and are indicators of damaged neurons that will eventually form the core of the infarct.

Figure 11: TTC staining in Long Evans rats subjected to MCAO ischemia.
Representative 2mm thick brain slices are arranged anterior (top) to posterior (bottom) and encompass the MCAO territory, which includes the striatum.

B. Frequency of mRNA granule formation

The total number of experimental Long Evans rats showed a much higher frequency of mRNA granule formation (80%) (Table 6) than the total number of experimental Wistar animals (11%) (Table 3). However, this is a misleading number because the experimental groups are not directly comparable in terms of the total number of rats. The Wistar set consisted mainly of transient MCAO, whereas the Long Evans set was mainly pMCAO. When compared in terms of experimental groups, the Wistar and Long Evans had comparable frequencies: 67% of 2I Wistar rats and 100% of the pMCAO groups of Long Evans rats had mRNA granules in some neurons. We will see below, however, that the affected areas were much larger in the Long Evans strain.

Table 6: mRNA granule frequency in Long Evans rats.

Experimental Group	n tested	n w mRNA granules	Percent
2I	5	5	100 %
2I/24R	5	0	0%
4I	5	5	100 %
6I	5	5	100 %
8I	5	5	100 %
total	25	20	80%

C. Systematic histology of mRNA granules in Long Evans MCAO

Co-staining pairs of pA FISH with IF for S6, PABP and HuR were performed across the 12 areas illustrated in Figure 10. Three co-stains were performed per animal to compare to both the Wistar results that used these stains and to compare to the previous work on global ischemia in the Jamison *et al*. study[102]. There were two main questions I wanted to ask with these studies: (1) Did mRNA granules form preferentially in any of the four histological regions: layer II/III, layer V, layer VI and striatum? (2) Did mRNA granules form preferentially in any of the three major MCAO-inducing brain areas: core, penumbra and (non-ischemic) contralateral hemisphere? Representative samples for layers II/III and V are shown in Figure 12, and for layer

VI and striatum in Figure 13. The samples shown are drawn mainly from the 2I and 4I groups.

The results to emerge from these studies are: (1) neurons of all 4 histological regions, layers II/III, V, VI and striatum, formed mRNA granules, (2) the mRNA granule-containing neurons were found preferentially in penumbral areas at the watershed between the MCA and ACA, (3) their colocalization patterns with S6, PABP and HuR were similar to those seen in the Wistar studies described in Chapter 2 and to those seen following global brain ischemia[102], and (4) shrunken/distorted neurons were present in the core areas fed directly by the MCA.

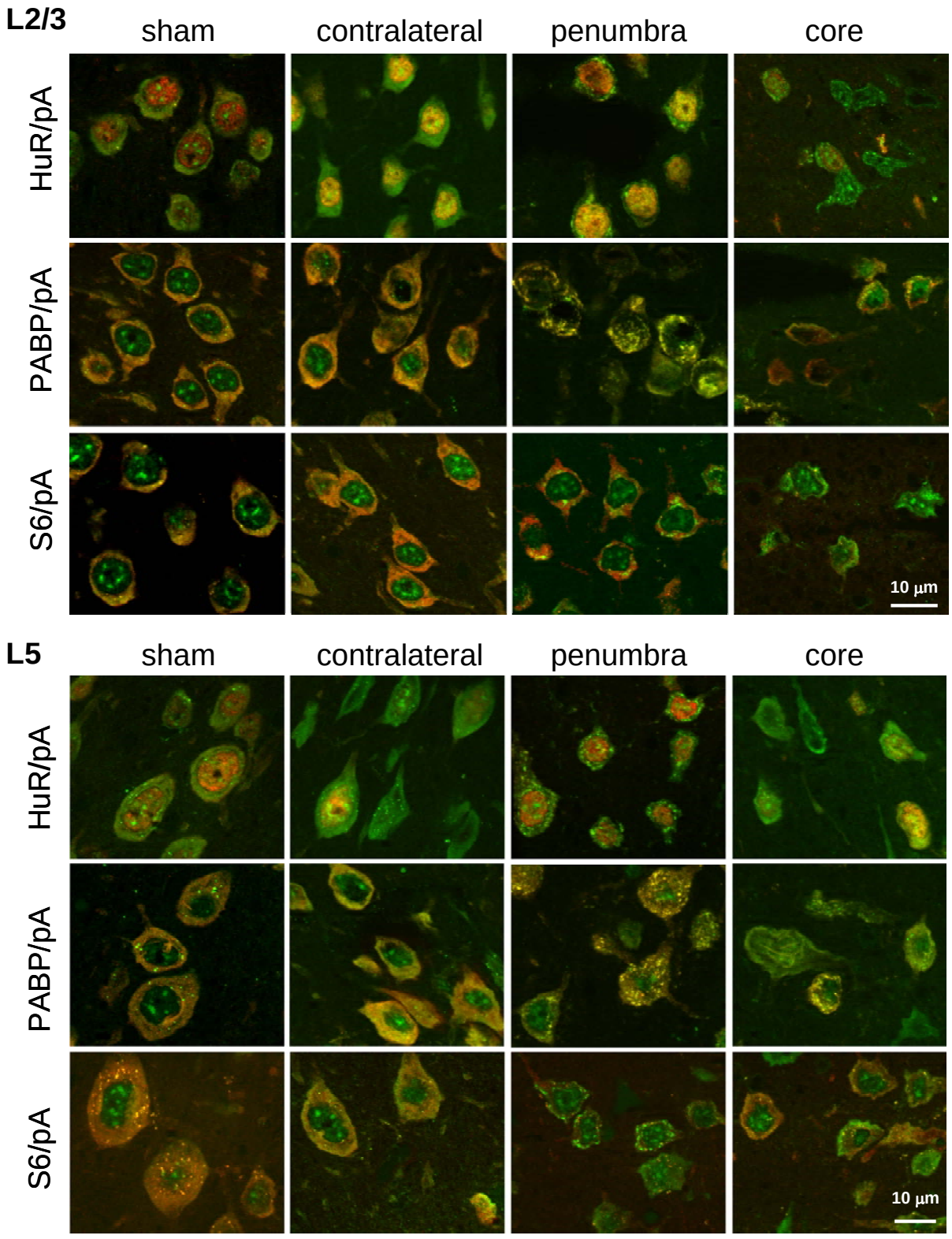

Figure 12: Layers II/III and V: sham, contralateral, penumbral and core pA & S6, PABP or HuR merged images. Scale bars in lower right panel apply to all panels for a given histological region.

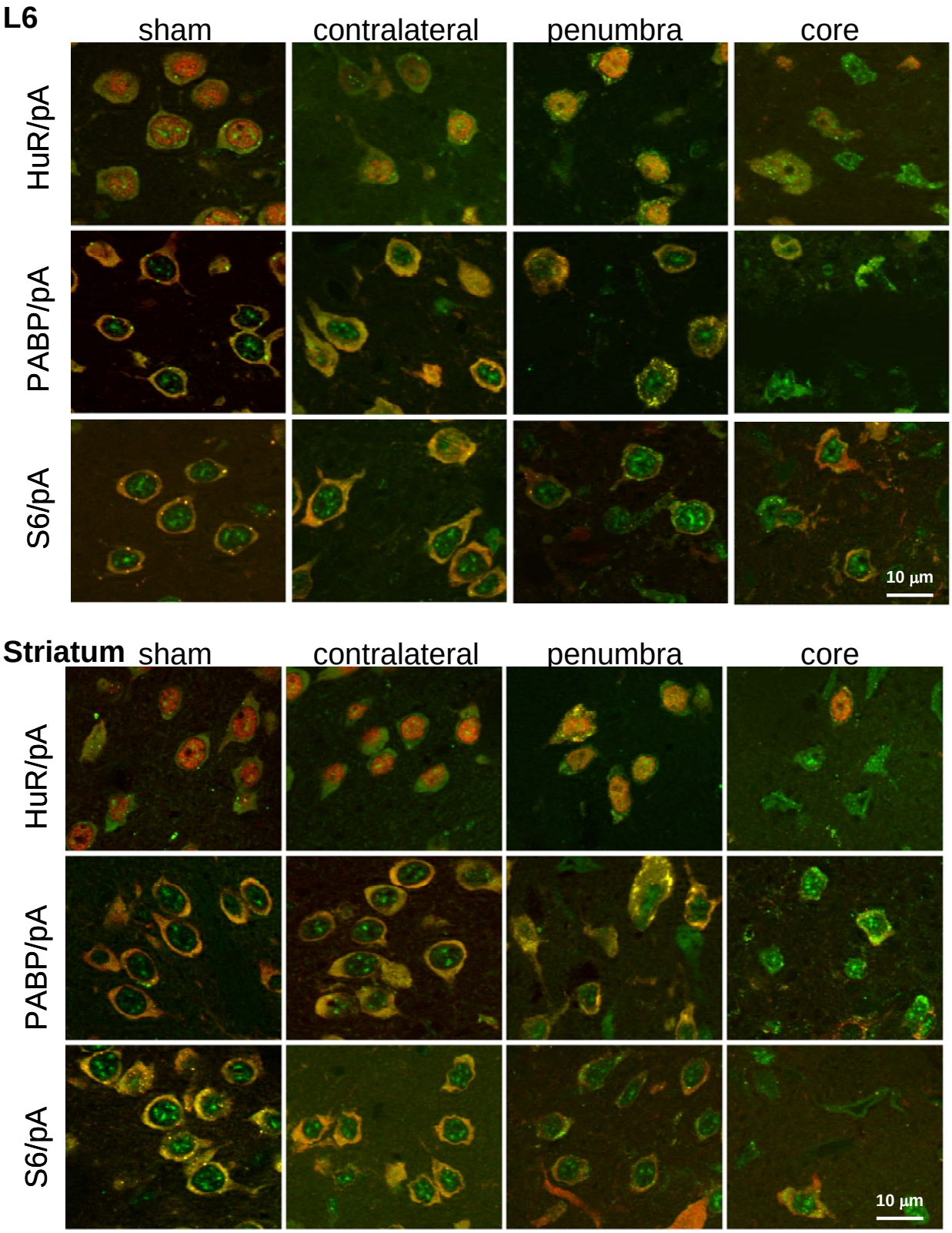

Figure 13: Layer VI and striatum: sham, contralateral, penumbral and core pA & S6, PABP or HuR merged images. Scale bars in lower right panel apply to all panels for a given histological region.

In addition, the core neurons generally had a weaker staining for the protein antigen, but the pA staining was good enough to discern the shape of the shrunken and/or distorted neurons. Finally, in general, the neurons of the four histological regions on the contralateral side resembled sham operated controls.

With regard to the colocalization patterns, in sham and contralateral neurons, S6 and PABP formed diffuse colocalization. When neurons showed mRNA granules, S6 did not, but PABP and HuR did colocalize with the mRNA granules. The colocalization with HuR was strong enough to form distinctly yellow mRNA granules, unlike the Wistar strain, but similar to CA3 following global brain ischemia[102].

D. 3D Volumetric analysis

The above colocalization studies showed that neurons in all cortical layers and the striatum could form mRNA granules, but there was quite a bit of variance in the distribution of the granules amongst these regions. 3D volumetric reconstructions were generated as a means to determine the relative distributions of neurons containing mRNA granules in the various regions. The reconstructions also served to assess the extent of the ischemic insult through a rostral to caudal extent in the brain.

A representative series of cross sections used to generate the 3D reconstruction of a 4I sample is shown in Figure 14. The top panels illustrate the appearances of areas assigned as either granular penumbra or shrunken/distorted core verses normal appearing, using the pA FISH/PABP IF co-staining of layer II cortical neurons. The bottom panel of Figure 14 shows an example of a 4I animal where mRNA-granule containing (green areas) and shrunken and distorted neurons (red areas) appeared in rostral-caudal cross sections. These areas are shown superimposed on the corresponding slices from the LONI rat brain dataset. Only half the dataset used for volumetric reconstruction is illustrated in the figure, therefore each slice is separated by 200µ.

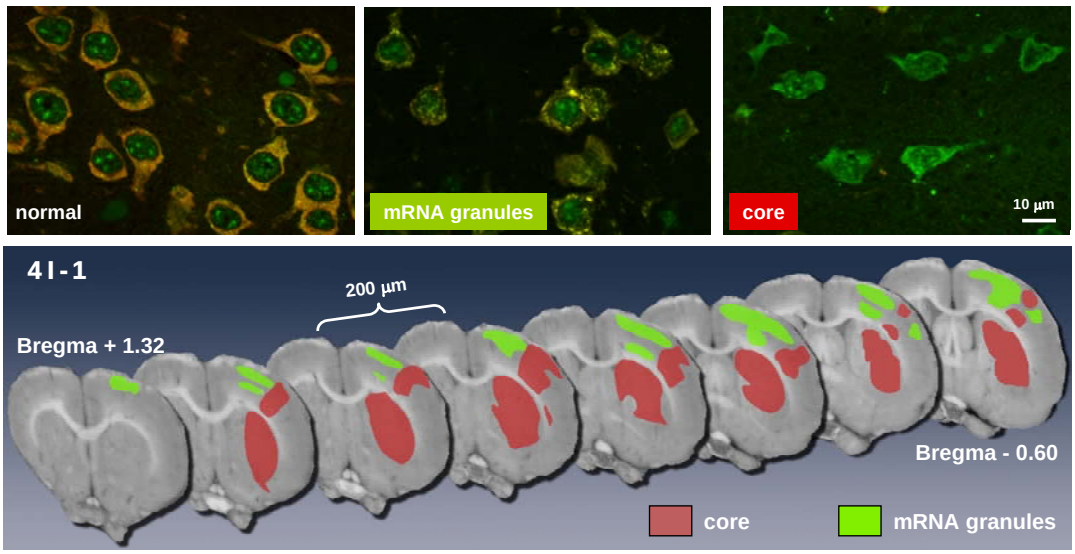

Figure 14: Cross-sections used for 3D reconstructions in Long Evans strain after pMCAO. Top: Example appearances of normal, granular and core areas in layer II. Scale bar on right panel applies to all three panels of the top row. Bottom: Rostral to caudal cross-sections show the extent of the granular penumbral (green) and core (red) areas through the MCA territory of a representative 4I samples.

For this particular example, no striatal neurons showed evidence of mRNA granules. The cells of the lateral striatum were shrunken and distorted, appearing similar to the top panel marked "core". Neurons of the medial striatum had the same appearance as contralateral and sham-operated striatal neurons (e.g. as in Figure 13). This animal also showed a substantial fraction of cerebral cortex to have a core phenotype that ran for some distance across all the cortical layers, mainly in somatosensory cortex. However, significant areas of cerebral cortex contained neurons expressing cytoplasmic mRNA granules. These areas were mostly medial to the core cortical areas, and were in the watershed area between the MCA and anterior cerebral artery territory.

Using the sequential cross sections, 3D volumes for the penumbra and core phenotypes over a range of pMCAO durations were generated (Figure 15). Quantitative analysis of the volumes for the 3D reconstructions from the pMCAO groups are as follows: at 2hrI, 72.8 ± 38.5% of the affected volume had mRNA granule containing neurons, and 27.2 ± 38.5%

contained distorted and shrunken cells. However, the relative volume percents did not clear statistically. There was a drop in the relative proportion of the affected volume of neurons containing mRNA granules to 15 ± 11.2%, 8.6 ± 8.0% and 0 % for the 4hrI, 6hrI and 8hrI groups respectively, and corresponding increases for the volume of core neuron phenotypes. The relative percents for the 4I and 6I groups cleared statistically (ANOVA $p < 0.05$, Tukey $p < 0.05$). An exponential curve fit of the decrease in relative volume containing mRNA granules (Figure 15, blue curve) gave a correlation coefficient (cc) equal to 0.91, whereas a linear fit gave a cc of 0.77 (Figure 15, magenta curve). The exponential drop in mRNA granule-containing neuron volume corresponds to expansion of the core into the penumbral region[124], as ischemia duration increases.

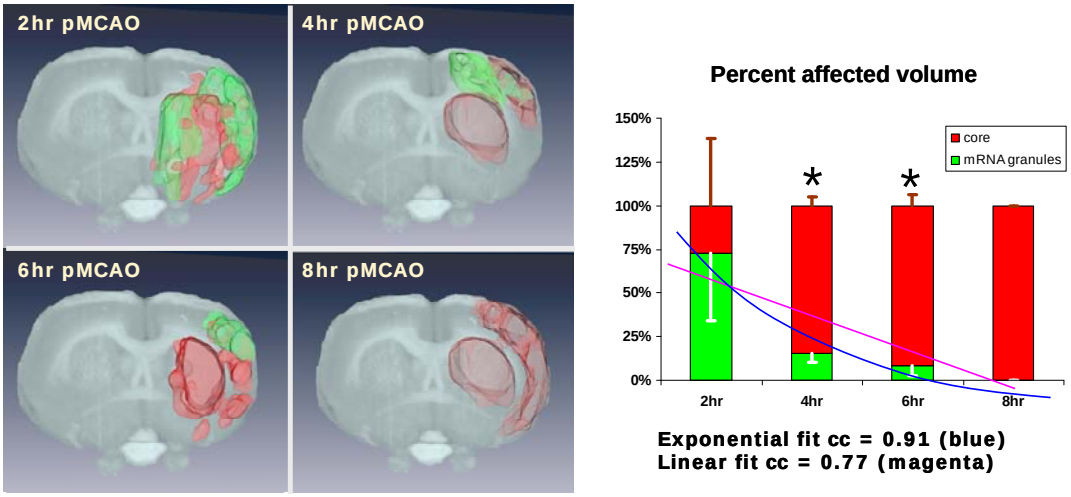

Figure 15: Quantification of mRNA granule-containing volumes in Long Evans pMCAO rats. Left: Representative 3D reconstructions from 2, 4, 6 and 8 hr of pMCAO in Long Evans rats. Right: Plot of percent affected volume occupied by mRNA granule-containing or core-like neurons. Blue curve is an exponential fit through the penumbral percents, and magenta curve is a linear fit. The correlation coefficients (cc) of the respective fits are indicated. There was a statistically significant difference (post hoc $p < 0.05$) for the relative percents of penumbra and core at the 4 hr and 6 hr experimental groups.

E. Colocalization in Layer II neurons

In this study, layer II/III mRNA granule forming neurons were assessed for colocalization with markers of organelles (Figures 16-22) and mRNA binding proteins (Figures

23-28). Figures 16-28 show staining in the three main MCAO regions: contralateral, penumbral and core, the latter two terms used as above. For these studies the results are shown in terms of the merged green and red channel and underneath are the individual green and red channels so the patterns of staining in the individual channels can be directly inspected along with the merged images. A summary of the staining patterns of the 13 antigens in the contralateral neurons and with the mRNA granules is provided in Table 7.

1. Double IF/pA FISH and Intracellular Organelle markers

For the contralateral, nonischemic hemisphere, the only organelle marker to show some degree of colocalization with pA mRNAs was protein disulfide isomerase (PDI, Figure 16), an endoplasmic reticulum (ER) localized enzyme used in the formation of disulfide bond. This is not unexpected, and the overlap of pA and PDI likely reflects the detection of rough ER, in which ribosomes are localized on the surface of the ER membrane. This would bring mRNA into close physical proximity to enzymes such as PDI.

However, in the penumbral neurons, the mRNA granules did not colocalize with PDI (Figure 16), GM130 (Figure 17) or TGN38 (Figure 18). GM130 is a 130 kDa "Golgi marker" protein localized to cis-Golgi. The 38 kDa trans-Golgi network marker localizes the trans-Golgi. The lack of colocalization indicates mRNA granules are not associated with the internal membranes making up the proximal secretory apparatus of the cell. The mRNA granules did not colocalize with cytochrome c oxidase, subunit IV (COX IV), an inner mitochondrial membrane protein involved in electron transport (Figure 19). Nor did they colocalize with α-tubulin (Figure 20) or with an antisera that detects the heavy (H) and medium (M) weight neurofilament proteins (NH-H/M, Figure 21) and thereby do not interact with microtubules or neuronal intermediate filaments, respectively. Unexpectedly, the mRNA granules did colocalize with the widely used neuronal marker, NeuN (Figure 22). "NeuN" is an abbreviation of "neuronal nuclei", and I used

this antiserum as a nuclei marker. However, we were surprised to observe the NeuN signal clearly colocalized with the mRNA granules outside of the nucleus. In sum, these results indicate that mRNA granules do not associate with the organelle markers tested.

2. Double IF/pA FISH and mRNA binding proteins

In the non-ischemic contralateral neurons, the one mRNA binding protein that strongly colocalized with cytoplasmic pA was ribosome p antigen (RPA, Figure 23) a marker of the large 60S ribosomal subunit[112]. Similar to S6, such colocalization would be expected to reflect mRNA associated with translating ribosomes. The only other markers that showed colocalization with pA in the contralateral neurons were TIA-1 and pp32. This colocalization occurred in the form of small punctate spots in the cytoplasm. Based on Foaz Kayali's work[101], we now know the TIA-1/pA spots in the cytoplasm are stress granules.

For the penumbral layer II neurons, the mRNA granules did not colocalize with RPA just as they did not colocalize with S6 (e.g. see pA/S6 co-stains in Figure 12 and Figure 13). Thus, the mRNA granules are sequestered away from the entire ribosome, both 40S and 60S subunits. The mRNA granules colocalized with HuR, an mRNA binding protein (Figure 24), but did not colocalize with the HuR cofactors APRIL and pp32 (Figures 25 and 26, respectively). ARPIL and pp32 are involved in the nuclear to cytoplasmic mRNA transport function of HuR[113]. The mRNA granules did not colocalize with the stress granule marker, TIA-1 either (Figure 27), ruling out the possibility of being stress granules. Lastly, there was no colocalization of the mRNA granules with TTP, an mRNA destabilizing protein that is associated with degradative processing bodies.[114] Based on the results here, mRNA granules that form following focal ischemia behave the same as those that occur following global ischemia[102], binding well-known mRNA binding proteins and sequestering mRNA away from ribosomal machinery.

Finally, it is striking that for each antigen studied, there is a decrease in protein antigen

staining in core neurons. Technically, this cannot be due to interference by the poly(T) probe because the FISH procedure is performed after the IF procedure.

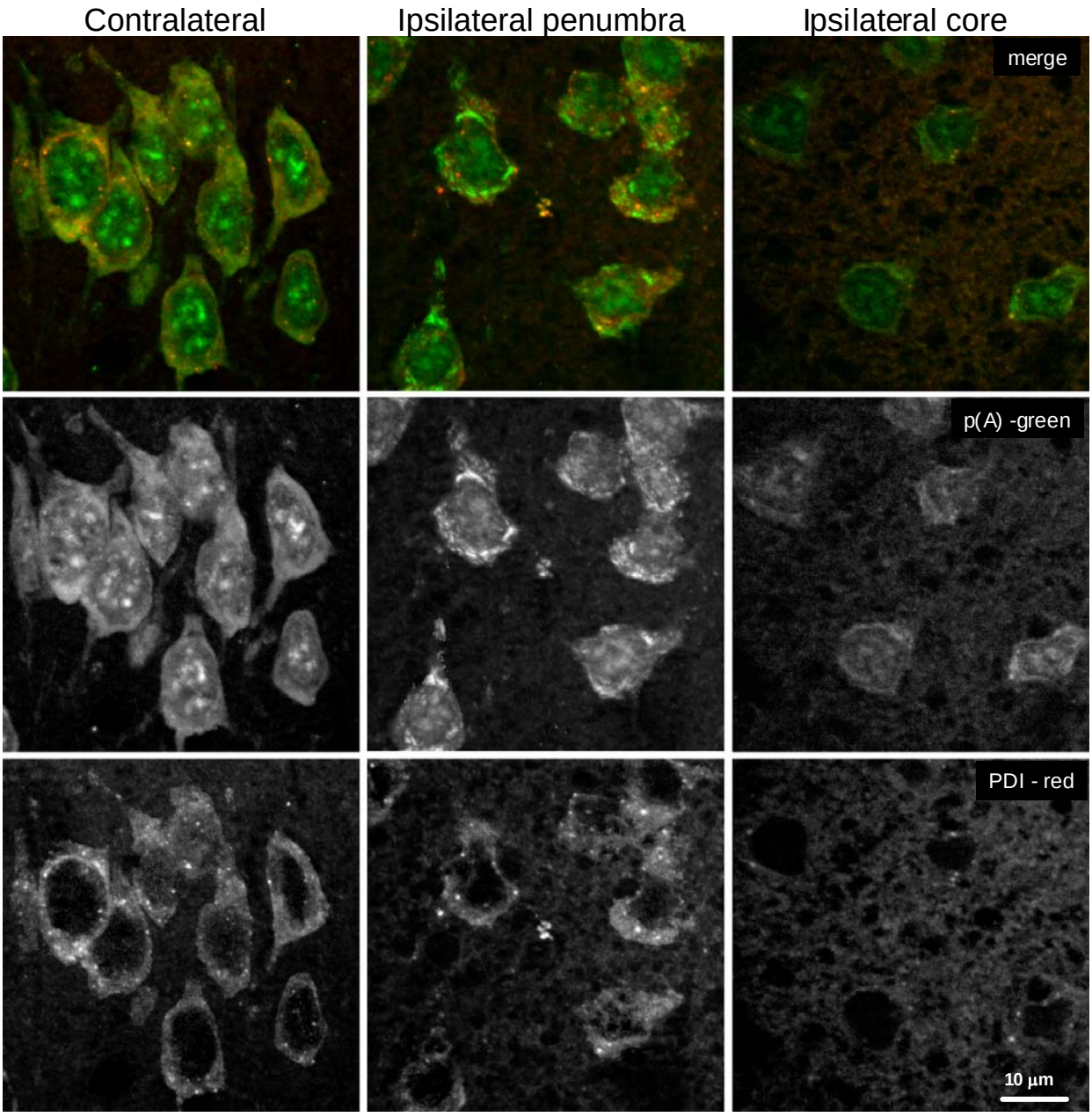

Figure 16: Layer II colocalization studies in Long Evans for pA & PDI.
Double FISH/IF for poly-adenylated mRNAs [p(A), green channel], and PDI (protein disulfide isomerase), a marker of the endoplasmic reticulum (red channel) in layer II of cerebral cortex following 2 hrs permanent MCAO ischemia. Images taken from coronal section approximately 1 mm anterior to Bregma using the coordinates of Paxinos and Watson (1998). Scale bar in lower right panel is 10 microns and applies to all panels.

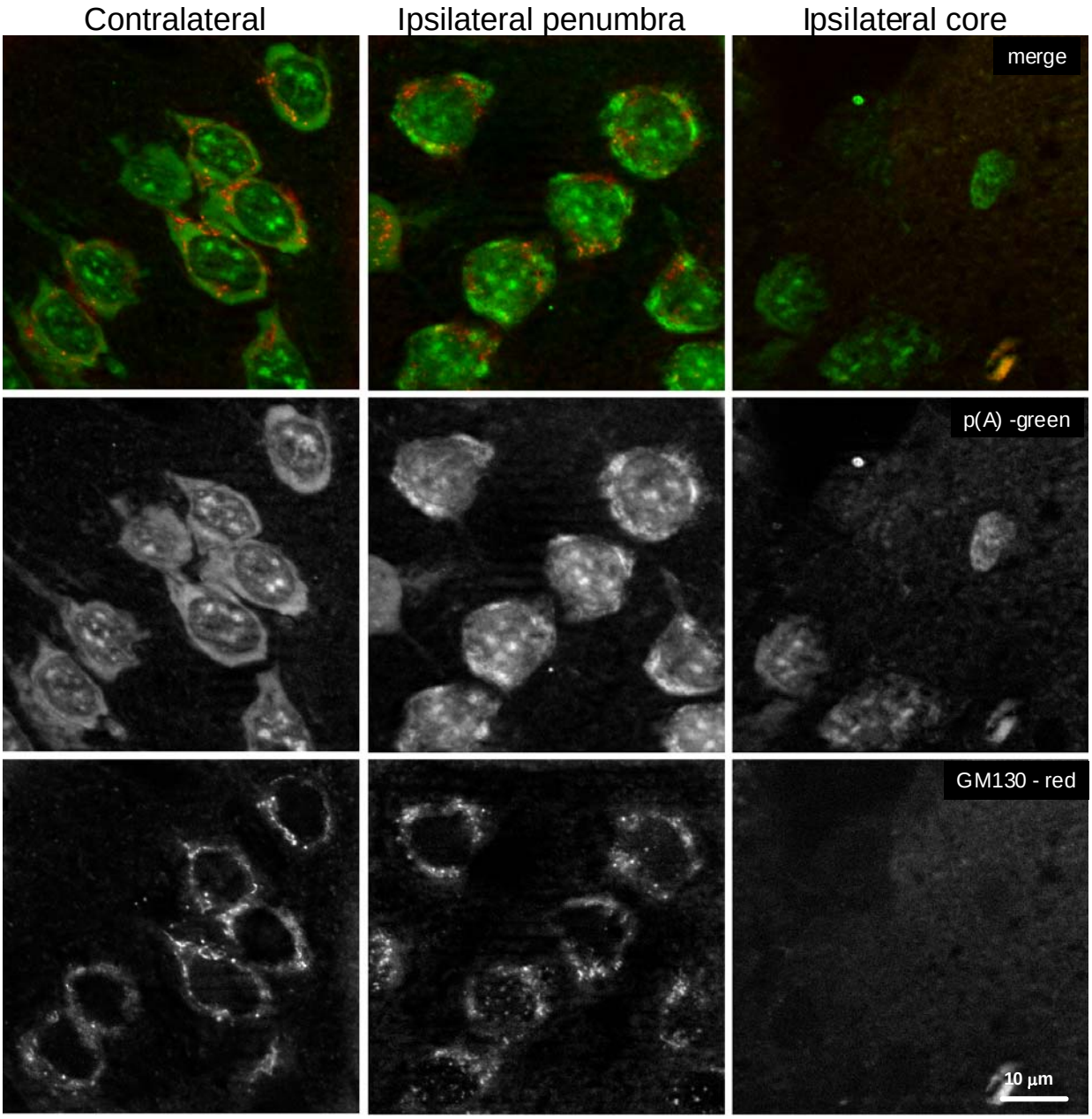

Figure 17: Layer II colocalization studies in Long Evans for pA & GM130.
Double FISH/IF for poly-adenylated mRNAs [p(A), green channel], and GM130, a marker of the cis-Golgi Apparatus (red channel) in layer II of cerebral cortex following 2 hrs permanent MCAO ischemia. Images taken from coronal section approximately 1 mm anterior to Bregma using the coordinates of Paxinos and Watson (1998). Scale bar in lower right panel is 10 microns and applies to all panels.

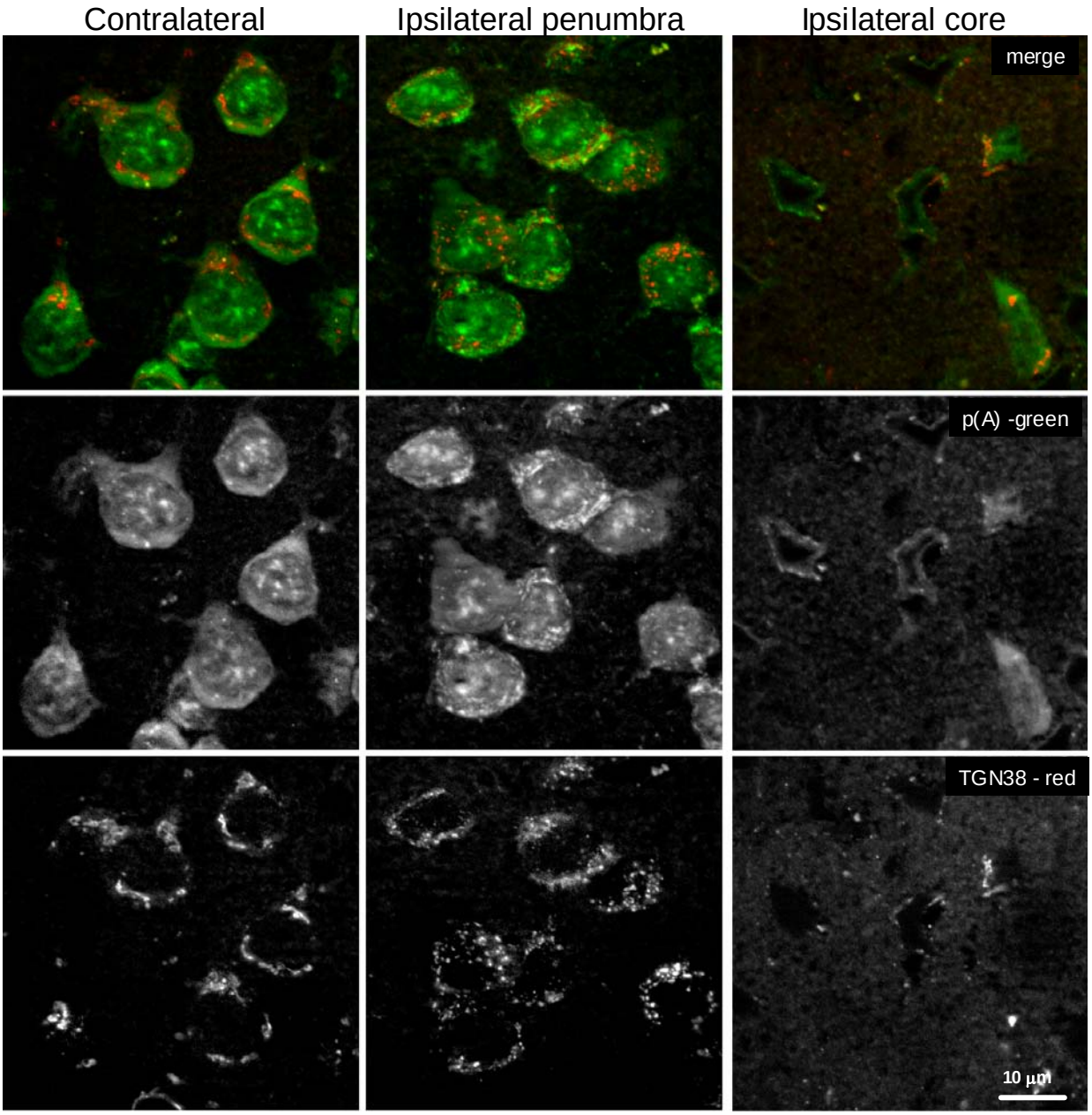

Figure 18: Layer II colocalization studies in Long Evans for pA & TGN38.
Double FISH/IF for poly-adenylated mRNAs [p(A), green channel], and TGN38, a marker of the trans-Golgi Network (red channel) in layer II of cerebral cortex following 2 hrs permanent MCAO ischemia. Images taken from coronal section approximately 1 mm anterior to Bregma using the coordinates of Paxinos and Watson (1998). Scale bar in lower right panel is 10 microns and applies to all panels.

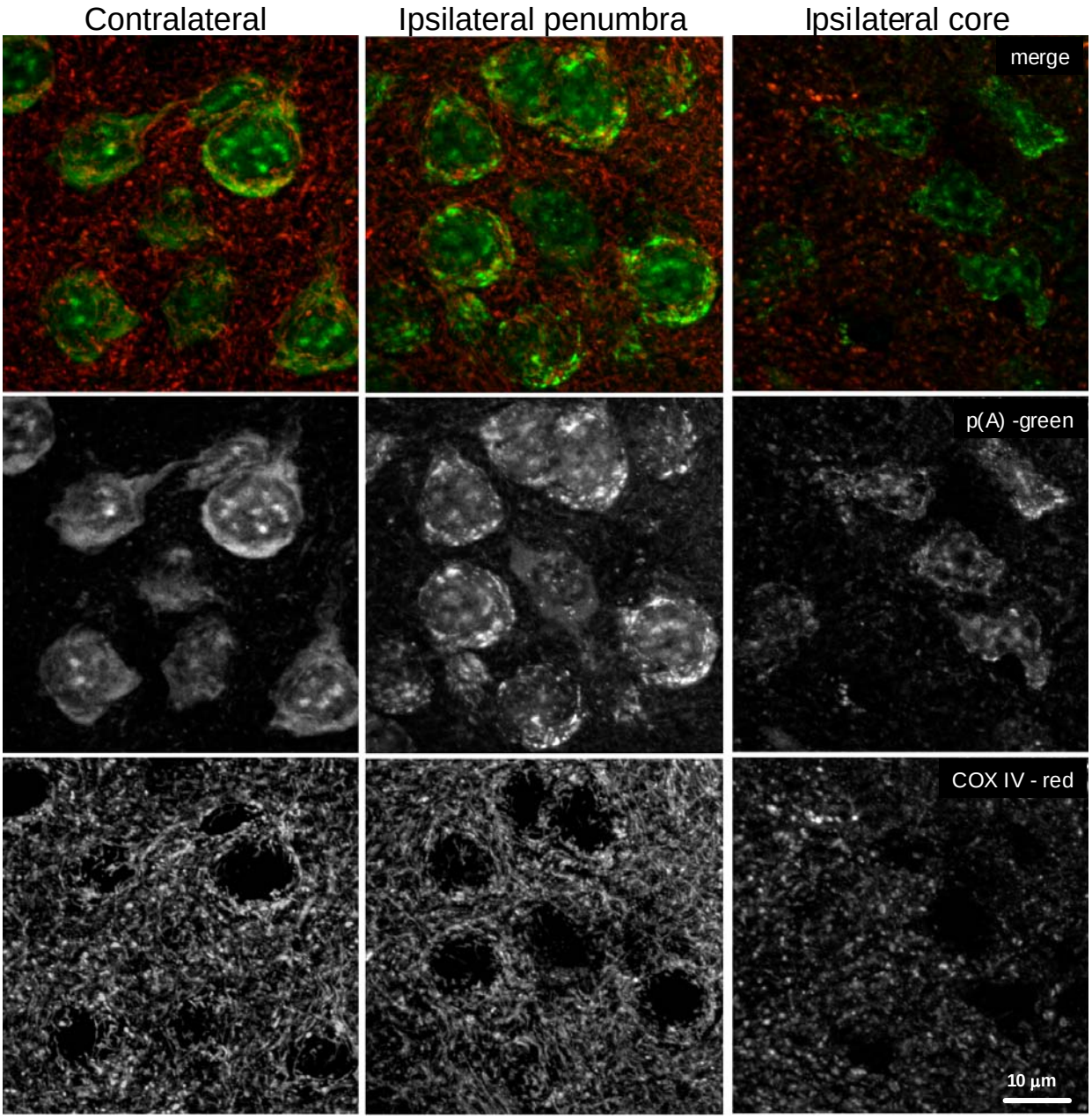

Figure 19: Layer II colocalization studies in Long Evans for pA & COX IV.
Double FISH/IF for poly-adenylated mRNAs [p(A), green channel], and COX IV (cytochrome c oxidase, subunit 4), a marker of the mitochondria (red channel) in layer II of cerebral cortex following 2 hrs permanent MCAO ischemia. Images taken from coronal section approximately 1 mm anterior to Bregma using the coordinates of Paxinos and Watson (1998). Scale bar in lower right panel is 10 microns and applies to all panels.

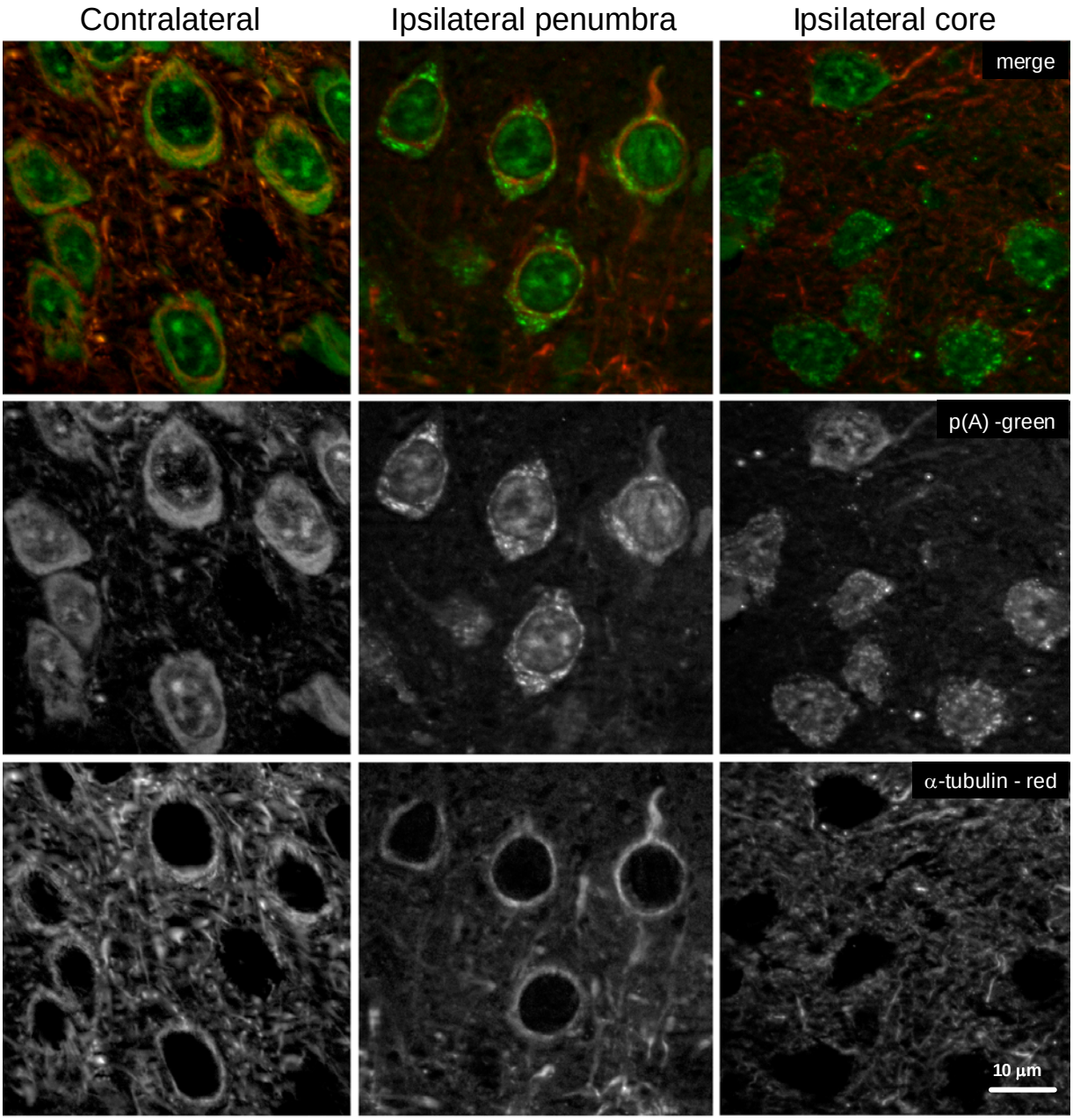

Figure 20: Layer II colocalization studies in Long Evans for pA & α-tubulin.
Double FISH/IF for poly-adenylated mRNAs [p(A), green channel], and α-tubulin, one of the main proteins of the microtubule component of the cytoskeleton (red channel) in layer II of cerebral cortex following 2 hrs permanent MCAO ischemia. Images taken from coronal section approximately 1 mm anterior to Bregma using the coordinates of Paxinos and Watson (1998). Scale bar in lower right panel is 10 microns and applies to all panels.

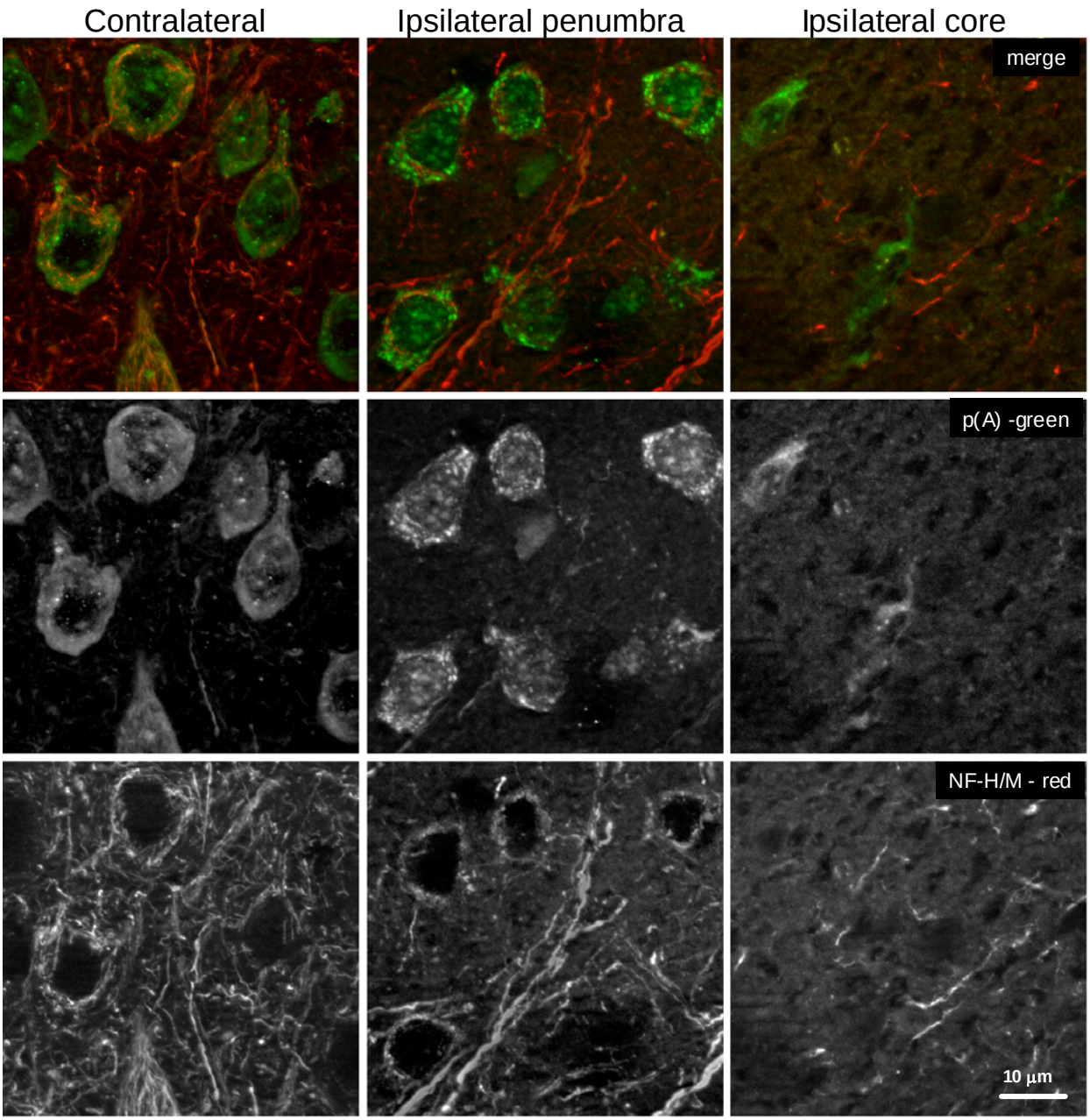

Figure 21: Layer II colocalization studies in Long Evans for pA & neurofilaments H and M. Double FISH/IF for poly-adenylated mRNAs [p(A), green channel], and neurofilaments H and M (NF-H/M), a marker of the intermediate filament component of the cytoskeleton (red channel) in layer II of cerebral cortex following 2 hrs permanent MCAO ischemia. Images taken from coronal section approximately 1 mm anterior to Bregma using the coordinates of Paxinos and Watson (1998). Scale bar in lower right panel is 10 microns and applies to all panels.

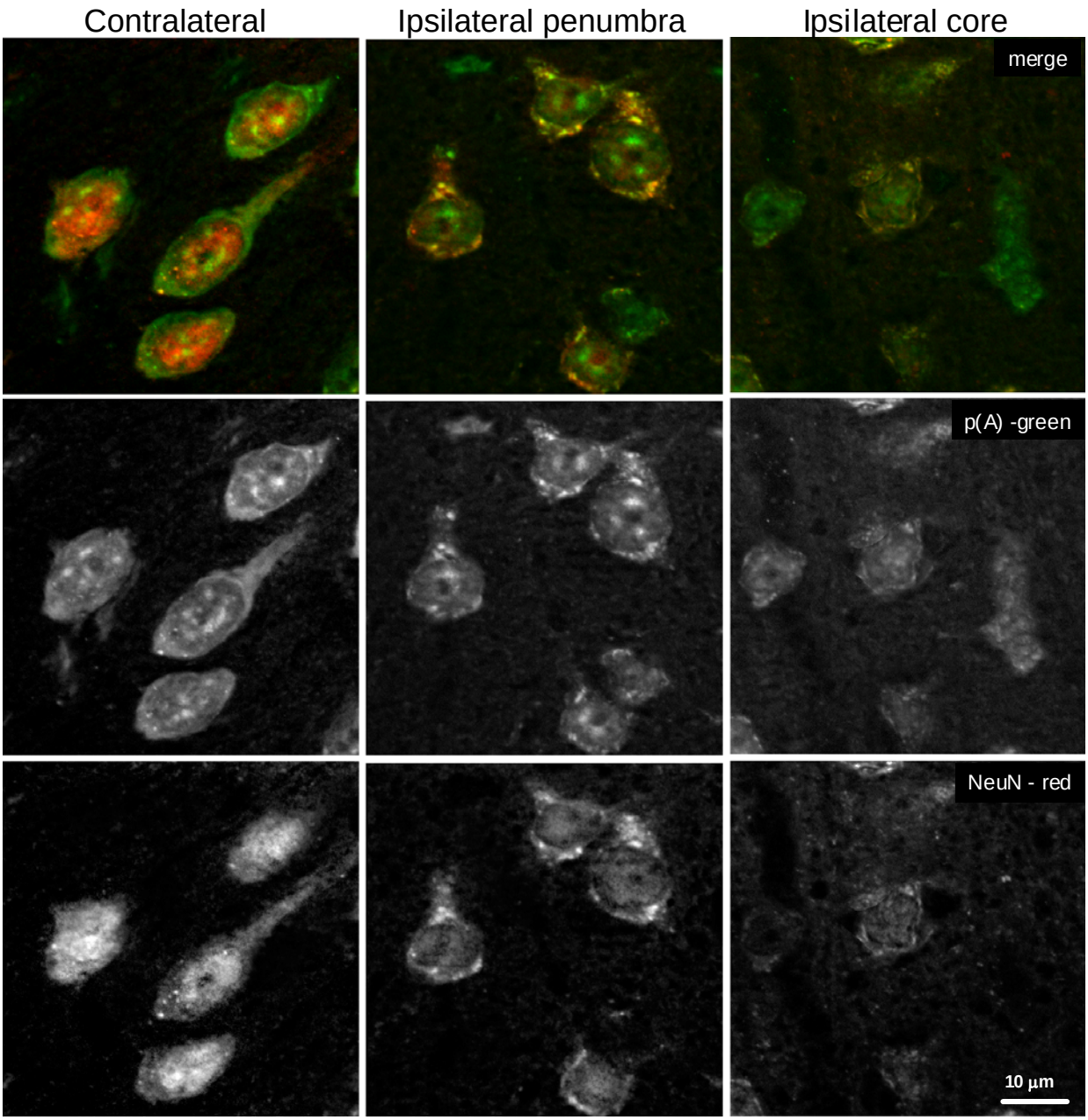

Figure 22: Layer II colocalization studies in Long Evans for pA & NeuN.
Double FISH/IF for poly-adenylated mRNAs [p(A), green channel], and NeuN, a marker of neuronal nuclei (red channel) in layer II of cerebral cortex following 2 hrs permanent MCAO ischemia. Images taken from coronal section approximately 1 mm anterior to Bregma using the coordinates of Paxinos and Watson (1998). Scale bar in lower right panel is 10 microns and applies to all panels.

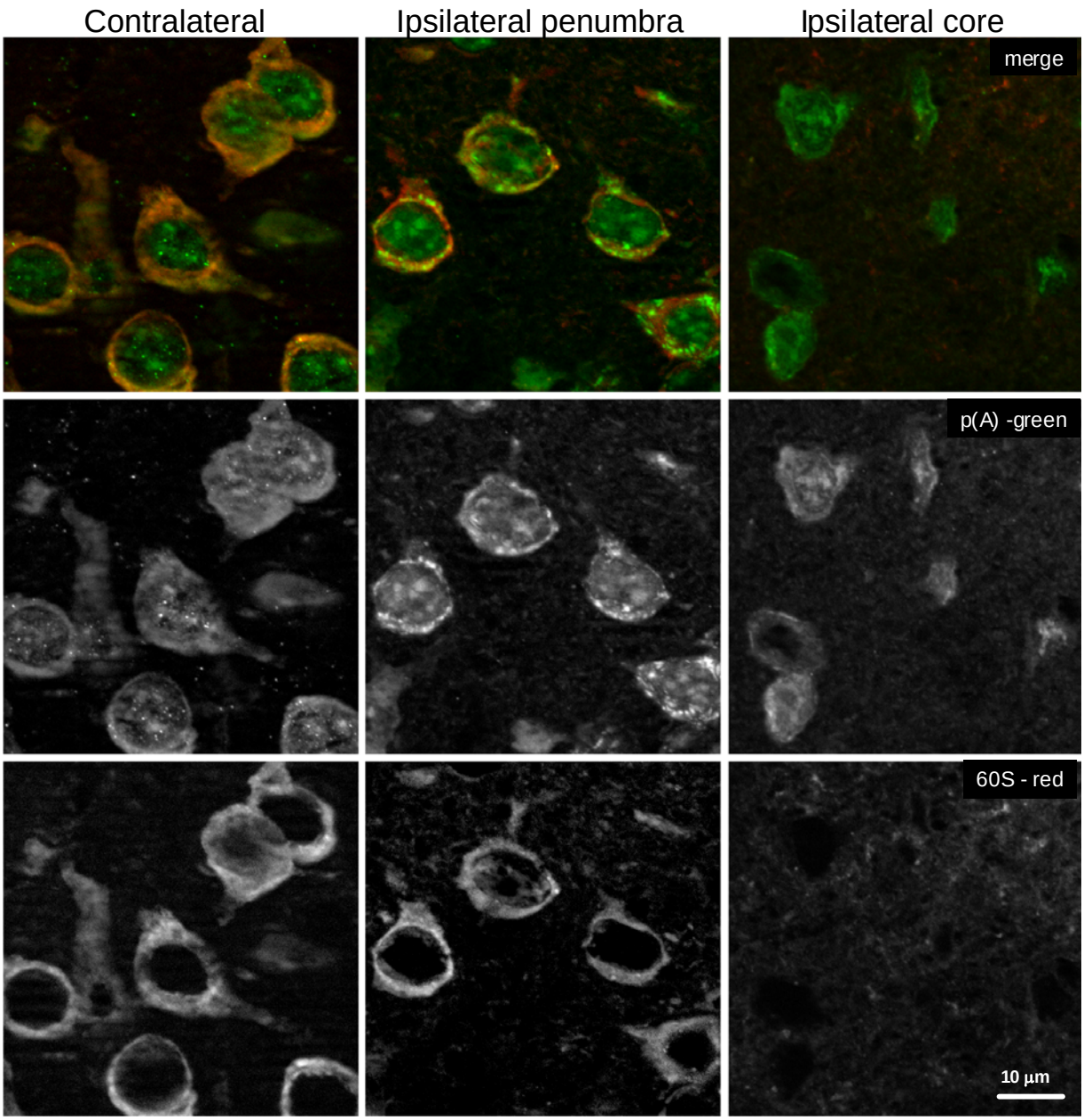

Figure 23: Layer II colocalization studies in Long Evans for pA & RPA.
Double FISH/IF for poly-adenylated mRNAs [p(A), green channel], and RPA, a marker of the large ribosomal subunit 60S (red channel) in layer II of cerebral cortex following 2 hrs permanent MCAO ischemia. Images taken from coronal section approximately 1 mm anterior to Bregma using the coordinates of Paxinos and Watson (1998). Scale bar in lower right panel is 10 microns and applies to all panels.

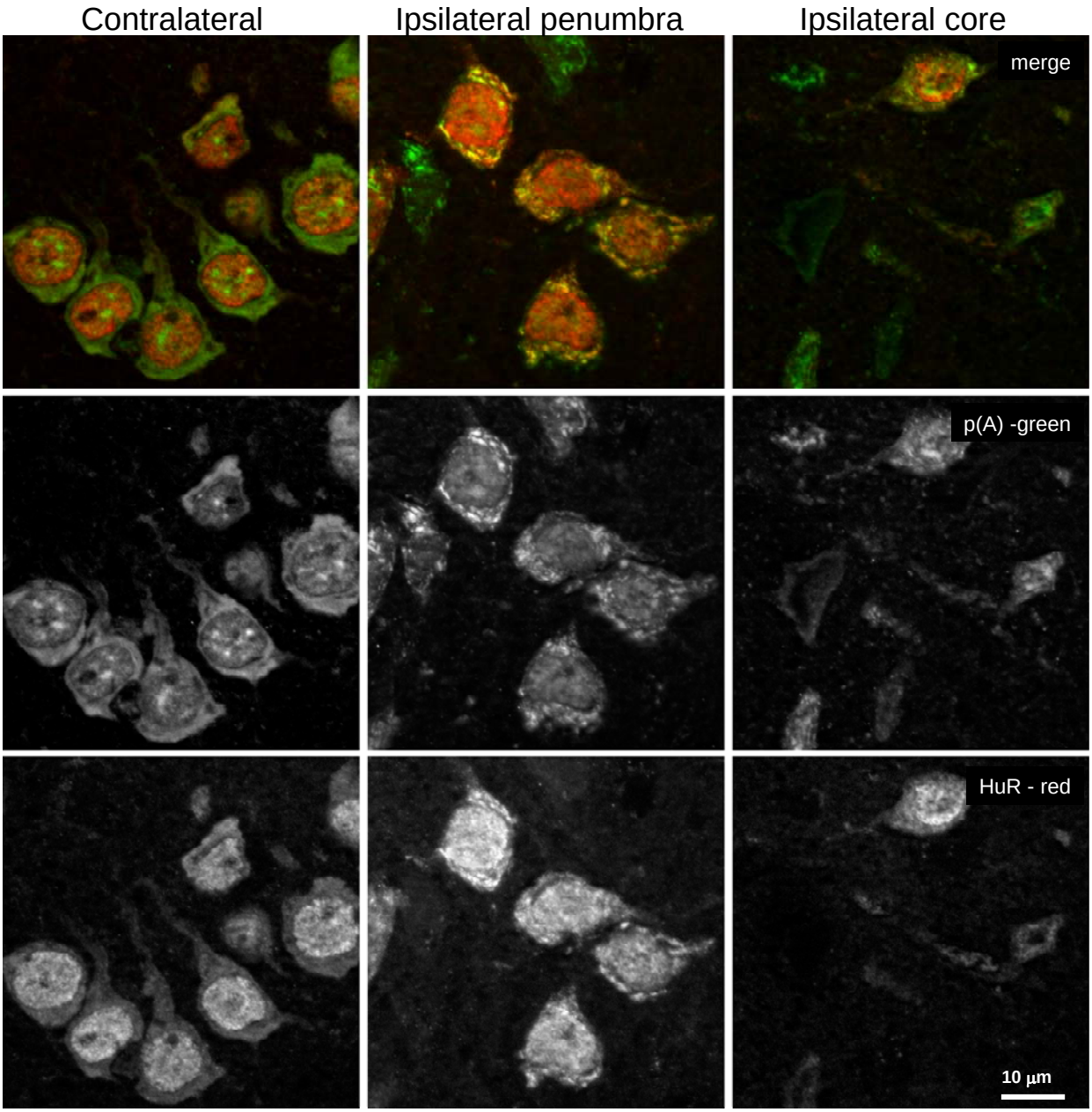

Figure 24: Layer II colocalization studies in Long Evans for pA & HuR.
Double FISH/IF for poly-adenylated mRNAs [p(A), green channel], and HuR, an mRNA binding protein that stabilizes adenine and uridine rich element (ARE)-containing mRNAs, in layer II of cerebral cortex following 2 hrs permanent MCAO ischemia. Images taken from coronal section approximately 1 mm anterior to Bregma using the coordinates of Paxinos and Watson (1998). Scale bar in lower right panel is 10 microns and applies to all panels.

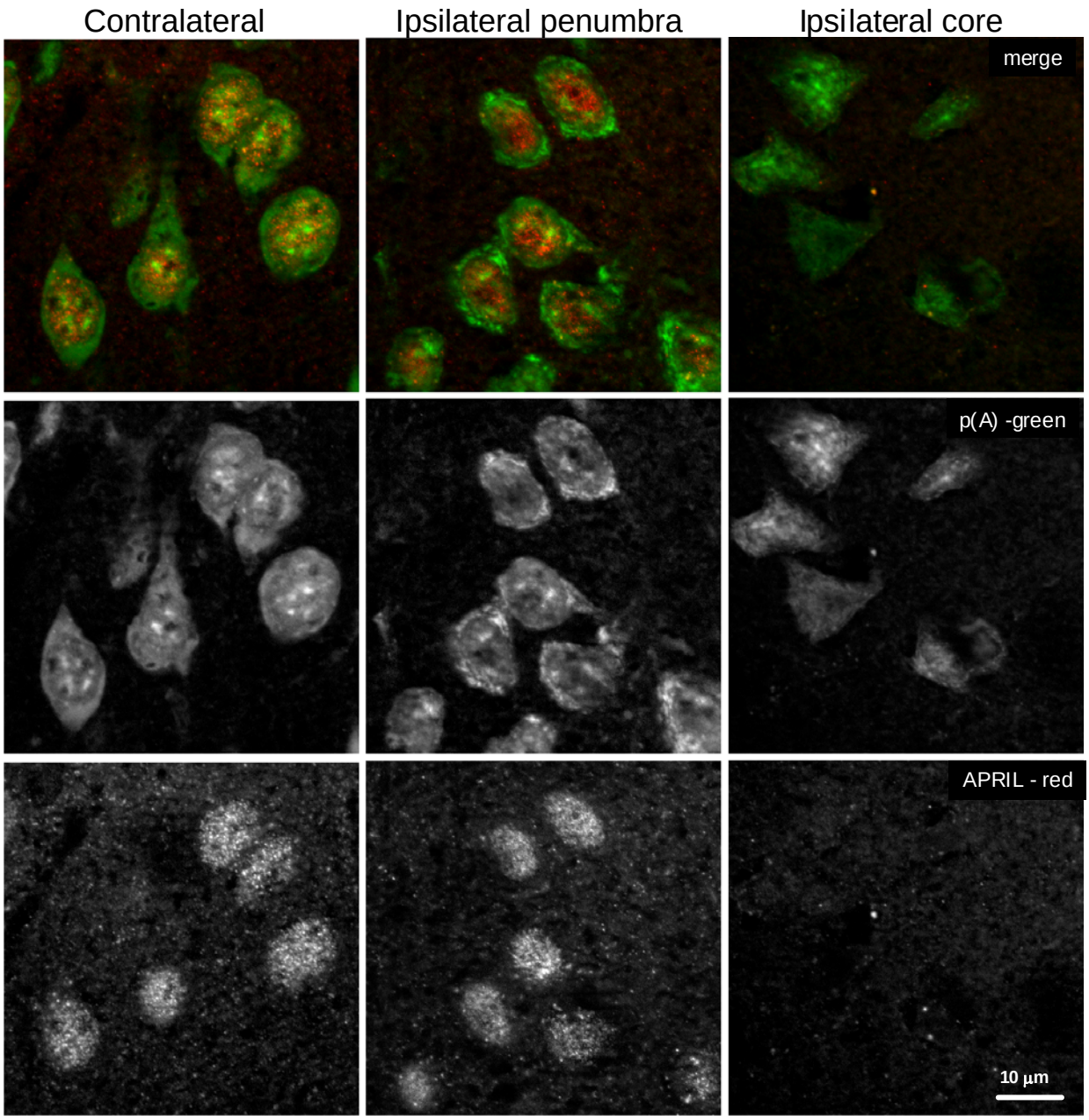

Figure 25: Layer II colocalization studies in Long Evans for pA & APRIL.
Double FISH/IF for poly-adenylated mRNAs [p(A), green channel], and APRIL (acidic protein rich in lysine), a HuR accessory protein (red channel) in layer II of cerebral cortex following 2 hrs permanent MCAO ischemia. Images taken from coronal section approximately 1 mm anterior to Bregma using the coordinates of Paxinos and Watson (1998). Scale bar in lower right panel is 10 microns and applies to all panels.

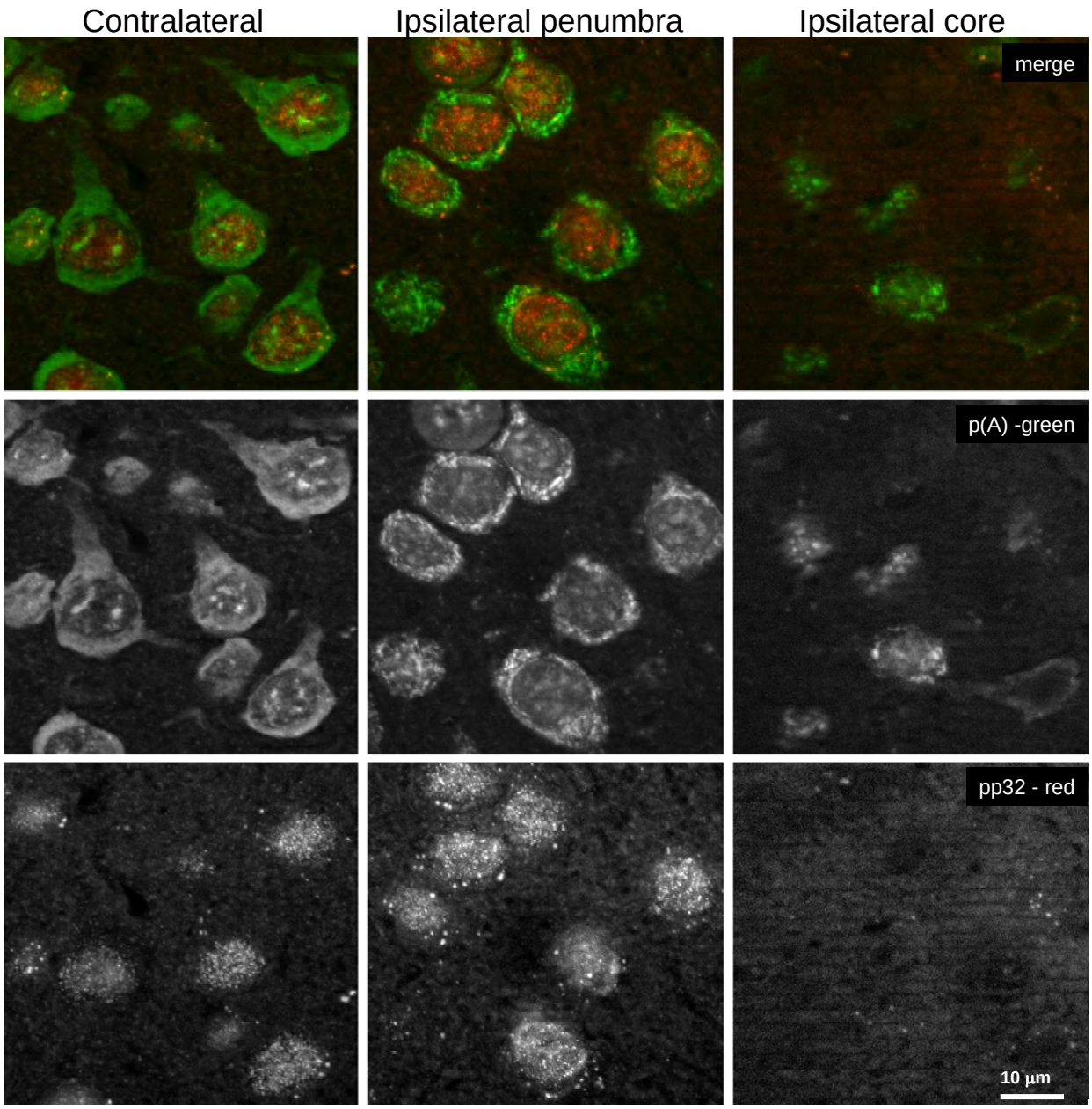

Figure 26: Layer II colocalization studies in Long Evans for pA & pp32.
Double FISH/IF for poly-adenylated mRNAs [p(A), green channel], and pp32 (red channel), a HuR accessory protein involved in mRNA nuclear export in layer II of cerebral cortex following 2 hrs permanent MCAO ischemia. Images taken from coronal section approximately 1 mm anterior to Bregma using the coordinates of Paxinos and Watson (1998). Scale bar in lower right panel is 10 microns and applies to all panels.

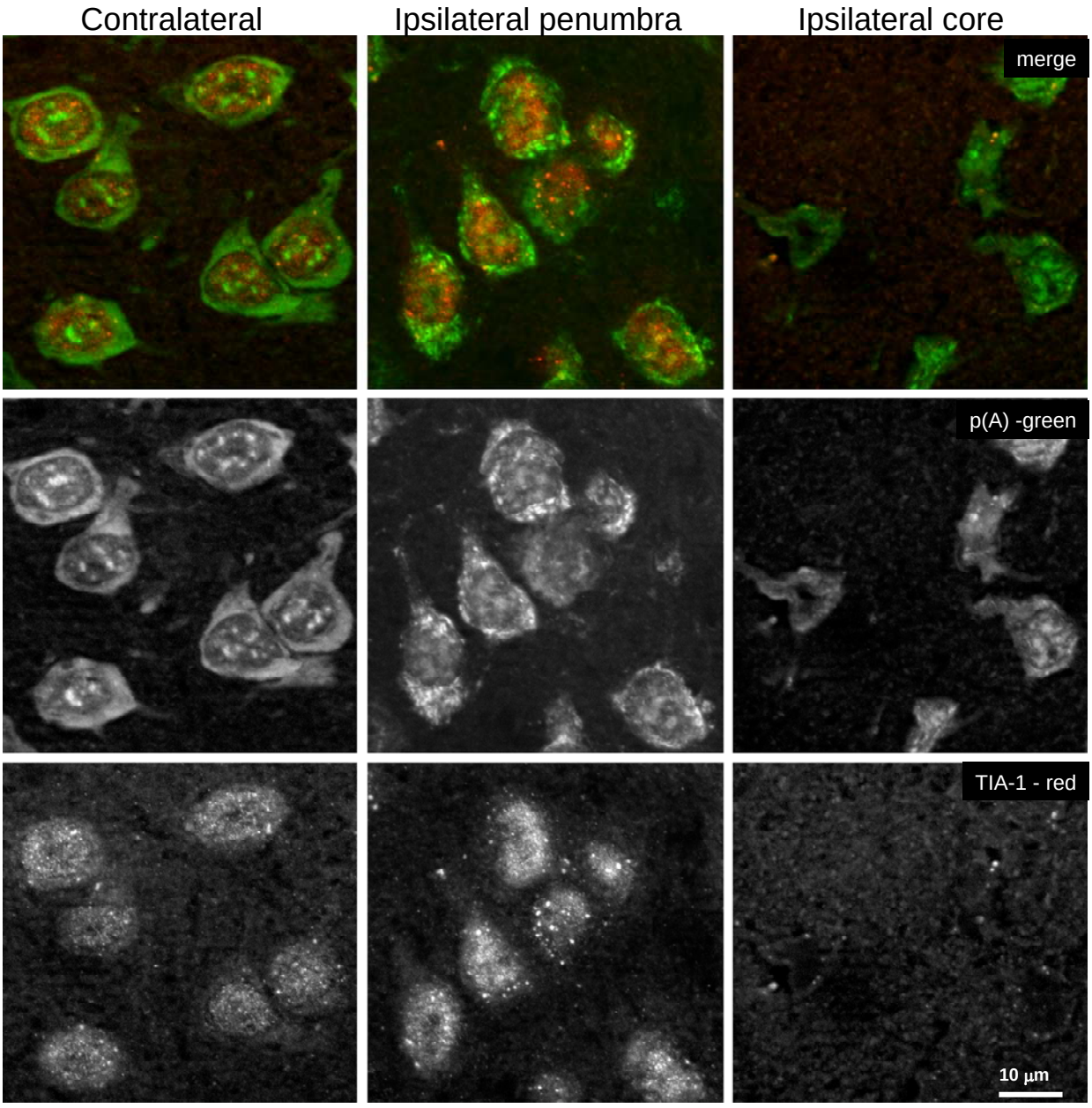

Figure 27: Layer II colocalization studies in Long Evans for pA & TIA-1.
Double FISH/IF for poly-adenylated mRNAs [p(A), green channel], and TIA-1 (red channel) , a canonical component of stress granules in layer II of cerebral cortex following 2 hrs permanent MCAO ischemia. Images taken from coronal section approximately 1 mm anterior to Bregma using the coordinates of Paxinos and Watson (1998). Scale bar in lower right panel is 10 microns and applies to all panels.

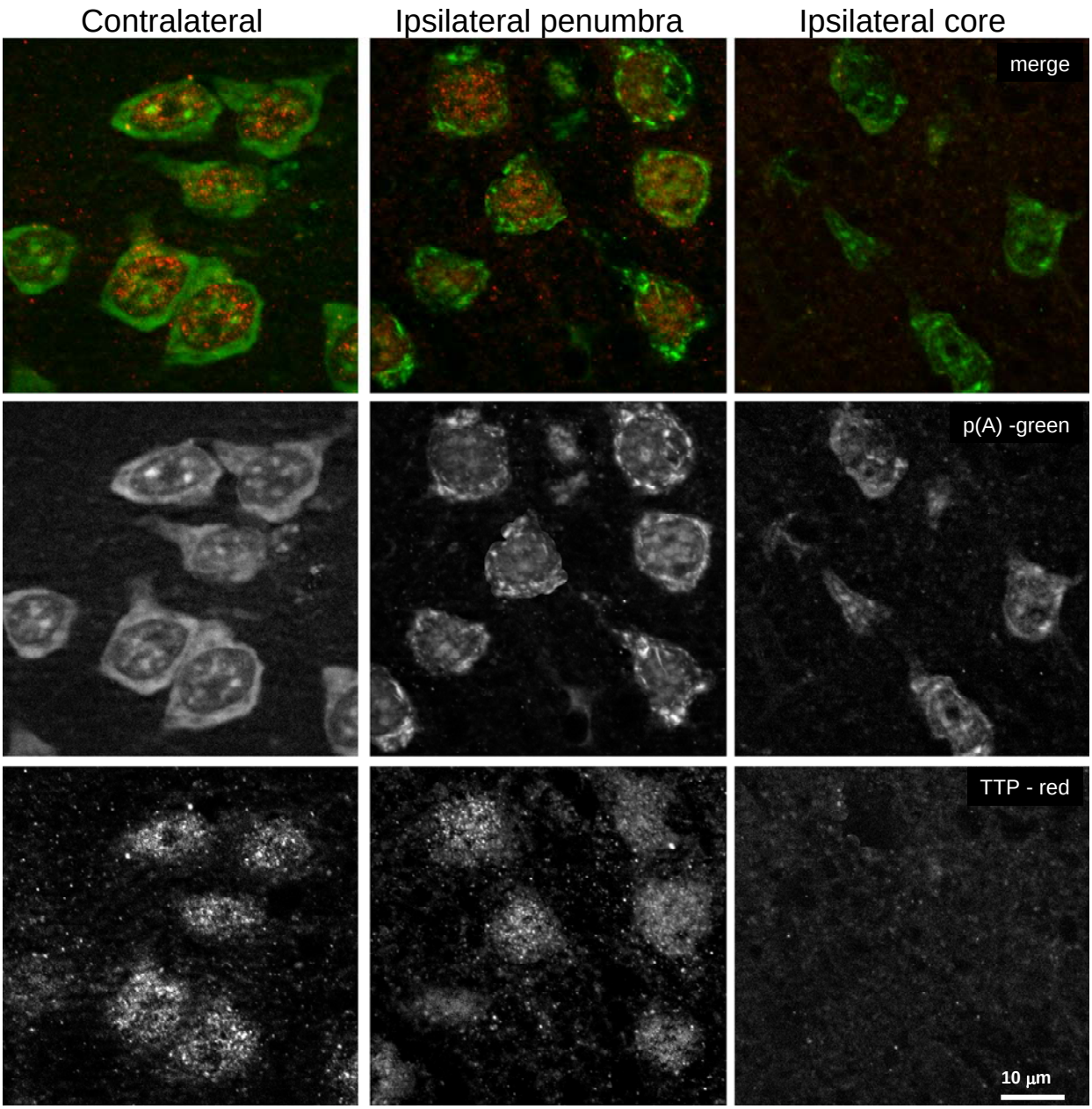

Figure 28: Layer II colocalization studies in Long Evans for pA & TTP.
Double FISH/IF for poly-adenylated mRNAs [p(A), green channel], and TTP (red channel), an enzyme involved in mRNA degradation and localized to processing bodies, in layer II of cerebral cortex following 2 hrs permanent MCAO ischemia. Images taken from coronal section approximately 1 mm anterior to Bregma using the coordinates of Paxinos and Watson (1998). Scale bar in lower right panel is 10 microns and applies to all panels.

Table 7: Summary of mRNA granule colocalization in Long Evans rats with pMCAO.

	Antigen	Marker of	CL with pA in contralateral cytoplasm	CL with mRNA granules	Figure No.
Organelle Markers	PDI	Endoplasmic reticulum	partial	No	16
	GM130	Cis-Golgi	No	No	17
	TGN38	Trans-Golgi	No	No	18
	Cytochrome C oxidase subunit IV	Mitochondria	No	No	19
	α-tubulin	Microtubules	No	No	20
	Neurofilament H/M	Intermediate filaments	No	No	21
	NeuN	Nucleus	No	Yes	22
mRNA binding proteins	Ribo P antigen	60S subunit	Yes	No	23
	HuR	mRNA BP	No	Yes	24
	APRIL	HuR cofactor	No	No	25
	pp32	HuR cofactor	Minor, punctate	No	26
	TIA-1	Stress granules	Minor, punctate	No	27
	TTP	Processing bodies	No	No	27

CL, colocalization. Other abbreviations as defined in the text.

CHAPTER FOUR: Effect of Diabetes - Methods and Results

I. Rationale

The systematic characterization of mRNA granule formation as a function of pMCAO duration in the Long Evans rat strain described in the previous chapter laid the framework to study the effect of diabetes on mRNA granule formation during focal cerebral ischemia. Combining the well-known fact that diabetes worsens outcome after focal ischemia with the new insight obtained from the time course and 3D distribution of neurons containing mRNA granules as a function of pMCAO duration described in Chapter 3 (Figure 15), it seemed reasonable to anticipate that diabetes might serve to accelerate the time course such that cessation of mRNA granule formation occurred at an earlier duration of pMCAO than the 8 hr pMCAO in the non-diabetics. I therefore repeated the design of the experimental groups in Chapter 3, but shortened the time course of pMCAO to cover the range 30 min to 6 hrs. Quite unexpectedly, this change did not make a difference to the results. As we describe in this chapter, diabetes completely inhibited mRNA granule formation in neurons during pMCAO.

II. Materials

STZ was purchased from Sigma Chemical Co. (St. Louis, MO). All other materials used were previously described in Chapters 2 and 3.

III. Methods

A. Animal model

An insulinopenic model of diabetes was induced in 8-week old male Long Evans rats by a single intraperitoneal (IP) injection of STZ (50 mg/kg dissolved in 0.1 mM sodium citrate, pH 4.5)[104,115]. Left hind limb saphenous vein blood samples were collected one week after STZ injection and plasma glucose was determined using an Accu-Chek® Advantage glucometer (Roche Diagnostics, Indianapolis, IN). Diabetes was defined by a blood glucose > 300 mg/dl,

with animals being used 4-6 weeks later without insulin supplements. Average blood glucose for the STZ-treated rats at the time of MCAO was 437 mg/dL ± 49.5. Unilateral focal brain ischemia was induced using the same model of MCAO described in Chapter 2. Diabetic experimental groups are listed in Table 8. NIC-d is the sham operated diabetic rats not subject to MCAO.

Table 8: Diabetic Long Evans experimental groups.

Experimental Group	Ischemia	Reperfusion	n
NIC-d	-	-	3
0.5I-d	30 min	-	4
1I-d	1hr	-	4
2I-d	2 hr	-	4
4I-d	4hr	-	4
6I-d	6hr	-	4

B. TTC staining

TTC staining was performed as described in Chapter 2. Only the 6I-d group was stained.

C. Immunofluorescence (IF) and Fluorescent in situ hybridization

Double-labeling PABP IF and pA FISH were performed as described in Chapter 2.

D. Volumetric reconstruction of pA staining

3D reconstruction of the brain following diabetes plus pMCAO was performed exactly as described in Chapter 3.

IV. Results

A. TTC staining

TTC staining was used to evaluate infarct volume in insulinopenic, chronically diabetic male Long Evans rats. Representative samples are shown in Figure 29. The NIC-d showed normal, deep red TTC staining, as did the 6I-d group. Since no infarct was observed in the 6I-d group, earlier time points of pMCAO were not tested for TTC staining.

Figure 29 : TTC staining in diabetic Long Evans rats following 6 hr pMCAO

B. Animal condition and mRNA granule frequency

Diabetic animals had average blood glucose of 437 ± 49.5 mg/dl and average weight loss of 4.57 ± 0.53 grams. This weight loss was not different from the variance of non-diabetic Long Evans used in Chapter 3. Three of the animals displayed muscle wasting and two of them developed cataracts.

Following histological examination of pA FISH/PABP IF stained slides no mRNA granules were detected in any neurons in any diabetic pMCAO group. The diabetic animals showed only shrunken and distorted, core-like areas of pA/PABP staining (data not shown, but essentially identical to Figure 14, top panel, core sample). Therefore, extensive colocalization studies such as described in Chapters 2 and 3 could not be performed.

C. Volumetric analysis

Volumetric analysis was performed as previously described in Chapter 3. Using the sequential cross sections, 3D volumes for the distorted/shrunken core neuronal phenotype of the experimental groups was generated (Figure 30). As indicated above, no mRNA granules were observed in neurons at any pMCAO duration, and therefore, reconstructed volumes show only the volumes of shrunken distorted neurons in red. Unlike the non-diabetics, some of the diabetic samples showed shrunken distorted neurons in the contralateral hemisphere and representative samples are shown for the 4I-d and 6I-d samples in Figure 30. One of the 1I-d samples and two each of the 4I-d and 6I-d samples showed bilateral damage. The volume of shrunken/distorted neurons in the contralateral hemisphere did not exceed 10% of the total affected volume.

Since no mRNA granules formed in neurons of diabetic MCAO animals, relative volumes could not be calculated. Instead, the "absolute" percent of affected brain was taken as the volume of core divided by the volume of one hemisphere of the LONI dataset and is plotted in Figure 30 (brown curve). In the 0.5I-d group, 27.7 ± 6.5% of the hemisphere volume had

shrunken/distorted neurons and this increased to 40.1 ± 9.0%, 46.9 ± 14% and 49.2 ± 17% at 1I, 4I and 6I, respectively. There was no statistical difference amongst the diabetic 1I, 4I and 6I groups, however, the 0.5I-d group differed statistically from the aforementioned groups (ANOVA $p = 0.044$, Tukey post hoc $p = 0.032$).

Also shown on the plot of Figure 30 is the percent of the LONI hemisphere volume taken up by the sum of the non-diabetic mRNA granule and non-diabetic core volumes (which had been shown as relative percents in Figure 15). When summed in this fashion the 1I, 2I, 4I and 8I percents of the LONI volume were 50.0 ± 26.9 %, 60.6 ± 15.8 %, 68.7 ± 11.3 %, and 63.7 ± 0.0 %, respectively. None of these summed volumes cleared statistically. Further, when an ANOVA was run comparing the 2I and 4I pMCAO time points between the diabetic and non-diabetic samples, these did not clear statistically (ANOVA $p = 0.327$).

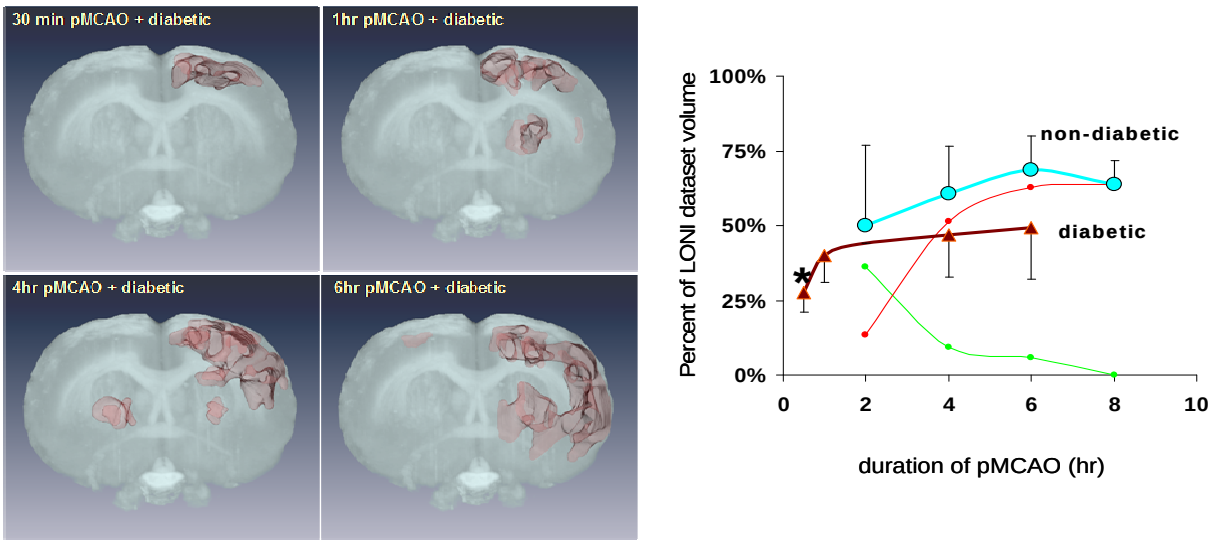

Figure 30: 3D reconstructions following pMCAO in diabetic rats.
Left: Representative 3D reconstructions of volumes of tissue containing shrunken/distorted neurons as identified by PABP/pA IF/FISH. Right: Percent of one hemisphere of the LONI dataset occupied by the core volume in diabetics (brown curve) or the core plus mRNA granule-containing volumes of the non-diabetics (cyan curve). The red and green curves are the averages of the volumes of the core and mRNA granule volumes, respectively, that are summed together to form the cyan curve. Red and green curves are shown for reference, and are shown without error bars to minimize distractions on the chart. Error bars on the cyan curve are the combined errors of the sum of the red and green curves. * Post hoc $p < 0.05$ for 0.5I-d compared to other diabetic groups.

There are two interesting conclusions drawn from the plot in Figure 30. First, diabetes did not increase the total volume of tissue affected by the pMCAO. The total volumes in both the diabetic and non-diabetic samples converged to roughly 50% of the reference volume, which was taken as one hemisphere of the rendered LONI dataset. Instead, and contrary to my hypothesis, diabetes did not increase the extent of injury after MCAO; it completely inhibited formation of the mRNA granules at any time point of MCAO.

Second, when the non-diabetic data is expressed as a percent of the reference volume, the sum of the mRNA granule-containing volume and the core volumes was essentially constant. As can be seen from the red and green lines on the plot of Figure 30, there was an exponential conversion of the mRNA granule containing volume to core volume as the duration of pMCAO increased.

CHAPTER FIVE: Discussion

I. Summary of Results

In the previous chapters I have described my studies assessing the histology of pA mRNAs in the rodent brain following focal ischemia. My main findings were:

1. In Wistar rats no infarct was detected out to 7 days reperfusion after 2 hr MCAO. Granulation of mRNA was sporadic and occurred at low frequency only in the 2I samples and was unaffected by anesthetic. The mRNA granules detected had the colocalization properties seen after global brain ischemia[102].
2. The frequency of mRNA granule-containing neurons was much greater in the Long Evans rat strain in the 2I group compared to the Wistar strain. Following 2 hr MCAO and 24 hr reperfusion, Long Evans rat brains showed a necrotic core.
3. The mRNA granules in the Long Evans rats following pMCAO…
    a. Were detected in layers II/III, V and VI of cerebral cortex, and striatum, and they occurred in ipsilateral penumbra.
    b. Had the colocalization properties seen after global brain ischemia[102].
    c. Did not colocalize with markers of ribosomal subunits or organelles but did colocalize with NeuN.
    d. Decreased in frequency with increased during of pMCAO and were not detected in the 8I group.
4. The volume occupied by mRNA granule-containing neurons transformed into a core-like shrunken and distorted neuronal phenotype with increased duration of pMCAO.
5. Diabetes inhibited formation of mRNA granules in neurons at all durations of pMCAO tested.
6. The volume of tissue showing distorted/shrunken neurons in diabetic samples approached

the same volume of core tissue in non-diabetics with increased duration of pMCAO.

In this chapter I will discuss the significance of these findings with respect to other studies in the literature and also with respect to new insights they provide about the response of the brain to focal ischemia and the response of the diabetic brain to focal ischemia.

II. Differences between Rat Strains

To begin, there was a striking difference in the way the Wistar and Long Evans rats responded to MCAO ischemia. Previous studies from other labs indicate a number of factors that would predispose the Wistar strain to be more resistant to a given ischemic stimulus compared to the Long Evans strain.

A. Strain Differences in Outcome

Wistar rats, compared to other common laboratory rat strains, were shown to have a greater number of MCA-ACA anastomoses or collaterals[106]. Collateral flow becomes important during focal ischemia to compensate in regions downstream of a focal occlusion[124] to increase blood flow to core and penumbra[116]. The importance of collateral flow was demonstrated by Oliff *et al*. who showed that when collateral flow was reduced by bilateral CCA occlusion, there was a significant increase in the mean cortical infarct volume[116,124]. In addition, subcortical regions like the striatum receive blood supply almost exclusively from the lateral striate arteries that originate from the MCA. Since these arteries are end-arterioles, the caudate-putamen does not receive sufficient collateral blood flow to keep the tissue viable following MCAO[106]. Most of the strain difference findings suggest that variations in outcome of focal ischemia may not be a technical issue, but may have to do with the type of animals used[116]. Thus, increased collateral blood flow is one explanation of why Wistar rats were more resistant to focal ischemia compared to Long Evans rats[106,116].

In addition to vascular anatomical differences, using laser Doppler flowmetry, Long

Evans rats demonstrated a more persistent and pronounced stable drop in cortical local cerebral blood flow (LCBF) (74.6 ± 8.9%) following 60 minutes of transient MCAO when compared to Wistar rats (49.0 ± 21.9%)[117]. The differences in blood flow could not be fully accounted for by anatomical differences in the vasculature and these authors speculated that intrinsic blood flow regulatory mechanisms may be more robust in the Wistar strain.

Factors such as these, allowing Wistars to maintain a higher blood flow during the MCAO period, could explain why, after 2 hr MCAO, the Wistar rat failed to show an infarct even out to 7 days reperfusion and the Long Evans strain showed an infarct at 24 hr reperfusion.

B. Strain Differences in mRNA granule Formation

The studies described above can also be used to explain why the incidence of mRNA granule formation was so much less in the Wistar compared to the Long Evans rats. Work from Hossmann's lab has measured many different metabolic and functional thresholds that occur at specific decrements of cerebral blood flow (CBF)[124]. For example, CBF must decrease below 20% for ATP levels to drop precipitously and for neurons to dissipate ion gradients[118]. Hossmann has documented that the threshold for TA occurs at ~ 50% reduction in CBF[119]. Based on the CBF study conducted by Prieto *et al*[117], CBF during MCAO averages around 50% in the Wistar, but averages around 30% for the Long Evans. Thus, the Wistar, on average, hovers at the threshold of TA onset, but the Long Evans is substantially below the 50% CBF threshold. Formation of mRNA granules has been shown to be a morphological correlate of TA[102], specifically because mRNA is sequestered away from ribosomal subunits. Therefore, the same explanation for improved outcome in the Wistar strain also provides a plausible explanation for the relative lack of mRNA granule formation following MCAO in this strain. Although protein synthesis was not directly measured in the studies described here, my results lead to the prediction that there would not be a cessation of protein synthesis in the Wistar brain

at least out to 2 hr MCAO and for any subsequent reperfusion duration. Indirect support for this prediction from the present studies was that I observed the successful translation of HSP70 protein in the Wistar strain at various durations of reperfusion (Figure 9). It is well documented that HSP70 translation does not occur in neurons destined to die by DND in both focal and global brain ischemia models, specifically because of the prolonged TA[1,86].

III. mRNA Granules in Focal Ischemic Neurons

Our previous study showed mRNA granules form following global brain ischemia[102]. The present study is the first demonstration of mRNA granule formation following focal brain ischemia. I performed extensive colocalization studies (Figure 12 and Figure 13) in order to determine if the mRNA granules that formed following focal ischemia were the same as those in the global model. Furthermore, I have extended the colocalization studies beyond those we published in the global model to assess cell organelles and additional mRNA binding proteins (Figures 16-28).

As stated above, the mRNA granules seen after MCAO failed to colocalize with the 40S and 60S ribosomal subunits. Presently, this is their most important characteristic as it provides an explanation for what has been an outstanding unresolved problem in the field, which is the cause of prolonged TA in post-ischemic brain neurons.

However, the additional colocalization studies begin to address more specifically what the mRNA granules are, and are not. They did not colocalize with markers of the ER or for cis- and trans-Golgi network. Thus, even though the mRNA granules are intimately involved with the translational system, they are not involved in the main proximal secretory systems for secreted and membrane localized protein synthesis. I also tested two markers of the cytoskeleton: α-tubulin and neurofilament proteins H/M. The lack of colocalization indicates the mRNA granules are not formed in association with microtubules or intermediate filaments. I had

tried several actin antibodies to look at the actin system, but was unable to get any of the tested actin antibodies to work in the FISH/IF double labeling procedure. Thus, the association of mRNA granules with the microfilament system is unresolved by my studies. The mRNA granules also did not colocalize with COX IV, a mitochondrial marker. Therefore, my studies rule out these organelle systems as playing a direct role in mRNA granule function.

Similar to the results with global brain ischemia[102], the mRNA granules did not colocalize with TIA-1 or TTP and therefore are not stress granules or processing bodies. They did colocalize with the known mRNA binding proteins PABP and HuR. Thus, the mRNA granules observed in the focal model are very similar to, if not identical to, those observed following global brain I/R.

However, one surprising finding was the colocalization of the cytoplasmic mRNA granules with NeuN, a neuronal nuclei marker. A recent study identified NeuN as the sequence-specific mRNA splicing factor Fox-3. Fox-3 is a component of nuclear speckles, which are morphological structures of the nuclear transcription and mRNA processing machinery that interacts with the nuclear matrix[120]. That NeuN has been identified as a protein involved in nuclear mRNA processing is consistent with our observation that NeuN colocalized in the mRNA granules. Furthermore, our result suggests that NeuN may function similarly to TIA-1, TTP and HuR, all of which are nuclear proteins involved in mRNA processing, but which translocate to the cytoplasm during cell stress and play roles in the ribonomic systems[76-81].

Since the mRNA granules colocalized with HuR, we tested two proteins known to function with HuR during the heat shock response: APRIL and pp32. Both of these proteins bind to and complex with HuR and its client mRNAs to mediate nuclear to cytoplasmic translocation of mRNAs upregulated during heat shock[79,80]. The logic of testing APRIL and pp32 was that if they colocalized with HuR and the mRNA granules, it would suggest all three

proteins were playing a role in the nuclear export of mRNAs. However, neither APRIL or pp32 colocalized in the mRNA granules, and this suggests HuR may be mediating a function different from that identified by the Steitz lab[79].

To summarize the colocalization studies, the mRNA granules detected after MCAO share the same characteristics as those seen after global ischemia, indicating they are likely the same structures. Further, the mRNA granules are not substantially colocalized with organelles but only select mRNA binding proteins.

IV. Time Course of mRNA granules in pMCAO

The observation that the relative proportions of mRNA granule-containing neurons decreased with pMCAO (plot, Figure 15), but that the sum of the volumes of mRNA granule-containing plus core-like neurons remained constant with pMCAO duration (plot, Figure 30) is one of the significant findings of my work. This observation is relevant to how penumbral neurons convert to core neurons and my findings contribute new insights to how this occurs.

As stated in the Background, rescuing the penumbra in an effort to improve outcome following an ischemic event is the goal of stroke research. There are two general approaches to stroke therapy. Therapies that induce reperfusion have had some success via surgical techniques and with application of tissue plasminogen activator (tPA). But even tPA usage occurs at the risk of hemo-compromising patients[121]. Neuroprotective strategies to halt the cause of cell death of penumbral neurons have been spectacular failures: every single one of over 100 clinical trials of stroke neuroprotection have failed[122,123]. Thus, the new insights into how potentially salvageable penumbral neurons convert to core-like neurons irreversibly committed to die are significant for the possibility of offering new neuroprotective strategies in the long run.

There are different mechanisms of penumbra-core conversion whether focal ischemia is transient or permanent, and whether the ischemia is occlusive or hemorrhagic[124]. Since I only

investigated permanent occlusive focal ischemia, my work applies only to this case.

The two images shown in Figure 31 are taken from a 2009 review by Hossmann on the pathophysiology of stroke injury and show the changes in the brain following pMCAO. The plot in Figure 31A shows how blood flow changes throughout the core area as a function of pMCAO duration. CBF is initially at its lowest, but increases somewhat as collateral circulation compensates for the occlusion. It should be noted he shows CBF to decrease to zero, but above I discussed that the average CBF decreases during rodent MCAO range from ~ 20-50% normal CBF.

The plot in Figure 31B shows the evolution of the infarct core with pMCAO duration. It can be seen how this rapidly increases and is almost maximum at 3 hr pMCAO and is maximum by 6 hr pMCAO. I have added to Figure 31B the curve of my results of the decrease in the volume of tissue where the neurons contained mRNA granules (green curve). It is striking that the decrease in mRNA granules is roughly a mirror image of the evolution of the infarct core. This decrease occurs in spite of the minor increase in CBF shown in the plot in A. Thus, the loss of ability of neurons to form mRNA granules directly correlates with production of infarct core.

It is also significant that I observed a rapid loss of mRNA-granule containing neurons between 2 and 4 hr pMCAO. This is precisely the time window that Hossmann has indicated as "therapeutic window" on his plot in Figure 31B. This correspondence would suggest that if we understood exactly why the neurons lost the ability to form mRNA granules with increased pMCAO duration, that this might be an important therapeutic target, and perhaps extend the duration of the "therapeutic window" shown in Dr. Hossmann's graph.

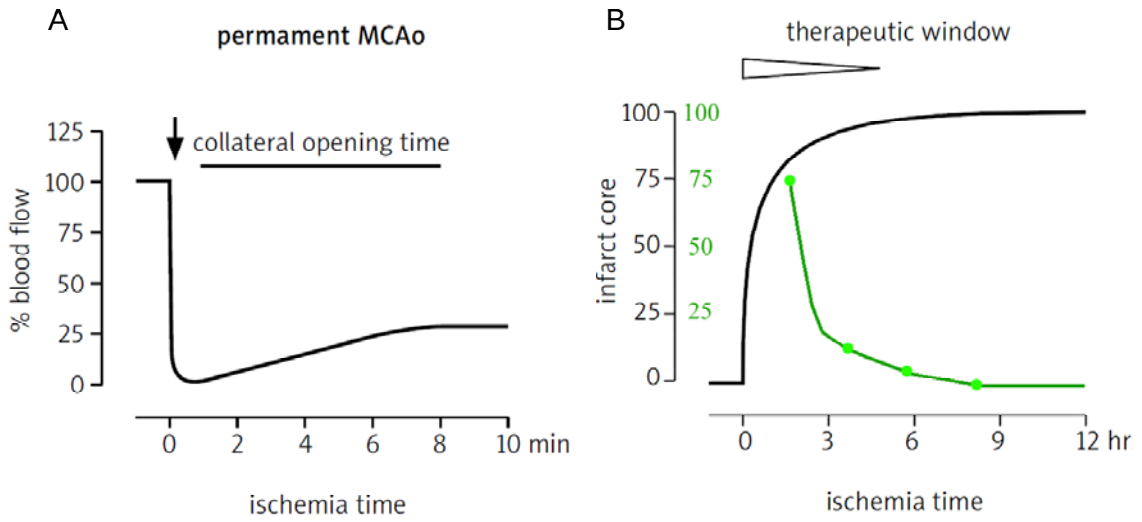

Figure 31: Changes in blood flow and core evolution during pMCAO. Adapted from [124].

V. Inhibition of mRNA Granulation by Diabetes

It was an unexpected finding that diabetes led to a complete inhibition of mRNA granule formation. It is well known that chronic diabetes causes a plethora of complications all of which have a negative impact on stroke outcome. These can be classified into three general categories: immunological, vascular and cellular. Each could plausibly contribute to the inhibition of the mRNA granules.

There is a series of processes in the inflammatory response that are associated with post-ischemic reperfusion that exacerbate brain injury even when diabetes is not present[115]. Chronic diabetes induces exaggerated inflammatory responses to brain I/R due to increase in leukocyte adhesion and emigration mediated by CD11/CD18-ICAM-1 and P-selectin and albumin leakages[125]. Matrix metalloproteinases (MMP), which are involved in the physiological turnover of the extracellular matrix, contribute to blood brain barrier leakage and cellular damage following focal brain I/R. MMP-2 and MMP-9 have been implicated in cerebral ischemia. MMP-9 is normally absent in brain but upregulated in response to injury. Early inhibition of MMP-9 led to reduction in infarct size at two weeks following permanent MCAO[125]. Such

adverse inflammatory responses would converge to create an extracellular environment that would upset the highly specific conditions required for neuronal function. In this way, inflammatory factors would serve to generally decrease neuronal fidelity, and this may contribute to diabetes inhibition of mRNA granule formation.

There is an increased risk of endothelial cell dysfunction and vascular smooth muscle impairment associated with chronic diabetes.[19] Diabetics were also shown to have impaired endothelium-dependent, nitric oxide-mediated vasodilation[126]. Hyperglycemia inhibits the production of nitric oxide via eNOS activation, thus blocking a potent vasodilator. Furthermore, when diabetes is present, there is also an increase in the production of vasoconstrictors, such as endothelin-1[127]. Studies have also shown impairment in collateral recruitment in chronic diabetes.[128]. Such vascular abnormalities in chronic diabetes may also contribute to the inhibition of mRNA granules in penumbral neurons, following diabetic MCAO. The vascular abnormalities would collectively serve to increase the intensity of the ischemic insult following MCAO, rendering the neurons incapable to respond properly to stress and leading to a greater volume of core-like neurons.

Finally, diabetes alters intracellular conditions in generally adverse ways. Examples include: decreased pH of the cytoplasm[129], increased production of free radical species[130,131], inhibition of the oxidative phosphorylation of mitochondria[132], and the activation of the intrinsic apoptotic pathways[96,104]. All of these are direct forms of damage inside the neuron, and as such, they could converge to inhibit the molecular mechanism of mRNA granule formation. For example, one could hypothesize that some crucial or rate limiting component needed for the formation of the mRNA granules is damaged by oxidative stress, or altered intracellular pH, rendering them inactive. Another possible mechanism is that some crucial component of the mRNA granules is a substrate of caspase 3 and degraded.

Thus, there are a number of plausible, experimentally testable hypotheses as to why diabetes inhibits mRNA granule formation.

VI. Limitations of the Present Studies

There are several limitations of the present study.

1. On one hand, the present study could be considered to be purely descriptive. There were no drug interventions or genetic knockouts used in the present work in the attempt to establish mechanism by the currently acceptable route. On the other hand, a histological demonstration that mRNA does not colocalize with ribosomal subunits is itself a mechanism of TA, one that has eluded 40 years of biochemical and molecular biological studies on ischemic brains. Whether one frames the present work as descriptive or mechanistic, it has clearly identified new phenomena that open up new and clinically important lines of research into two of the biggest clinical problems today: stroke and diabetes.
2. No attempt was made to ascertain information about molecular mechanisms of the formation or the function of the mRNA granules. However, that diabetes inhibits their formation provides a system that can be used in the future to begin to address the mechanisms of their formation.
3. As described in the previous section, diabetes leads to a large number of possible mechanisms for the inhibition of mRNA granule formation. The present studies did not investigate any of these.

VII. Future Directions

Future directions follow directly from the limitations of the present study:

1. Seek information about the molecular mechanisms of mRNA granule formation, and about their role and function in the neurons of the ischemic and reperfused brain. Some

ways to begin to move in this direction would be to use specific pharmacologic agents or to use genetic knockouts to assess the role of specific proteins in either mRNA granule formation of function. For example, as described in Background, Ca^{2+} ion is a critical trigger for many subsequent molecular changes in the neurons after ischemia. Calcium channel blockers or NMDA antagonists could be used to determine if Ca^{2+} also plays an upstream role in mRNA granule formation. Another example would be to administer agents that directly alter the translational system. For example, cycloheximide is a well known protein synthesis inhibitor whose mode of operation is to prevent polysomes from dissociating. Since it is well known that polysomes dissociate in neurons after I/R, would preventing their dissociation with cycloheximide alter mRNA granule formation? Genetically altered mice could also be used in a similar fashion to test the role of specific proteins.

2. The present work studied specifically mRNA granules after pMCAO. Now that the time course of mRNA granule formation in pMCAO has been identified, the next step is to study a time course of transient MCAO, and assess the mRNA granules and how they correlate with outcome. For example, I can now predict that following 2hr MCAO, there should be mRNA granules for at least some duration of subsequent reperfusion. However, following 8 hr MCAO, there should be no mRNA granules at subsequent reperfusion durations.
3. Another future direction is to begin to study specific adverse effects of diabetes to see which may be involved in the inhibition of mRNA granule formation. Some of these effects can be separated from diabetes, such as hyperglycemia.

VIII. Summary and Conclusions

I had hypothesized that mRNA granules form in brain after focal ischemia. My research

showed how this phenomenon is dependent on the strain used, which, based on information from the literature, was related to blood flow rates during MCAO, and hence the amount or degree of ischemia generated in the different rat strains. I have contributed new insights into how penumbral brain tissue converts to core as ischemia duration increases. Neurons that might have survived at lesser durations of focal ischemia no longer form mRNA granules with increased ischemia duration. Previously this had been understood only in terms of "threshold" magnitudes[118], but my work begins to identify specific cellular mechanisms mediating this conversion in neuronal phenotypes. Finally, the work reported here discovered the unexpected finding that diabetes completely abrogates the mRNA granule response in the neurons of the focal ischemic brain. This adds an additional effect of diabetes on brain that clearly will contribute to worsened outcome in the diabetic brain after stroke and opens up a new line of investigation into how diabetes exerts adverse affect on ribonomic pathways in neurons.

As the work I did relied on the work of other researchers before me, I sincerely hope my work can be a stepping stone for future studies that will lead to a clear and full understanding of the insidious effects of both diabetes and stroke and lead one day to successful treatments that can alleviate the pain and suffering of both stroke victims and diabetic patients.

REFERENCES

[1] Hossmann KA. Disturbances of cerebral protein synthesis and ischemic cell death. Prog Brain Res 1993; 96:161-77.

[2] Althausen S, Mengesdorf T, Mies G, Olah L, Nairn AC, Proud CG, Paschen W. Changes in the phosphorylation of initiation factor eIF-2α elongation factor eEF-2 and p70 S6 kinase after transient focal cerebral ischemia in mice. J. Neurochem. 2001; 78: 779-787.

[3] Chong JY, Sacco RL. Epidemiology of stroke in young adults: race/ethnic differences. J. Throm. Thrombolysis 2005 Oct:20(2): 77-83

[4] Caplan LR. Transient ischemic attack: definition and natural history. Curr Atheroscler Rep. 2006 Jul;8(4):276-80.

[5] Lipton P. Ischemic cell death in brain neurons. Physiol Rev. 1999 Oct;79(4):1431-568.

[6] Kirino T. Ischemic Tolerance. J Cereb Blood Flow Metab. 2002 Nov;22(11):1283-96.

[7] Buchan AM, Slivka A, Xue. The effect of the NMDA receptor antagonist MK-801 on cerebral blood flow and infarct volume in experimental focal stroke.

[8] Garcia JH, Yoshida Y, Chen H, Li Y, Zhang ZG, Lian J, Chen S, Chopp M. Progression from ischemic injury to infarct following middle cerebral artery occlusion in the rat. Am J Pathol. 1993 Feb;142(2):623-35.

[9] Siesjö BK. Pathophysiology and treatment of focal cerebral ischemia. Part II: Mechanisms of damage and treatment. J Neurosurg. 1992 Sep;77(3):337-54.

[10] Garcia JH, Liu KF, Ho KL. Neuronal necrosis after middle cerebral artery occlusion in Wistar rats progresses at different time intervals in the caudoputamen and the cortex. Stroke. 1995 Apr;26(4):636-42.

[11] Du C, Hu R, Csernansky CA, Hsu CY, Choi DW. Very delayed infarction after mild focal cerebral ischemia: a role for apoptosis? J Cereb Blood Flow Metab. 1996 Mar;16(2):195-201.

[12] Li Y, Powers C, Jiang N, Chopp M. Intact, injured, necrotic and apoptotic cells after focal cerebral ischemia in the rat. J Neurol Sci. 1998 Apr 1;156(2):119-32.

[13] http://www.diabetes.org/diabetes-basics/diabetes-statistics

[14] http://www.who.int/mediacentre/factsheets/fs312/en/

[15] Matthaei S. Pathophysiology and pharmacological treatment of insulin resistance. Endocrine Reviews. 2000; 21(6):585-618.

[16] Poitout V, Robertson RP. Secondary beta cell failure in type 2 diabetes-A convergence of glucotoxicity and lipotoxicity. Endocrinology, 2002; 143(2):339-342.

[17] Mahler RJ, Adler ML. Type 2 diabetes mellitus: Update on diagnosis, pathophysiology, and treatment. J Clin Endoc and Metab.1999; 84(4):1165-1169.

[18] Rask-Madsen C, King GL. Mechanisms of disease: endothelial dysfunction in insulin resistance and diabetes. Nature. 2007; 3(1):46-56.

[19] Beckman, JS, Creager MA, Libby P. Diabetes and Atherosclerosis: Epidemiology, pathophysiology, and management. JAMA. 2002; 287(19):2570-2581.

[20] Ginsberg MD. Adventures in the pathophysiology of brain ischemia: penumbra, gene expression, neuroprotection. Stroke. 2003; 34:214-223.

[21] Yao H, Takasawa R, Fukuda K, Shiokawa D, Sadanaga-Akiyoshi F, Ibayashi S, Tanuma S, Uchimura H. DNA fragmentation in ischemic core and penumbra in focal cerebral ischemia in rats. Brain Research 2001; 91(1-2):112-118.

[22] Li Z, Britton M, Sima AAF, Dunbar JC. Diabetes enhances apoptosis induced by cerebral ischemia. Life Sciences. 2004; 76: 249-262.

[23] McLaughlin B. The kinder side of killer proteases: caspase activation contributes to neuroprotection and CNS remodeling. Apoptosis. 2004 Mar;9(2):111-21.

[24] Weigl M, Tenze G, Steinlechner B, Skhirtladze K, Reining G, Bernardo M, Pedicelli E, Dworschak M. (2005) A systematic review of currently available pharmacological neuroprotective agents as a sole intervention before anticipated or induced cardiac arrest. *Resuscitation* 65:21-39

[25] Laughlin SB and Sejnowski TJ. Communication in neuronal networks. Science 2003; 301:1870-1874.

[26] Krause GS, White BC, Aust SD, Nayini NR, Kumar K. Brain cell death following ischemia and reperfusion: a proposed biochemical sequence. Crit Care Med 1988;16:714-26

[27] Durukan A, Tatlisumak T. Acute ischemic stroke: overview of major experimental rodent models, pathophysiology, and therapy of focal cerebral ischemia. Pharmacol Biochem Behav. 2007 May;87(1):179-97

[28] Silver IA, Erecińska M. Intracellular and extracellular changes of [Ca2+] in hypoxia and ischemia in rat brain in vivo. J Gen Physiol. 1990 May;95(5):837-66.

[29] Hossmann KA. Periinfarct depolarizations. Cerebrovasc Brain Metab Rev. 1996 Fall;8(3):195-208.

[30] Nedergaard M, Hansen AJ. Characterization of cortical depolarizations evoked in focal cerebral ischemia. J Cereb Blood Flow Metab. 1993 Jul;13(4):568-74.

[31] Busch E, Gyngell ML, Eis M, Hoehn-Berlage M, Hossmann KA. Potassium-induced cortical spreading depressions during focal ischemia in rats: contribution to lesion growth assessed by diffusion-weighted NMR and biochemical imaging. J. Cereb. Blood Flow Metab. 1996; 16:1090–1099.

[32] Back T, Ginsberg MD, Dietrich WD, Watson BD. Induction of spreading depression in the ischemic hemisphere following experimental middle cerebral artery occlusion: effect on infarct morphology. J. Cereb. Blood Flow Metab. 1996; 16:202–213.

[33] Martone ME, Jones YZ, Young SJ, Ellisman MH, Zivin JA, Hu BR. Modification of postsynaptic densities after transient cerebral ischemia: a quantitative and three dimensional ultrastructural study. J Neurosci 1999 Mar 15;19(6):1988-97.

[34] Sloviter RS. Hippocampal pathology and pathophysiology in temporal lobe epilepsy. Neurologia. 1996 Dec; 11 Suppl 4:29-32.

[35] Hossmann KA. The bistable network model of brain ischemia. Exp Stroke Transl Med (2010) 3(1): 56-58.

[36] Sun GY, Xu J, Jensen MD, Simonyi A. Phospholipase A2 in the central nervous system: implications for neurodegenerative diseases. J Lipid Res. 2004 Feb;45(2):205-13.

[37] Farooqui AA, Horrocks LA. Brain phospholipases A2: a perspective on the history. Prostaglandins Leukot Essent Fatty Acids. 2004 Sep;71(3):161-9.

[38] Radi R, Beckman JS, Bush KM, Freeman BA. Peroxynitrite oxidation of sulfhydryls: The cytotoxic potential of superoxide and nitric oxide. J Biol Chem 1991; 266:4244-4250.

[39] Beckman JS, Beckman TW, Chen J, Marshall PA, Freeman BA. Apparent hydroxyl radical production by peroxynitrite: Implications for endothelial injury from nitric oxide and superoxide. Proc Natl Acad Sci USA 1990; 87:1620-1624.

[40] Ushijima K, Miyazaki H, Morioka T. Immunohistochemical localization of glutathione peroxidase in the brain of the rat. Resuscitation 1986;13:97-105

[41] Aust SD, Morehouse LA, Thomas CE. Role of metals in oxygen radical reactions. J Free Radic Biol Med 1985; 1:3-25.

[42] Mergenthaler P, Dirnagl U, Meisel A. Pathophysiology of stroke: lessons from animal models. Metab Brain Dis. 2004 Dec;19(3-4):151-67.

[43] Lo CJ, Lin JG, Kuo JS, Chiang SY, Chen SC, Liao ET, Hsieh CL. Effect of salvia miltiorrhiza bunge on cerebral infarct in ischemia-reperfusion injured rats. Am J Chin Med. 2003;31(2):191-200.

[44] Solenski NJ, Kwan AL, Yanamoto H, Bennett JP, Kassell NF, Lee KS. Differential hydroxylation of salicylate in core and penumbra regions during focal reversible cerebral ischemia. Stroke. 1997; 28:2545–2552.

[45] Beckman JS. Peroxynitrite versus hydroxyl radical: the role of nitric oxide in superoxide-dependent cerebral injury. Ann. NY Acad Sci. 1994; 738: 69–75.

[46] Nogawa S, Forster C, Zhang F, Nagayama M, Ross ME, Iadecola C. Interaction between inducible nitric oxide synthase and cyclooxygenase-2 after cerebral ischemia. Proc. Natl. Acad. Sci. USA 1998; 95:10966–10971.

[47] O'Neil BJ, McKeown TR, DeGracia DJ, Alousi SS, Rafols JA, White BC. Cell death, calcium mobilization, and immunostaining for phosphorylated eukaryotic initiation 2- factor 2-alpha (eIF2a) in neuronally-differentiated NB-104 cells: arachidonate and radical medicated injury mechanisms. Radical-mediated injury mechanisms. Resuscitation 1999;41:71-83.

[48] Suzuki L, Poot M, Gerrity RG, Bornfeldt KE. Diabetes accelerates smooth muscle accumulation in lesions of atherosclerosis: Lack of direct growth-promoting effects of high glucose levels. Diabetes. 2001; 50:851-860

[49] Stroemer RP, Rothwell NJ. Cortical protection by localized striatal injection of IL-1RA following cerebral ischemia in the rat. J. Cereb. Blood Flow Metab. 1997; 17:597–604.

[50] Hara H, Friedlander RM, Gagliardini V. Inhibition of interleukin 1b converting enzyme family proteases reduces ischemic and excitotoxic neuronal damage. Proc. Natl. Acad. Sci. USA. 1997; 94:2007–2012.

[51] Braun, JS, Jander S, Schroeter M, Witte OW, Stoll G. Spatiotemporal relationship of apoptotic cell death to lymphomonocytic infiltration in photochemically induced focal ischemia of the rat cerebral cortex. Acta Neuropathol. 1996; 92:255–263.

[52] Zhang RL, Chopp M, Chen H, Garcia JH. Temporal profile of ischemic tissue damage, neutrophil response and vascular plugging following permanent and transient (2H) middle cerebral artery occlusion in the rat. J. Neurol. Sci.1994;125:3–10.

[53] Chen, JW, Zhang L, Lian X, Hwang F. Effect of hydroxyl radical on Na-K ATPase activity of the brain microsomal membranes. Cell Biol. Int. Rep. 1992; 16:927–936.

[54] Kleihaus P and Hossmann KA. Protein synthesis in the cat brain after prolonged cerebral ischemia. Brain Res. 1971 Dec 24;35(2):409-18

[55] Gingras A.C., Raught B, and Sonenberg N. eIF4 Initiation Factors: Effectors of mRNA Recruitment To Ribosomes and Regulators of Translation. Annu. Rev. Biochem 1999. 68:913-63.

[56] Lamphear BJ, Kirchweger R, Skern T, Rhoades RE. Mapping of functional domains in eukaryotic protein synthesis initiation factor 4G with picornaviral proteases. J Biol Chem 1995; 270:21975-21983.

[57] Rowlands A. G., Panniers, R., and Henshaw, E. C. The catalytic mechanism of guanine nucleotide exchange factor action and competitive inhibition by phosphorylated eukaryotic initiation factor 2. J. Biol. Chem. 1988; 263: 5526-5533.

[58] Bu X, Haas DW, Hagedorn CH. Novel phosphorylation sites of eukaryotic initiation factor-4F and of the p25 and p220 subunits. J Biol Chem 1993; 268:4975-4978.

[59] Svitkin YV, Imataka H, Khaleqhpour K, Kahvejian A, Liebiq HD, Sonenberq N. Poly(A)-binding protein interaction with eIF4G stimulates picornavirus IRES-dependent translation. RNA. 2001 Dec;7(12):1743-52

[60] Byrd MP, Zamora M, Lloyd RE. Translation of eukaryotic translation initiation factor 4G1 (eIF4G1) proceeds from multiple mRNAs containing a novel cap-dependent internal ribosome entry site (IRES) that is active during poliovirus infection. J Biol Chem. 2005 May 13;280(19):18610-22.

[61] Marissen WE and Lloyd RE. Eukaryotic translation initiation factor 4G is targeted for proteolytic cleavage by caspase 3 during inhibition of translation in apoptotic cells. Mol Cell Biol 1998 Dec;18(12):7565-74.

[62] Hu BR, Wieloch T. Stress-induced inhibition of protein synthesis initiation: modulation of initiation factor 2 and guanine nucleotide exchange factor activities following transient cerebral ischemia in the rat. J Neurosci. 1993 May;13(5):1830-8.

[63] Burda J, Martin ME, Garcia A, Alcazar A, Fando JL, Salinas M. Phosphorylation of the α subunit of initiation factor 2 correlates with the inhibition of translation following transient cerebral ischemia in the rat. Biochem J. 1994; 302:335-338.

[64] DeGracia DJ, Neumar RW, White, BC, Krause GS. Global brain ischemia and reperfusion: Modifications in eukaryotic initiation factors are associated with inhibition of translation initiation. J Neurochem 1996; 67:2005-2012.

[65] DeGracia DJ, Sullivan JM, Neumar RW, Alousi SS, Hikade KR, Pittman JE, White BC, Rafols JA, Krause GS. Effect of brain ischemia and reperfusion on the localization of phosphorylated eukaryotic initiation factor 2α. J Cereb Blood Flow and Metab 1997; 17:1291-1302.

[66] Kumar R, Azam S, Sullivan JM, Owen CR, Cavener DR, Zhang P, Ron D, Harding HP, Chen JJ, Han A, White BC, Krause GS, DeGracia DJ. Brain ischemia and reperfusion activates the eukaryotic initiation factor 2α kinase, PERK. J Neurochem 2001; 77:1418-1421.

[67] Zhao H, Sapolsky RM, Steinberg GK. Interrupting reperfusion as a stroke therapy: ischemic postconditioning reduces infarct size after focal ischemia in rats. J Cereb Blood Flow Metab. 2006 Sep;26(9):1114-21.

[68] Davis DP, Patel PM. Ischemic preconditioning in the brain. Curr Opin Anaesthesiol. 2003 Oct;16(5):447-52.

[69] DeGracia DJ, Jamison JT, Szymanski JJ, Lewis MK. Translation arrest and ribonomics in post-ischemic brain: layers and layers of players. J Neurochem. 2008 Sep;106(6):2288-301.

[70] Martin De La Vega C, Burda J, Nemethova M, Quevedo C, Alcazar A, Martin M.E., Danielisova V, Fando J.L. and Salinas M. Possible mechanisms involved in the down-regulation of translation during transient global ischaemia in the rat brain. Biochem. J. 2001; 357:819-826.

[71] Hu B.R., Janelidze S., Ginsberg M.D., Busto R., Perez-Pinzon M., Sick T.J., Siesjo B.K., and Liu C.L.; Protein Aggregation After Focal Brain Ischemia and Reperfusion, Journal of Cerebral Blood Flow and Metabolism 2001; 21:865-875.

[72] Liu CL, Ge P, Zhang F, Hu BR. Co-translational protein aggregation after transient cerebral ischemia. Neuroscience. 2005;134(4):1273-84.

[73] Van Leeuwen FW, Hol EM, Fischer DF. Frameshift proteins in Alzheimer's disease and in the other conformational disorders: time for the ubiquitin-proteasome system. J Alzheimers Dis. 2006; 9:319-25.

[74] Hu B.R., Martone M.E., Jones Y.Z., and Liu C.L.; Protein Aggregation after Transient Cerebral Ischemia, The Journal of Neuroscience, May 1, 2000, 20(9):3191-3199.

[75] Zhang F, Liu CL, Hu BR. Irreversible aggregation of protein synthesis machinery after focal brain ischemia. J. Neurochem. 2006 Jul;98(1):102-12.

[76] Mansfield KD, Keene JD. The ribonome: a dominant force in co-ordinating gene expression. Biol Cell. 2009 Mar;101(3):169-81.

[77] Anderson P, Kedersha N. Stress granules. Curr Biol. 2009 May 26;19(10):R397-8.

[78] Nissan T, Parker R. Analyzing P-bodies in Saccharomyces cerevisiae. Methods Enzymol. 2008;448:507-20.

[79] Brennan CM, Steitz JA. HuR and mRNA stability. Cell Mol Life Sci. 2001 Feb;58(2):266-77.

[80] Atasoy U, Watson J, Patel D, Keene JD. ELAV protein HuA (HuR) can redistribute between nucleus and cytoplasm and is upregulated during serum stimulation and T cell activation. J Cell Sci. 1998 Nov;111 (Pt 21):3145-56.

[81] Keene JD, Tenenbaum SA. Eukaryotic mRNPs may represent posttranscriptional operons. Mol Cell. 2002 Jun;9(6):1161-7.

[82] Maruno M, Yanagihara T. Progressive loss of messenger RNA and delayed neuronal death following transient cerebral ischemia in gerbils. Neurosci Lett. 1990 Jul 31;115(2-3):155-60.

[83] Matsumoto K, Yamada K, Hayakawa T, Sakaguchi T, Mogami H. RNA synthesis and processing in the gerbil brain after transient hindbrain ischaemia. Neurol Res. 1990: 12:45-48.

[84] Kedersha N, Tisdale S, Hickman T, Anderson P. Real-time and quantitative imaging of mammalian stress granules and processing bodies. Methods Enzymol. 2008;448:521-52.

[85] Kumar R, Krause GS, Yoshida H, Mori K, DeGracia DJ. Dysfunction of the unfolded protein response during global brain ischemia and reperfusion. J Cereb Blood Flow Metab. 2003 Apr;23(4):462-71.

[86] DeGracia DJ. Mini review; Acute and Persistent Protein Synthesis Inhibition Following Cerebral Reperfusion, Journal of Neuroscience Research 2004; 77:771-776.

[87] Montie HL, Haezebrouck AJ, Gutwald JC, DeGracia DJ. PERK is activated differentially in peripheral organs following cardiac arrest and resuscitation. Resuscitation. 2005 Mar; 66:379-389.

[88] Montie HL, Kayali F, Haezebrouck AJ, Rossi NF, DeGracia DJ. Renal ischemia and reperfusion activates the eIF2 alpha kinase PERK. Biochimica etBiophysica Acta. 2005 Apr; 1741:314-324.

[89] Smith ML, Bendek G, Dahlgren N, Rosén I, Wieloch T, Siesjö BK. Models for studying long-term recovery following forebrain ischemia in the rat. 2. A 2-vessel occlusion model. Acta Neurol Scand. 1984 Jun;69(6):385-401.

[90] DeGracia DJ, Rudolph J, Roberts GG, Rafols JA, Wang J. Convergence of stress granules and protein aggregates in hippocampal cornu ammonis 1 at later reperfusion following global brain ischemia. Neuroscience. 2007 May 11;146(2):562-72.

[91] DeGracia DJ, Rafols JA, Morley SJ, Kayali F. Immunohistochemical mapping of total and phosphorylated eukaryotic initiation factor 4G in rat hippocampus following global brain ischemia and reperfusion. Neuroscience. 2006;139(4):1235-48.

[92] Kedersha N, Stoecklin G, Ayodele M, Yacono P, Lykke-Andersen J, Fritzler MJ, Scheuner D, Kaufman RJ, Golan DE, Anderson P. Stress granules and processing bodies are dynamically linked sites of mRNP remodeling. J Cell Biol. 2005 Jun 20;169(6):871-84.

[93] Tchórzewski M. The acidic ribosomal P proteins. Int J Biochem Cell Biol. 2002 Aug;34(8):911-5.

[94] Oliff HS, Weber E, Miyazaki B, Marek P. Infarct volume varies with rat strain and vendor in focal cerebral ischemia induced by transcranial middle cerebral artery occlusion. Brain Res. 1995 Nov 20;699(2):329-31.

[95] Li ZG, Britton M, Sima AA, Dunbar JC. Diabetes enhances apoptosis induced by cerebral ischemia. Life Sci. 2004 Dec 3;76(3):249-62.

[96] Rizk NN, Rafols JA, Dunbar JC. Cerebral ischemia-induced apoptosis and necrosis in normal and diabetic rats: effects of insulin and C-peptide. Brain Res. 2006 Jun 22;1096(1):204-12.

[97] Schifilliti D, Grasso G, Conti A, Fodale V. Anaesthetic-related neuroprotection: intravenous or inhalational agents? CNS Drugs. 2010 Nov 1;24(11):893-907.

[98] Hatashita T, Ito M, Miyaoka M, Ishii S. Chronological alterations of regional cerebral blood flow, glucose utilization, and edema formation after focal ischemia in hypertensive and normotensive rats. Significance of hypertension. Adv Neurol. 1990;52:29-37.

[99] Hatfield RH, Mendelow AD, Perry RH, Alvarez LM, Modha P. Triphenyltetrazolium chloride (TTC) as a marker for ischaemic changes in rat brain following permanent middle cerebral artery occlusion. Neuropathol Appl Neurobiol. 1991 Feb;17(1):61-7.

[100] Isayama K, Pitts LH, Nishimura MC. Evaluation of 2,3,5-triphenyltetrazolium chloride staining to delineate rat brain infarcts. Stroke. 1991 Nov;22(11):1394-8.

[101] Kayali F, Montie HL, Rafols JA, DeGracia DJ. Prolonged translation arrest in reperfused hippocampal cornu Ammonis 1 is mediated by stress granules. Neuroscience. 2005;134(4):1223-45.

[102] Jamison JT, Kayali F, Rudolph J, Marshall M, Kimball SR, DeGracia DJ. Persistent redistribution of poly-adenylated mRNAs correlates with translation arrest and cell death following global brain ischemia and reperfusion. Neuroscience. 2008 Jun 23;154(2):504-20

[103] Bessert DA, Skoff RP. High-resolution in situ hybridization and TUNEL staining with free-floating brain sections. J Histochem Cytochem. 1999 May;47(5):693-702.

[104] Rizk NN, Rafols J, Dunbar JC. Cerebral ischemia induced apoptosis and necrosis in normal and diabetic rats. Brain Res. 2005 Aug 16;1053(1-2):1-9.

[105] Walberer M, Stolz E, Müller C, Friedrich C, Rottger C, Blaes F, Kaps M, Fisher M, Bachmann G, Gerriets T. Experimental stroke: ischaemic lesion volume and oedema formation differ among rat strains (a comparison between Wistar and Sprague-Dawley rats using MRI). Lab Anim. 2006 Jan;40(1):1-8.

[106] Oliff HS, Coyle P, Weber E. Rat strain and vendor differences in collateral anastomoses. J Cereb Blood Flow Metab. 1997 May;17(5):571-6.

[107] Kinouchi H, Sharp FR, Koistinaho J, Hicks K, Kamii H, Chan PH. Induction of heat shock hsp70 mRNA and HSP70 kDa protein in neurons in the 'penumbra' following focal cerebral ischemia in the rat. Brain Res. 1993 Aug 13;619(1-2):334-8.

[108] Yenari MA, Liu J, Zheng Z, Vexler ZS, Lee JE, Giffard RG. Antiapoptotic and anti-inflammatory mechanisms of heat-shock protein protection. Ann N Y Acad Sci. 2005 Aug;1053:74-83.

[109] Paxinos G, Watson C. *The Rat Brain in Stereotaxic Coordinates* (5th ed). 2005: Elsevier Academic Press, Amsterdam.

[110] Toga AW, Santori EM, Hazani R, Ambach K. A 3D digital map of rat brain. Brain Res Bull. 1995;38(1):77-85.

[111] Benedek A, Móricz K, Jurányi Z, Gigler G, Lévay G, Hársing LG Jr, Mátyus P, Szénási G, Albert M. Use of TTC staining for the evaluation of tissue injury in the early phases of reperfusion after focal cerebral ischemia in rats. Brain Res. 2006 Oct 20;1116(1):159-65.

[112] Bonfa E, Marshak-Rothstein A, Weissbach H, Brot N, Elkon K (1988) Frequency and epitope recognition of anti-ribosome P antibodies from humans with systemic lupus erythematosus and MRL/lpr mice are similar. J Immunol 140:3434-3437.

[113] Gallouzi IE, Brennan CM, Steitz JA (2001) Protein ligands mediate the CRM1-dependent export of HuR in response to heat shock. *RNA* **7**, 1348-1361.

[114] Fenger-Grøn, Martin, Christy Fillman, Bodil Norrild and Jens Lykke-Andersen. Multiple Processing Body Factors and the ARE Binding Protein TTP Activate mRNA Decapping. Molecular Cell. 2005 Dec 22 Volume 20, Issue 6, 905-915.

[115] Chen H, Wu XJ, Lu XY, Zhu L, Wang LP, Yang HT, Chen HZ, Yuan WJ. Phosphorylated heat shock protein 27 is involved in enhanced heart tolerance to ischemia in short-term type 1 diabetic rats. Acta Pharmacol Sin. 2005 Jul;26(7):806-12.

[116] Oliff HS, Weber E, Eilon G, Marek P. The role of strain/vendor differences on the outcome of focal ischemia induced by intraluminal middle cerebral artery occlusion in the rat. Brain Res. 1995 Mar 27;675(1-2):20-6.

[117] Prieto R, Carceller F, Roda JM, Avendaño C. The intraluminal thread model revisited: rat strain differences in local cerebral blood flow. Neurological Research. 2005 Jan;27(1).

[118] Hossmann K-A. Viability thresholds and the penumbra of focal ischemia. Ann Neurol 1994; 36: 557-565.

[119] Mies G, Ishimaru S, Xie Y, Seo K, Hossmann KA. Ischemic thresholds of cerebral protein synthesis and energy state following middle cerebral artery occlusion in rat. J Cereb Blood Flow Metab. 1991 Sep;11(5):753-61.

[120] Dent MA, Segura-Anaya E, Alva-Medina J, Aranda-Anzaldo A. NeuN/Fox-3 is an intrinsic component of the neuronal nuclear matrix. FEBS Lett. 2010 Jul 2;584(13):2767-71.

[121] Sena ES, Briscoe CL, Howells DW, Donnan GA, Sandercock PA, Macleod MR. Factors affecting the apparent efficacy and safety of tissue plasminogen activator in thrombotic occlusion models of stroke: systematic review and meta-analysis. J Cereb Blood Flow Metab. 2010 Dec;30(12):1905-13.

[122] O'Collins VE, Macleod MR, Donnan GA, Horky LL, van der Worp BH, Howells DW. 1,026 experimental treatments in acute stroke. Ann Neurol. 2006 Mar;59(3):467-77.

[123] Braeuninger S, Kleinschnitz C. Rodent models of focal cerebral ischemia: procedural pitfalls and translational problems. Experimental & Translational Stroke Medicine. 2009 Nov 25; 1:8.

[124] Hossmann KA. Pathophysiology and therapy of experimental stroke. Cell Mol Neurobiol. 2006 Oct-Nov;26(7-8):1057-83.

[125] Panés J, Kurose I, Rodriguez-Vaca D, Anderson DC, Miyasaka M, Tso P, Granger DN. Diabetes exacerbates inflammatory responses to ischemia-reperfusion. Circulation. 1996 Jan 1;93(1):161-7.

[126] Zhou M, Yesilkaya A, Ullrich V. Peroxynitrite inactivates prostacyclin synthase by heme-thiolatecatalyzed tyrosine nitration. Drug Metab Rev. 1999;31:343-349.

[127] Kalani M. The importance of endothelin-1 for microvascular dysfunction in diabetes. Vasc Health Risk Manag. 2008;4(5):1061-8.

[128] van Golde JM, Ruiter MS, Schaper NC, Vöö S, Waltenberger J, Backes WH, Post MJ, Huijberts MS. Impaired collateral recruitment and outward remodeling in experimental diabetes. Diabetes. 2008 Oct;57(10):2818-23.

[129] Siesjö BK, Katsura KI, Kristián T, Li PA, Siesjö P. Molecular mechanisms of acidosis-mediated damage. Acta Neurochir Suppl. 1996;66:8-14.

[130] Rains JL, Jain SK. Oxidative stress, insulin signaling, and diabetes. Free Radic Biol Med. 2011 Mar 1;50(5):567-75.

[131] Chrissobolis S, Miller AA, Drummond GR, Kemp-Harper BK, Sobey CG. Oxidative stress and endothelial dysfunction in cerebrovascular disease. Front Biosci. 2011 Jan 1;16:1733-45.

[132] Mastrocola R, Restivo F, Vercellinatto I, Danni O, Brignardello E, Aragno M, Boccuzzi G. Oxidative and nitrosative stress in brain mitochondria of diabetic rats. J Endocrinol. 2005 Oct;187(1):37-44.

ABSTRACT

MECHANISMS OF TRANSLATION ARREST FOLLOWING FOCAL BRAIN ISCHEMIA

by

MONIQUE K. LEWIS

August 2011

Advisor: Donald J. DeGracia, Ph.D.

Major: Physiology

Degree: Doctor of Philosophy

Diabetes affects 25 million and stroke affects ¾ million people a year in the USA. Diabetes increases the risk of stroke and worsens stroke outcome, but the causes for this are not fully known. Neurons destined to die following brain ischemia undergo a persistent translation arrest that prevents successful expression of protective cellular responses. Recent work has revealed the translation arrest following global ischemia is due to sequestration of mRNA in the form of mRNA granules away from ribosomal subunits, thereby precluding translation. I hypothesize that mRNA granules form during focal brain ischemia and this effect is worsened in diabetics subjected to focal brain ischemia. MCAO was performed for durations ranging from 2-8 hr and mRNA granules assessed by fluorescence in situ histochemistry. Long Evans rats showed strong mRNA granule formation in penumbra at 2 hr ischemia but not Wistar rats. In the Long Evans strain, the volume of brain containing neurons expressing mRNA granules decreased exponentially from 2 to 8 hr focal brain ischemia such that no mRNA granules were detected at 8 hr ischemia. Colocalization studies of mRNA granules with a panel of organelle and mRNA binding protein markers showed these to colocalize with PABP, HuR and NeuN. mRNA granules did not colocalize with markers of ribosomal subunits, endoplasmic reticulum, cis- and trans-Golgi networks, mitochondria, microtubules, intermediate filaments, stress granules, processing bodies or the HuR accessory proteins APRIL and pp32. Diabetes completely abrogated the formation of mRNA granules following any duration of focal ischemia

tested. Thus, mRNA granules form in penumbral neurons following focal brain ischemia and mediate translation arrest in these neurons. This response is inhibited by diabetes. Since mRNA granules are part of the ribonomic regulation of neuronal stress responses, their inhibition by diabetes provides an additional mechanism whereby diabetes worsens outcome after focal brain ischemia.

AUTOBIOGRAPHICAL STATEMENT

EDUCATION

Wayne State University Detroit, MI

Ph.D in Physiology planned graduation date: August 2011

Wayne State University

Masters in Basic Medical Sciences December 2004

Thesis: The Impact of Hypertension in Type-1 Diabetic Nephropathy

Advisor: Dr. David Lawson

University of Michigan Ann Arbor, MI

BA in Sociology May 1997

PUBLICATIONS

Jamison JT. Lewis MK, Kreipke CW. Rafols J. DeGracia DJ. Polyadenylated mRNA staining reveals distinct neuronal phenotypes following endothelin 1, focal brain ischemia, and global brain ischemia/ reperfusion. Neurological Research 2011;33(2):145-161.

DeGracia DJ, Jamison JT, Szymanski JJ, Lewis MK. Translation arrest and ribonomics in post-ischemic brain: layers and layers of players. J Neurochem. 2008;106(6):2288-301.

Jamison JT, Kayali F, Rudolph J, Marshall M, Kimball SR, DeGracia DJ. Persistent redistribution of poly-adenylated mRNAs correlates with translation arrest and cell death following global brain ischemia and reperfusion. Neuroscience. 2008;154(2):504-20.

Roberts GG, Di Loreto MJ, Marshall M, Wang J, DeGracia DJ. Hippocampal cellular stress responses after global brain ischemia and reperfusion. Antioxid Redox Signal. 2007;9(12):2265-75.